FUNCTIONAL STUDY OF G PROTEIN SIGNALING DURING GROWTH AND DEVELOPMENT OF THE SOCIAL AMOEBA *DICTYOSTELIUM DISCOIDEUM*

By

Yuantai Wu

Dissertation

Submitted to the Faculty of the

Graduate School of Vanderbilt University

in partial fulfillment of the requirements

for the degree of

DOCTOR OF PHILOSOPHY

in

Biological Sciences

August, 2013

Nashville, Tennessee

Approved:

Professor James Patton

Professor Chris Janetopoulos

Professor Chang Chung

Professor Charles Singleton

To my beloved wife Xiaoxi and my parents, for their infinite support.

ACKNOWLEDGEMENTS

This work would not have been possible without the financial support from the National Institutes of Health, the Vanderbilt Discovery Grant Program and the Department of Biological Sciences. I am grateful to our supportive Department of Biological Sciences for providing us the Gislea Mosig Travel Fund, which provided me the opportunity to meet with my colleagues in the *Dictyostelium* community.

I am especially indebted to Dr. Chris Janetopoulos. As my mentor, he guided me into the exciting G protein signaling field and led the challenging journey in my graduate study. He also provided me unwavering support and allowed me to test my "crazy" ideas. His work ethic, motivation and creativity have set me a good example of what a good scientist should be.

I would like to thank the members of my Dissertation Committee for their guidance and comments over the past four years as I started to screen the folic acid receptors. I would especially like to thank Dr. Charles Singleton. He provided me with a lot of helpful suggestions on writing the qualifying exam proposal, helped me on how to characterize the development of the amoeba, generously provided me reagents and allowed me to use the microscope in his lab.

Nobody has been more important to me during my graduate study than my wife Xiaoxi. She endured my impatience in our everyday life, pushed me when I hesitated, encouraged me when I was under stress and helped me with difficulties I met in my experiments. She provided unending inspiration during my research. I could not imagine what I could have done without her.

TABLE OF CONTENTS

Page

DEDICATION ..... ……..ii

ACKNOWLEDGEMENTS iii

LIST OF TABLES vi

LIST OF FIGURES vii

LIST OF ABBREVIATIONS x

Chapter

I. A BRIEF INTRODUCTION TO THE SOCIAL AMOEBA *DICTYOSTELIUM DISCOIDEUM* 1

II. SCREEN OF POTENTIAL FOLIC ACID RECEPTORS 4

Abstract 4
Introduction 4
Materials and Methods 8
Results 14
Discussion 18

III. SYSTEMATIC ANALYSIS OF GAMMA-AMINOBUTYRIC ACID (GABA) METABOLISM AND FUNCTION 20

Abstract 20
Introduction 21
Materials and Methods 24
Results 30
Discussion 55

IV. THE G ALPHA SUBUNIT GA8 INHIBITS PROLIFERATION, PROMOTES ADHESION AND REGULATES CELL DIFFERENTIATION 61

Abstract 61

Introduction 62
Materials and methods 64
Results 74
Discussion 106

V. SUMMARY AND PERSPECTIVE 112

REFERENCES 118

LIST OF TABLES

Table Page

1. Primers used for RT-PCR in chapter II 10

2. Primers used for gene knockout in chapter II 13

3. Primers used in chapter III 26

4. Summary of mutants obtained from dictybase. 65

5. Primer sequences used in chapter IV 68

LIST OF FIGURES

Figure Page

1. The structure of folic acid 1

2. The developmental cycle of *Dictyostelium discoideum* 2

3. Transcriptional changes of several candidate genes upon folic acid stimulation.. 15

4. Folic acid chemotaxis assay for *grlB* null mutant 16

5. Development of Ax2 and *grlB* mutants on DB agar 17

6. Early developmental phenotypes of *grlB* mutants. 31

7. Effect of exogenous GABA on early development 32

8. GABA synthesis and secretion in wild-type and mutant *D. discoideum* strains during early development 33

9. GABA secretion during axenic growth 34

10. Transcriptional changes of *gadA* and *gadB* in different mutants 36

11. Early developmental phenotypes of *gad* mutants 37

12. Early developmental phenotypes of *gad* overexpressors 37

13. Co-development of WT::*gfp* and WT::*gadB* cells 39

14. Regulation of GABA degradation and secretion 41

15. Localization of GabT-GFP in axenic cells 41

16. Early development of *gabT* mutants 42

17. Early development of *DdvGAT* mutant..... 44

18. Localization of GFP-DdvGAT in axenic cells..... 44

19. Effect of Latrunculin A and Nocodazole on GABA secretion 45

20. GABA binding in vegetative cells and early gene expression in *grlB*- cells..... 47

21. Early development of *grlE*- and *grlB-/grlE*- mutants 48

22. Distribution of GrlB-GFP during early development 49

23. Expression of "early genes" during early development of *grlB*- cells..... 50

24. The percentage of detergent-resistant spores in different GABA mutants 52

25. Overexpression of *gadB* in different Gα subunit null mutants 54

26. Characterization of nuclei per cell and cell proliferation in adherent cells lacking or overexpressing Gα8 75

27. Characterization of nuclei per cell and cell proliferation in shaking cells lacking or overexpressing Gα8 76

28. Expression of Gα8 in different mutants..... 77

29. Proliferation of different *gα8* mutants in suspension..... 79

30. Phenotypic characterization of Gα1 overexpression in wild-type Ax2 cells..... 80

31. Induction of adhesion in response to Gα8 overexpression 82

32. Expression of CadA and Gα8 in vegetative growing cells 83

33. Effect of Gα8 overexpression on cell-cell cohesion 84

34. Effect of Gα8 on cell-substrate adhesion 86

35. Localization of Gα8 in wild-type Ax2 and *gβ*- cells 88

36. Effect of different mutant forms of Gα8 on cell division. 89

37. Subcellular localization of Gα8 mutants 90

38. The induction of cytokinesis defects by the heterotrimer Gα8βγ 91

39. Distribution of Gα8 and Gβ during cytokinesis 93

40. Overexpression of *gα8* in *cadA*- cells 94

41. Overexpression of Gα8 in *paxB*- cells 95

42. Overexpression of Gα8 in *sadA*- cells 97

43. Early development of Gα8 mutants 98

44. Expression of Gα8 and adhesion molecules during early development 99

45. Distribution of Gα8 in multiceullular structures 101

46. Distribution of *ga8*- and *gα8* overexpression cells in chimeras 103

47. Spore formation and spatial patterning during culmination 105

LIST OF ABBREVIATIONS

ACA, adenylyl cyclase of aggregation stage

ALC, anterior-like cell

Bp, base pair

Bsr, blasticidin S resistance

Cad, calcium-dependent adhesion

cAMP, 3'-5'-cyclic adenosine monophosphate

cAR, cAMP receptor

CsA, contact site A

DAPI, 4′, 6-diamidino-2-phenylindole

DB, developmental buffer

EDTA, ethylenediaminetetraacetic acid

EGTA, ethylene glycol tetraacetic acid

GABA, γ-aminobutyric acid

GabT, GABA transaminase

Gad, glutamate decarboxylase

GAT, GABA transporter

GDP, guanosine 5′-diphosphate

GEF, guanine exchange factor

GPCR, G protein coupled receptor

GTP, guanosine-5'-triphosphate

Htt, Huntingtin

IgG, immunoglobulin G

PBS, phosphate buffered saline

PDE, phosphodiesterase

PI(3,4,5)P3, phosphatidylinositol-3,4,5-triphosphate

PI3K, phosphatidylinositol-3 kinase

PLP, pyridoxal phosphate

qPCR, quantitative PCR

RT-PCR, reverse-transcription PCR

Sad, substrate adhesion

SDF, spore differentiation factor

SSA, succinic-semialdehyde

SSADH, succinic semialdehyde dehydrogenase

TCA, tricarboxylic-acid

Tgr, transmembrane, IPT, IG, E-set, Repeat protein

vGAT, vesicular GABA transporter

CHAPTER I

A BRIEF INTRODUCTION TO THE SOCIAL AMOEBA *DICTYOSTELIUM DISCOIDEUM*

Since the first isolation of the social amoeba *Dictyostelium discoideum* from the hard wood forest outside of Ashville, North Carolina by Kenneth Raper (Raper, 1935), this organism has been extensively studied and established as a model system to study many fundamental biological processes including phagocytosis, chemotaxis and differentiation. These solitary amoebae usually have a size of 10-20 μm in diameter. They are professional phagocytes living in the soil, and utilize a bacterial metabolite, folic acid (see structure in Fig. 1), to track down bacteria during the vegetative stage.

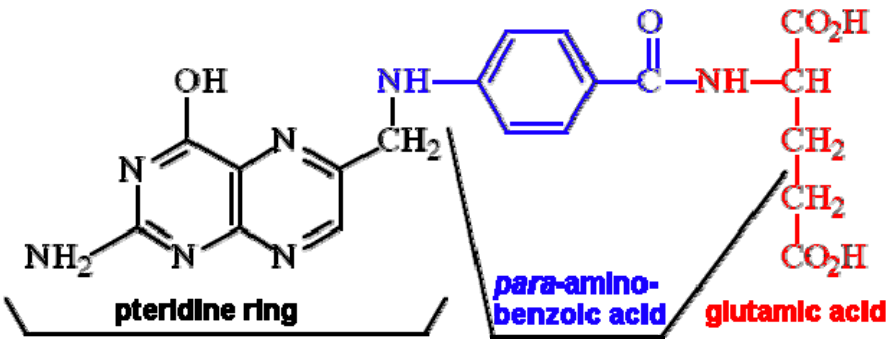

Figure 1. The structure of folic acid (Adapted from Dominic Taylor and Paul May in University of Bristol, Bristol, UK).

When food sources are scarce, starvation triggers a complicated developmental process in the social amoeba. The developmental process is shown schematically in Fig. 2. Upon starvation, up to 100,000 cells sense propagating cAMP waves and chemotax toward the aggregation center. These aggregating cells have their own territory and form

an intact mound by the end of streaming. At the mound stage, homogeneous cells specify into two different types of cells: pre-spore and pre-stalk cells. After a series of morphological changes depicted in Fig. 2, pre-stalk cells finally differentiate into the upright stalk supporting the sorus which is driven from pre-spore cells. The cooperation of multiple cells in the developmental cycle defines the "social" trait of *D. discoideum*.

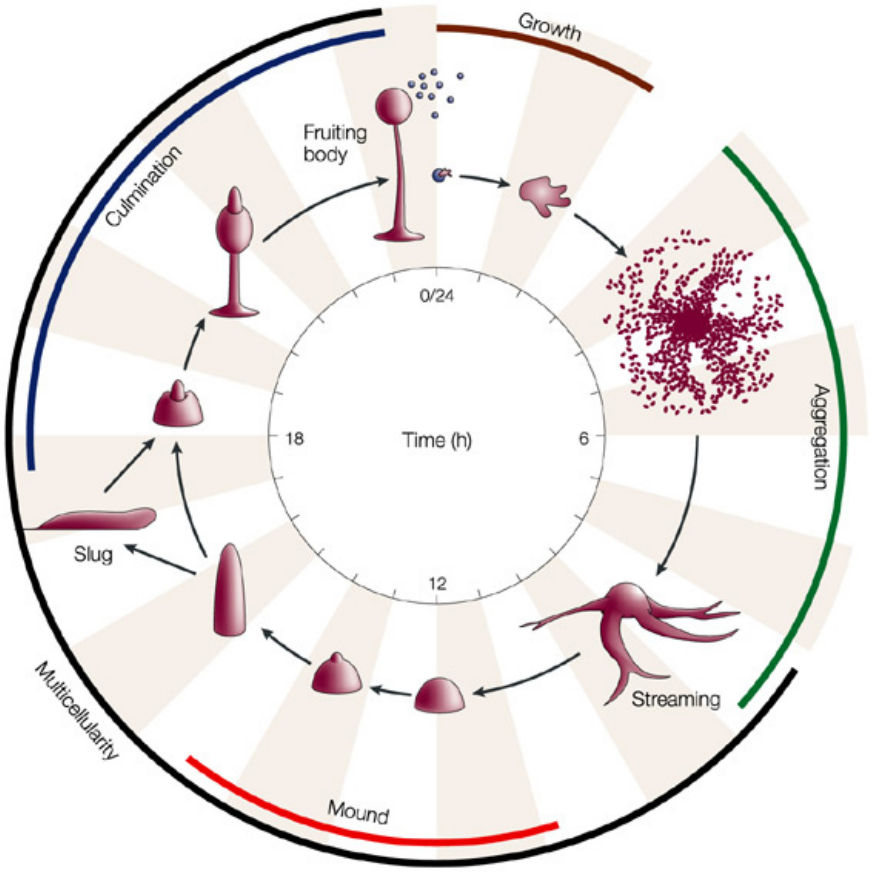

Figure 2. The developmental cycle of *Dictyostelium discoideum* (Chisholm and Firtel, 2004).

In this thesis, I focus on two different aspects of the life cycle of the social amoeba. First, how is it that the amoebae sense folic acid? Folic acid has been identified as a chemo-attractant for decades. However, the folic acid receptor has yet to be

identified. Previous studies revealed that the G protein subunits Gα4 and Gβ are required for folic acid sensing (Hadwiger et al., 1994; Wu et al., 1995). Therefore I narrowed my search to putative G protein coupled receptors (GPCRs) in the *D. discoideum* genome.

Second, the transcriptional profile of the *D. discoideum* genome undergoes a dramatic change involving more than 25% of the genes during the transition from growth to development (Van Driessche et al., 2002). Cells cease dividing, and the expression of genes required for basic metabolism gradually diminishes. Meanwhile, genes required for development such as cAMP signaling components and cell-cell adhesion molecules are up-regulated. Given the unexpected large number of putative GPCRs and G protein alpha subunits, I will elucidate the functions of some of them in this transition and later development.

CHAPTER II

SCREEN OF POTENTIAL FOLIC ACID RECEPTORS

ABSTRACT

The solitary soil amoeba *Dictyostelium discoideum* utilizes the bacterial metabolite folic acid as a chemo-attractant to track down bacteria. Previous studies indicate that cells without the G protein alpha subunit Gα4 or the G beta subunit Gβ lose their chemotactic capacity toward folic acid, suggesting the potential folic acid receptor(s) is a G protein coupled receptor (GPCR). Genomic analysis of the amoeba revealed 61 putative GPCRs. I hypothesized that the folic acid receptor is among 46 of these putative GPCRs and the transcriptional level of the folic acid receptor is induced upon folic acid stimulation, therefore the transcriptional level of all putative GPCRs was examined after folic acid stimulation by reverse-transcription PCR. Two $GABA_B$ receptor-like family members, *grlB* and *grlD*, and five frizzled/smoothened-like family members, *fslA*, *fslB*, *fslJ*,*fslK* and *fslH* exhibited substantial transcriptional up-regulation. However, disruption of each gene (except *fslJ* which was not disrupted) did not lead to the loss of chemotactic ability toward folic acid. Potential explanations are discussed in the discussion.

INTRODUCTION

In nature, the survival of all organisms largely depends on the capacity to sense and respond to environmental cues. Various important extracellular stimuli, including neurotransmitters, growth factors, chemokines, odorants, and light, are relayed to intracellular effectors by activation of plasma membrane-bound receptors. Of all these receptors, serpentine G protein coupled receptors (GPCRs) form the largest superfamily.

The major families of GPCRs are family 1, including β-adrenergic, odorant receptor and light receptor; family 2, secretin family; family 3, metabotropic glutamate/$GABA_B$ family; family 4, pheromone receptors and family 5, frizzled/smoothened family. In humans, more than 1000 genes encoding GPCRs have been revealed, which represent about 4% of the entire protein-coding genome (Fredriksson et al., 2003; Howard et al., 2001). Several hereditary human diseases have been related to mutations within specific GPCRs or heterotrimeric G proteins (Spiegel and Weinstein, 2004). Moreover, GPCRs represent a major therapeutic target, and more than 30% of all currently marketed drugs are modulators of specific GPCRs (Wise et al., 2002).

The amoeboid protozoan *Dictyostelium discoideum* grow as single independent cells in the soil and utilize bacteria and yeast as a natural food source by phagocytosis. However, axenic mutant strains can obtain nutrients from liquid media through a process called pinocytosis (Doherty and McMahon, 2009). The first axenic strain was isolated by culturing a non-axenic natural strain in liquid medium (Sussman and Sussman, 1967). *Dictyostelium* cells have a segregated growth and developmental cycle. When facing adverse environments such as nutrient depletion, up to 100,000 cells can aggregate and undergo a series of morphological changes to form a multicellular fruiting body containing environmental-resistant spores. *Dictyostelium* is a powerful system extremely suitable for studying many key physiological processes, including cell motility, chemotaxis, cytokinesis, signal transduction and cell differentiation, which are highly conserved in mammalian systems (Eichinger et al., 2005). Moreover, the genetically tractable characteristic of this model provides several advantages for the analysis of gene function.

Sequence alignment revealed a total number of 61 genes encoding putative GPCRs in *Dictyostelium* genome (Eichinger et al., 2005; Heidel et al., 2011). Detailed analysis showed that 1 gene *lrlA* belongs to family 2 (secretin family), 17 genes (*grlA-H*, *grlJ-R*) to family 3 (metabotropic glutamate/$GABA_B$ family), 25 genes (*fslA-H*, *fslJ-Q*, *fscA-H*, *fscJ*) to family 5 (frizzled/smoothened family), 12 genes (*cAR1-4*, *CrlA-H*) to a unique cAR/Crl (cAMP receptor/cAMP receptor like) family, 1 gene similar to orphan vertebrate GPR89 and 5 genes related to human trans-membrane protein 145 (Heidel et al., 2011; Prabhu and Eichinger, 2006). 4 cAMP receptors (cARs) and 3 cAMP receptor-like proteins have been previously characterized (Manahan et al., 2004; Raisley et al., 2004). Surprisingly, families 2, 3 and 5 were thought to be exclusive to higher eukaryotes. Although the function of these receptors in *Dictyostelium* largely remains a mystery, three $GABA_B$ receptor-like proteins (GrlA, GrlE and GrlJ) were found to be involved in sporulation (Anjard and Loomis, 2006; Prabhu et al., 2007a; Prabhu et al., 2007b). With the exception of the cAMP receptors, the ligands for most receptors are unknown. However, γ-aminobutyric acid (GABA) is thought to be the ligand for GrlB and GrlE (Anjard and Loomis, 2006; Wu and Janetopoulos, 2013b). In addition, the *Dictyostelium* genome encodes 14 Gα subunits, 2 Gβ subunits and 1 Gγ subunit. Functions of the 9 Gα subunits, 1 Gβ subunit and the Gγ subunit have been described in detail (Brandon and Podgorski, 1997; Brzostowski et al., 2002; Hadwiger and Firtel, 1992; Hadwiger et al., 1996; Kumagai et al., 1991; Lilly et al., 1993; Wu et al., 1994; Wu and Janetopoulos, 2013a; Zhang et al., 2001). Since the number of Gα subunits is insufficient, one Gα subunit is likely to couple to several receptors. Previous studies have shown that the

cAMP receptor is coupled to the Gα2 subunit (Janetopoulos et al., 2001; Kumagai et al., 1991), and GrlE is likely to be coupled to the Gα7 subunit (Anjard et al., 2009).

cAMP signaling has been intensively studied in *Dictyostelium*, and cAR1 and cAR3 serve as major cAMP receptors in the signaling pathway (Manahan et al., 2004). Starvation elicits a developmental program and cAMP chemotaxis happens at the early stage of development. A cell stochastically starts to release the chemo-attractant cAMP and provides a shallow cAMP gradient for surrounding cells. Thousands of polarized cells synchronously sense this gradient and stream toward the cAMP signaling center. Meanwhile, cells signal each other by periodically releasing cAMP to form oscillations of cAMP at approximately 6-minute intervals, which are propagated through the cell monolayer. During this process, the chemo-attractant cAMP binds and activates the cAMP receptor. The activation of the cAMP receptor leads to GDP/GTP exchange for Gα2 and subsequent dissociation of the Gα2 subunit from the Gβγ dimer, both of which possibly release from the plasma membrane and regulate many downstream effectors (Elzie et al., 2009).

Dictyostelium cells also exhibit chemotactic ability when preying upon bacteria. *Dictyostelium* cells utilize environmental bacterial metabolites such as folic acid to track down bacteria. Axenic *Dictyostelium* cells respond poorly toward folic acid. However, axenic cells co-cultured with bacteria will soon restore folic acid chemotactic ability. Studies have shown that axenic cells can regain their chemotactic ability when folic acid is supplied in pulses (Wurster and Schubiger, 1977). Folic acid-induced chemotaxis was discovered decades ago, however, the receptor for folic acid still remains elusive. To help elucidate genes regulating this pathway, a delicate device was designed to screen

chemical mutagenized mutants for folic acid chemotactic defects (Segall et al., 1987) and mutants exhibiting different types of alterations were collected. One of these mutants showed altered folic acid affinity and abolished folic acid chemotaxis (Segall et al., 1988). The gene related to this mutant was identified as *gα4* (Hadwiger et al., 1994), suggesting the folic acid receptor likely couples to the Gα4 subunit. Responses to folic acid decrease after the onset of development, but a basal folic acid affinity remains until 12 hours of development (Tillinghast and Newell, 1987). Like cAMP receptors, it is possible that there may be redundant folic acid receptors. Folic acid binding assays revealed two different types of binding sites (Hadwiger et al., 1994), implying the existence of two different kinds of receptors. Folic acid signaling shares most of the components with cAMP signaling downstream of heterotrimeric G proteins (Srinivasan et al., 2012), however, the biggest difference between these two pathways is the generation of cytoskeletal polarity. During folic acid chemotaxis, cells form many random pseudopods during detection of the gradient while in cAMP chemotaxis, cells generate front-back cytoskeletal polarity and display an elongated cell shape (Mahadeo and Parent, 2006). Identifying the folic acid receptor(s) can greatly help us understand folic acid signaling and shed light on the mechanisms governing chemotaxis.

MATERIALS AND METHODS

Cell culture and folic acid stimulation

Wild-type Ax2 cells were maintained in HL-5 medium at 22°C. For folic acid pulse, 5 ml cell culture in HL-5 medium containing 1×10^6 cells per ml was shaken at

110 rpm, and pulsed periodically with 10μM folic acid at 6-minute intervals for 4 hours. Unpulsed cells were used as a negative control. After folic acid pulse, the folic acid chemotaxis of control cells and pulsed cells was examined by micropipette needle assay. The folic acid pulsed cells exhibited robust folic acid chemotaxis, whereas the control cells exhibited little response.

Reverse-transcription PCR (RT-PCR)

Total RNA was prepared from pulsed cells or control cells using the TRIzol reagent (Invitrogen). Total RNA extracts were treated with amplification grade DNase I (Invitrogen) to remove contaminating DNA. 1 μg of total DNase I-treated RNA was reverse-transcribed into first strand cDNA using the SuperScript III First-Strand Synthesis System (Invitrogen). PCR for specific GPCR genes was performed using the synthesized first strand cDNA as templates. The primers used for RT-PCR were listed in Table 1.

Generation of mutants

All mutants were generated in the wild-type AX2 background using the vector pLPBLP (Faix et al., 2004). The 5' homologous region and the 3' homologous region for each gene were amplified from the genomic DNA and directionally cloned into the vector pLPBLP. Primers used to amplify these regions for each GPCR gene were listed in Table 2. The resulting construct was linearized by NotI and 2 μg linear DNA was electroporated into 5×10^6 cells. Cells were then selected with 10 μg/ml Blasticidin S for 10 days. The clones were isolated, diluted and then clonally spread on a *Klebsiella aerogenes* lawn for

5 days. The size of plaques was measured and successful gene disruption in plaques was confirmed by PCR of genomic DNA using one primer inside the Bsr cassette and one primer outside the homologous region on the genome (Charette and Cosson, 2004). At least 2 different clones were isolated and phenotypes were confirmed.

Chemotaxis micropipette assay

Different GPCR mutants were cultured with *K. aerogenes* bacteria overnight. Cells were collected and washed with developmental buffer (DB：5 mM Na_2HPO_4, 5 mM KH_2PO_4, 0.2 mM $CaCl_2$, 2 mM $MgSO_4$，pH 6.5) to remove residual bacteria. Cells were then spread on a one-well Lab-Tek chamber containing 2ml DB. A micropipette (Femtotips, eppendorf) filled with 10μM folic acid was positioned proximately to the bottom surface. Chemotaxis of the cells was filmed at 15-second intervals and 120 frames were taken at 40× (1.35 NA) objective on a Zeiss inverted microscope.

Table 1. Primers used for RT-PCR in chapter II (GPCR gene disruptions with known unaffected folic acid chemotactic capacity were not studied.)

Family	Name	Primers	PCR product
CAR/CRL	*crlG*	F:5'-AATAGCAACACATATCCAAAC R:5'-ATATAACTACCACTACCACC	432 bp
	crlE	F:5'-GAACGTTCAACAATTATTTGC R:5'-ACACTTGTTGTTGTTGTCTC	383 bp
	crlC	R: 5'- GCAACCTCACACCATCCATCAG F: 5'- TCAATTACAATTGGCAATGG	490 bp
	crlD	F:5'-GGACATTAGCAATCTCTATG R:5'-TAATGATGATGAAGAACATGC	431 bp
	crlF	F:5'-TATACCACAATTCAGTGACG R:5'-TTGTGAAATACAATGGCACC	401 bp
	RpkA	F:5'-ATGCATTTGATTCTTCTCATG R:5'-TCGTAATTCTTGAACAGTATC	451 bp

Table 1, continued

	cAR1	F:5'-TTTGCATGTTGGTTGTGGAC R:5'-GATACACTCAAATAGGTGTG	473 bp
Frizzled/ smoothened	*fslP*	F:5'-CAATTTGGTGCGATTACTTC R:5'-AATACATTCTGCCCAAACTG	471 bp
	fslQ	F:5'-GTCACCAATGATTGCATATG R:5'-TTCACATTGTGATGGATCAC	469 bp
	fscA	F:5'-GTAACTGGTTTAGCTTGTTG R:5'-AATCTAATGAAGCACCATCC	514 bp
	fscB	F:5'-GGTAGATTTGCAAGACAATC R:5'-AACAAATACCTAATGGTGCC	307 bp
	fscC	F:5'-TATGCAAGGCAATCAGATAC R:5'-GTAGGTAGGTTGATTTGCTG	486 bp
	fscD	F:5'-TGTACTTCACCATGTCCAAG R:5'-CAAATCCATTAACCAACAGC	531 bp
	fscE	F:5'-TGTGTTCAACCATGTCCATC R:5'-GCATCAATGTAACCATACTG	503 bp
	fscF	F:5'-CAATGTGTTCAGATATGTGG R:5'-ATACATTGCAGAACCTAACC	332 bp
	fscG	F:5'-TTAGGTTGTTGGTTAGGTTC R:5'-TTTGCTACTGACATTCTTGG	341 bp
	fscH	F:5'-GGATGTCCATCAGAAACAAG R:5'-GGACAAGTATATGAATCTGG	581 bp
	fscJ	F:5'-TGGTTAGGTTCTGTTATGTG R:5'-CATCCAACTTGTTCTGCAAG	449 bp
	fslA	F:5'-CATGATTCAAGATGTGTTGC R:5'-TGAACCTGTTGTTTGAACAC	528 bp
	fslB	F:5'-ACTGGTTCATTAGCATGTTG R:5'-ATCACGTGCATTTTGAGATG	432 bp
	fslC	F:5'-TCAATCTGATGTTGCATGTG R:5'-ACCACCAACTAACAATACAC	418 bp
	fslD	F:5'-TGTGTTCTTTGGTCAATGAC R:5'-GATGCTGAAACTGTAACTAC	365 bp
	fslE	F:5'-GAATGTTGGGTTAGAGAAAG R:5'-TATCTCTTGCAACTCTTGAG	424 bp
	fslF	F:5'-TGTGTGTTATGGTCAATGAC R:5'-GTTGTGAAGCATTCTTCTTG	485 bp
	fslG	F:5'-GTTGGATTAGAGATAGATGG R:5'-TTCATACCAGGAATCTCTTG	434 bp
	fslH	F:5'-ACATTGGTTCCATTAGGTAC R:5'-TAGGGAATTGCTGAATCTTC	380 bp
	fslJ	F:5'-AATACAACTTGTGTAGTGGG R:5'-TTGACACAATTGGTGGTATC	469 bp

Table 1, continued

	fslK	F:5'-GTAGTTTGGATTGAATCTGG R:5'-AATGCAATGCAATACACTCC	386 bp
	fslL	F:5'-TTGTGTAGTACCAAATCCAG R:5'-TTGCAATACCTAAGGGTATC	563 bp
	fslM	F:5'-TCCACTTTACACCAATGAAC R:5'-TAATGGTCCAAAGAAGAGTG	532 bp
	fslN	F:5'-TAGATGTTCATCACAACCTG R:5'-CTTGGACATTGATCATTTCC	579 bp
	fslO	F:5'-TATGCAGTTCAAGAAGCTAG R:5'-GTTGCAACATAAGATGGAAC	362 bp
$GABA_B$ receptor-like	*grlB*	F:5'-ATCCAATGTACATTGACCTC R:5'-AACTCTTGCTCTACAAGTTC	374 bp
	grlC	F:5'-CAATGTTACAGGTATCACTC R:5'-CCAAGTGTAACTAACCAAAG	363 bp
	grlD	F:5'-GGTAATGATGGGTTTAGTAG R:5'-CAATGTTGATGCACCAGAAC	442 bp
	grlF	F:5'-CCATCATATGGTGATTCAAC R:5'-ATACCAGTTCTAGATTCAGC	464 bp
	grlG	F:5'-AACTCCAAGAGCTATTCATC R:5'-CTTCCATTGCATACATGATC	411 bp
	grlH	F:5'-GTGTTAGCACTGATACAATC R:5'-CATGAATGAGTACTCATTGG	463 bp
	grlK	F:5'-CAACCAAACACAACAAACTG R:5'-TCACAACCAAACTACCAATC	382 bp
	grlL	F:5'-CTATGAAGCTGCAACTATGG R:5'-TGATGCCATCCAAATCTTTG	517 bp
	grlM	F:5'-TACCAAAGATCTTCTCATCC R:5'-GAACGAATTGATGGTGTATC	342 bp
	grlO	F:5'-CTTGTCAAGGTAGAGTTTGG R:5'-GATGATGATGATGAAGATGG	475 bp
	grlP	F:5'-TCAACAACAACAACGACAAG R:5'-GATTGAGAAGATGGAGATAG	498 bp
	grlQ	F:5'-TATCATTCAACACCTGGAAC R:5'-CCTTCACCTATATCATCTTC	419 bp
	grlR	F:5'-ATTGTCAAGAAGGTCAAGAC R:5'-ATCGTGTAACTCTTCAACAC	389 bp
Secretin	*lrlA*	F:5'-GAGATATCATTCAGGTCATC R:5'-CCATGAACTTCCAATTGATAC	447 bp

Table 2. Primers used for gene knockout in chapter II. Nucleotides labeled in red indicate restriction sites.

Primer name	Primer sequence (5'-3')
grlB5-F-KpnI	GGGGTACCAAGTGGTGACTTTTCAGATC
grlB5-R-SalI	GCGTCGACTCCGAGGTCAATGTACATTG
grlB3-F-PstI	AACTGCAGGAAGGAACTTGTAGAGCAAG
grlB3-R-BamHI	CGGGATCCCATCTTCAGTATCACTACTG
grlD5-F-SalI	GCGTCGACTGTTCAAGTCAAGATCATGC
grlD5-R-HindIII	CCCAAGCTTGGGATAATCTTGGTGTTCTC
grlD3-F-PstI	AACTGCAGGGTAATGATGGGTTTAGTAG
grlD3-R-SpeI	GAACATATCACTAGTTCCAC
fslA5-F-SalI	GCGTCGACAGACCATGTAGAGAATCATG
fslA5-R-HindIII	CCCAAGCTTGCAACACATCTTGAATCATG
fslA3-F-PstI	AACTGCAGGTTGGATTATGAGTAATTCAG
fslA3-R-SpeI	GGACTAGTAAATCATCATCATCACCACC
fslH5-F-SalI	GCGTCGACATGTGTGCAATGATGTTTCC
fslH5-R-HindIII	CCCAAGCTTTACACCTGAAACTGACATTC
fslH3-F-PstI	AACTGCAGGATAGAGTATGTGTTGCATC
fslH3-R-SpeI	GGACTAGTTAGGGAATTGCTGAATCTTC
fslB5-F-KpnI	GGGGTACCATATGGAGCAGGATTAGTTG
fslB5-R-HindIII	CCCAAGCTTTTGATGCCATTTCTTCTCTG
fslB3-F-PstI	AACTGCAGGCAGTTCAATCAGATGTTTC
fslB3-R-NotI	TTGCGGCCGCTGAAGTTGGATTTGTACCAC
fslK-F-KpnI	GGGGTACCGTATAGAATGCACATGACTG
fslK-R-HindIII	CCCAAGCTTGTTGTGCTTCTGTATATGTG
fslK-F-BamHI	CGGGATCCAAGAGTTTGTTTGGATACTTG
fslK-R-SpeI	GGACTAGTCCAGATTCAATCCAAACTAC

RESULTS

The cAMP receptor cAR1 expression level increases rapidly after the onset of cAMP chemotaxis, indicating that the expression level of cAR1 has significant positive correlation with cAMP stimulation. Axenic cells restore folic acid chemotactic ability by feeding on bacteria or by being merely stimulated with folic acid pulses. It was therefore hypothesized that the ability to sense a folic acid gradient would be coordinated with elevated levels of folic acid receptor. To avoid undesired expression changes during phagocytosis and potential effects of other chemo-attractants released by bacteria, axenic cells from HL5 medium were pulsed periodically with 10 μM folic acid at 6-minute intervals for 4 hours. RT-PCR was performed to examine transcriptional changes of 46 putative GPCRs. GPCRs that exhibited significant mRNA expression level changes upon folic acid stimulation are shown in Fig. 3A. Several genes were up-regulated when pulsed with folic acid, especially *fslH*, *grlB*, and *grlD*. *grlB* was previously shown to be up-regulated when cells grow on bacteria (Sillo et al., 2008). Most of these receptor expression levels decreased after 4 hours of starvation (Fig. 3A). Interestingly, the cAMP receptor cAR1 also shows slight up-regulation when cells were pulsed with folic acid. During the pulse of folic acid, we speculated that phosphatidylinositol-3,4,5-triphosphate [PI(3,4,5)P3] generated by phosphatidylinositol-3 kinases (PI3Ks) accumulated periodically and in turn activated downstream adenylyl cyclase (ACA). Therefore, cAMP was secreted periodically to generate a cAMP stimulation and induce cAMP signaling. Interestingly, cells exhibited weak chemotaxis toward cAMP after pulsing with folic acid (data not shown). Since the folic acid receptor is coupled to the Gα4 subunit, we used *ga4* null cells (Hadwiger et al., 1994) as a control background to perform RT-PCR for these

genes (Fig. 3B). Also, to avoid the effect of cAMP signaling, *aca* null cells (Pitt et al., 1992) were used. The receptors didn't show detectable changes when Gα4 was absent, while *fslA*, *fslH* and *grlD* were up-regulated when ACA was absent, suggesting these receptors might be involved in folic acid signaling but not cAMP signaling (Fig. 3B).

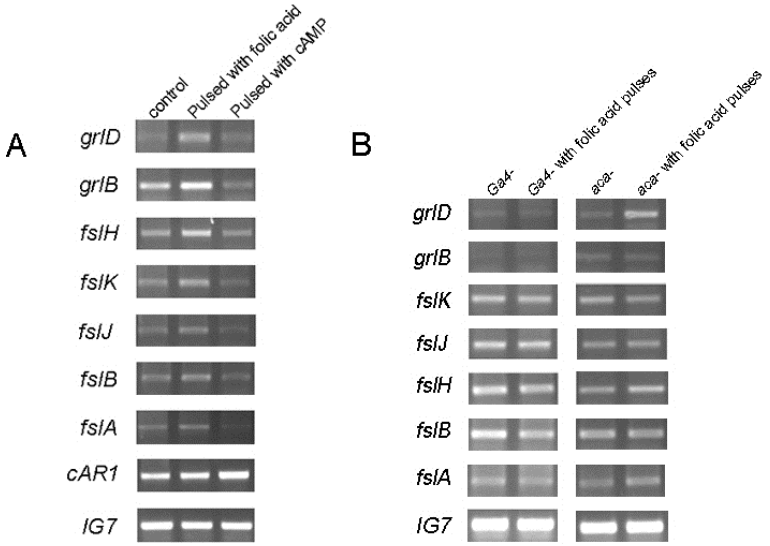

Figure 3. Transcriptional changes of several candidate genes upon folic acid stimulation. (A) mRNA level changes in the absence of chemo-attractant and with folic acid or cAMP. Axenic wild-type Ax2 cells were pulsed with 10μM folic acid in HL5 for 4 hours. Un-pulsed axenic cells were used as control. For cAMP pulses, axenic cells were pulsed with 10μM cAMP in DB for 4 hours. (B) mRNA level changes of these genes in *ga4* and *aca* nulls after folic acid pulses.

Null mutants for *fslA*, *fslB*, *fslK*, *fslH*, *grlB* and *grlD* were then generated by homologous recombination. For each mutant, a chemotaxis micropipette assay was applied using folic acid as the chemo-attractant. Unfortunately, none of these null mutants showed folic acid chemotactic defects, suggesting the folic acid receptor might be redundant or other GPCRs might acts as folic acid receptors. The *grlB* null mutant is

shown as an example in Fig. 4. These mutants showed normal size plaques on SM agar plates with bacteria after 5 days incubation, while mutants with impaired folic acid chemotactic ability such as *gα4* null mutant and *gβ* null mutant showed significantly smaller plaques (van Es et al., 2001), again suggesting that these GPCRs are not or not sole folic acid receptors.

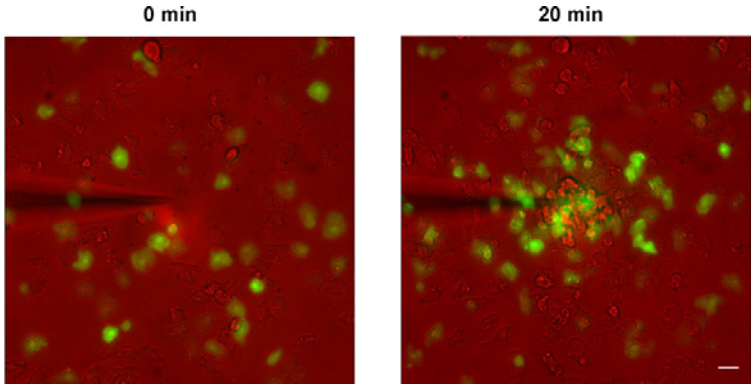

Figure 4. Folic acid chemotaxis assay for *grlB* null mutant. Equal amounts of Ax2 and PH-GFP labeled *grlB* null cells were mixed and cultured with bacteria overnight. Then cells were washed twice with DB and plated on a one-well glass chamber in DB. The needle was filled with 10μM folic acid. Bar, 10μm.

The developmental processes for each mutant were also examined. Only *grlB* null mutants showed a developmental defect. These mutants were delayed by 2 hours during aggregation (Fig. 5), suggesting GrlB is involved in early development.

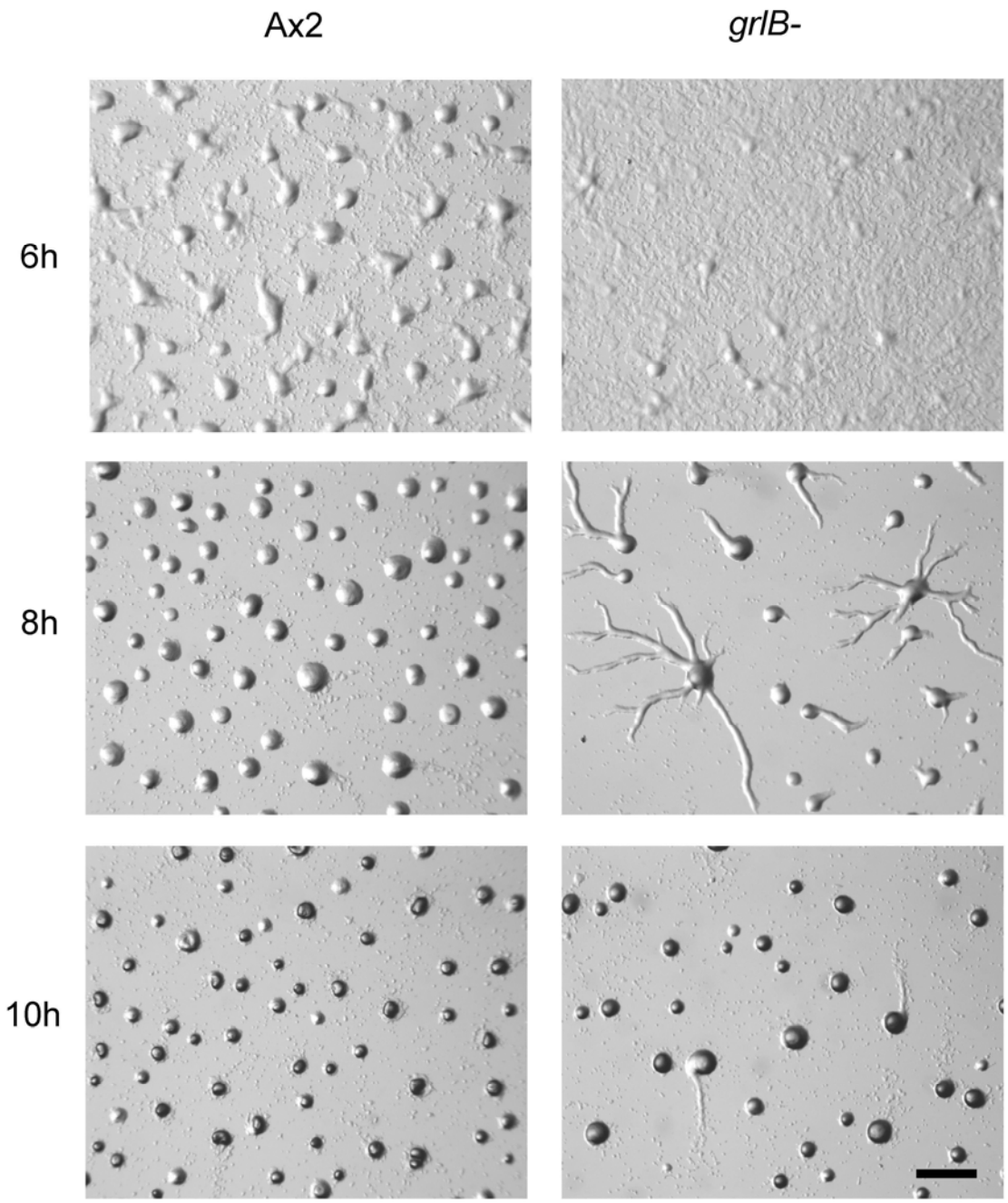

Figure 5. Development of Ax2 and *grlB* mutants on DB agar. 5×10^6 cells were washed twice with DB and plated on a non-nutrient DB agar plate. Bar, 1mm.

DISCUSSION

Though the attempt to isolate folic acid receptors failed, several possibilities could explain the result. The cAMP receptor cAR1 shows both transcriptional and protein level up-regulation during cAMP chemotaxis, however, the activation of the folic acid receptor may be translationally controlled. If this is true, no significant transcriptional change of the folic acid receptor should be observed. Another possibility is that the activation of the folic acid receptor requires a co-factor or a chaperone, and both transcriptional and protein levels of the folic acid receptor remain unchanged during folic acid chemotaxis. The folic acid receptor remains inactive in axenic cells, and folic acid stimulation activates a co-factor or a chaperone which in turn activates the dormant folic acid receptor.

Second, the folic acid receptor may be redundant. The ability to sense bacteria is vital for the survival of the amoeba in nature, therefore the complexity of the folic acid receptor are likely evolved to ensure efficient predation. A similar case is the cAMP receptor family. 4 cAMP receptors (cAR1-4) have been discovered with different cAMP affinity, and cAR1 and cAR3 play major roles during cAMP chemotaxis in early development (Johnson et al., 1993; Klein et al., 1988; Saxe et al., 1991). The possible existence of redundancy and too many GPCR candidates make it difficult to generate a mutant lacking the folic acid response.

Third, the GPCR candidate pool I used may not cover all putative GPCRs in the genome. When I was studying all putative GPCRs, the number of total GPCRs was 55 (Eichinger et al., 2005). A year later, the number was updated to 61 (Heidel et al., 2011). Besides, TMHMM program predicting trans-membrane helices revealed more than 100

proteins in the *Dictyostelium* genome with 6-8 trans-membrane helices (the serpentine receptor cAR1 is only predicted to have six trans-membrane domains in this program). The unexpected number of putative GPCRs in this simple eukaryote greatly increases the difficulty of "finding a needle in the haystack".

CHAPTER III

SYSTEMATIC ANALYSIS OF GAMMA-AMINOBUTYRIC ACID (GABA) METABOLISM AND FUNCTION

ABSTRACT

In the previous chapter, GrlB was shown to regulate early development. Since the disruption of GrlB reduced GABA affinity, and my preliminary work suggested the first role of GABA in early development, I investigated the homeostasis of GABA metabolism by disrupting genes related to GABA metabolism and signaling. Extracellular levels of GABA are tightly regulated during early development, and GABA is generated by the glutamate decarboxylase, GadB, during growth and in early development. However, overexpression of the prespore-specific homologue, GadA, in the presence of GadB reduces production of extracellular GABA. Perturbation of extracellular GABA levels delays the process of aggregation. Cytosolic GABA is degraded by the GABA transaminase, GabT, in the mitochondria. Disruption of a putative vesicular GABA transporter (vGAT) homologue DdvGAT reduces secreted GABA. I identified the $GABA_B$ receptor-like family member GrlB as the major GABA receptor during early development, and either disruption or overexpression of GrlB delays aggregation. This delay is likely the result of an abolished pre-starvation response and late expression of several "early" developmental genes. Distinct genes are employed for GABA generation during sporulation. During sporulation, GadA alone is required for generating GABA and DdvGAT is likely responsible for GABA secretion. GrlE but not GrlB is the GABA receptor during late development. The work in this chapter has been published (Wu and Janetopoulos, 2013b).

INTRODUCTION

GABA is an amino acid molecule that exists in most, if not all, prokaryotes and eukaryotes (Jakoby and Fredericks, 1959; Roberts et al., 1953; Roberts and Frankel, 1950; Steward et al., 1949). It is synthesized primarily from glutamate catalyzed by cytosolic glutamic acid decarboxylase (GAD). Cytosolic GABA is transported by membrane-bound transporters into the extracellular environment and to different organelles and plays various roles. GABA is first metabolically catabolized by the mitochondrial GABA transaminase (GABA-T) into succinic-semialdehyde (SSA), and then into succinate by succinic semialdehyde dehydrogenase (SSADH), which ultimately allows the GABA carbon skeleton to enter the tricarboxylic-acid (TCA) cycle. This pathway mainly composed of these three enzymes (GAD, GABA-T, SSADH) bypasses two steps of the TCA cycle and is called the GABA shunt (Shelp et al., 2012).

The presence of GABA is ubiquitous and multiple functions have evolved. In plants, GABA is rapidly accumulated in response to a variety of biotic and abiotic stresses, including bacterial invasion, insect herbivorous behavior, and oxidative stress and osmotic shock. The GABA shunt also contributes to nitrogen metabolism and carbon:nitrogen balance, demonstrating its importance as a metabolite in many physiological processes (Bouche and Fromm, 2004). GABA can also function as a signaling molecule in pollen tube growth and guidance (Palanivelu et al., 2003). In invertebrates and vertebrates, GABA acts as a potent inhibitory neurotransmitter. GABA achieves postsynaptic inhibition by hyperpolarizing the cell through ionotropic and G protein-coupled metabotropic receptors in the adult brain (Kleppner and Tobin, 2002). However, opposite effects of GABA have been reported during nervous system

development (Owens and Kriegstein, 2002). Misregulation of GABA has been linked to several neuronal diseases, including epilepsy (Meldrum, 1989) and Huntington's disease (Reddy et al., 1999).

The social amoeba *Dictyostelium discoideum* preys on bacteria during the solitary vegetative stage, whereas thousands of cells aggregate to form multicellular structures when food sources are depleted (Kessin, 2001). This organism also produces GABA in both vegetative and developmental stages (Ehrenman et al., 2004). Two genes encoding GAD, *gadA* and *gadB*, have been identified in the *D. discoideum* genome (Iranfar et al., 2003). These two proteins share high protein sequence identity (73%) but display distinct temporal expression patterns, suggesting they function non-redundantly in growth and development. Microarray analysis showed that *gadA* mRNA expression dramatically increases at 10 hours after development and peaks at 18 hours during the culmination stage (Iranfar et al., 2001), whereas *gadB* mRNA is expressed in vegetative cells and diminishes after the onset of starvation (Iranfar et al., 2003). Only one GABA transaminase gene, *gabT*, has been identified in the *D. discoideum* genome (Anjard et al., 2009). No *D. discoideum* ionotropic GABA receptor homologue was found. Strikingly, 17 genes (*grlA-H*, *grlJ-R*) encoding homologues of $GABA_B$ metabotropic receptors have been reported (Eichinger et al., 2005; Heidel et al., 2011; Prabhu and Eichinger, 2006). Among them, only GrlE shares a well conserved N-terminal ligand binding domain (Taniura et al., 2006), and this has been proven to be the bona fide GABA receptor (Anjard and Loomis, 2006).

The role of GABA has been clearly defined as a signaling cue in sporulation in *D. discoideum*. Disruption of GadA, which theoretically abolishes GABA synthesis in

prespore cells, prevents the GABA triggered release of the precursor of spore differentiation factor-2 (SDF-2) and thus results in decreased viable spores (Anjard and Loomis, 2006). Consistent with this finding, disruption of GrlE, the GABA receptor at this stage, phenocopies the *gadA*- mutant (Anjard and Loomis, 2006). In addition, either disruption of *gabT* or direct addition of the irreversible GABA transaminase inhibitor vigabatrin promotes SDF-2 production and induces spore maturation (Anjard et al., 2009). *grlE*- cells also exhibit rapid growth in suspension and a delay in early development (Taniura et al., 2006), however, the mechanism remains unknown. The functions of several other members of the $GABA_B$ receptor-like family which are induced in sporulation have also been explored. Disruption of GrlA shows a delay in late development and GrlA possibly acts as the SDF-3 receptor (Anjard et al., 2009; Prabhu et al., 2007a), while loss of GrlJ shows precocious development and malformed spores (Prabhu et al., 2007b).

Although the role of GABA in late development has been studied, the role of GABA in other developmental stages remains obscure. In addition, there is very little fundamental data on the homeostasis of GABA. In this chapter, I identified a $GABA_B$ receptor-like family member GrlB as a GABA receptor during early development and further characterized the synthesis, degradation and signaling of GABA in *D. discoideum*.

MATERIALS AND METHODS

Materials

γ-aminobutyric acid (GABA), GTPγS, and vigabatrin were purchased from Sigma (St. Louis, MO), $GABA_B$ receptor antagonist CGP55845 from Tocris (Ellisville, MO), Mitotracker Red CMXRos from Invitrogen (Eugene, OR) and 2,3-^{3}H(N)-GABA from American Radiolabelled Chemical (St. Louis, MO). The pLPBLP vector, the plasmid pDEX-NLS-Cre and a series of the *actin15* promoter driven pDM expressing vectors were provided by dictyBase (*http://dictybase.org/*). Mouse anti-CsA antibody (33-294-17) and mouse anti-Discoidin I (80-52-13) monoclonal antibodies were obtained from the Developmental Studies Hybridoma Bank at the University of Iowa. Mouse anti-actin monoclonal antibody (MAB1501R) was purchased from Millipore.

Cell culture and development

For axenic growth in HL5 medium at 22°C, all cell strains were either cultured in petri dishes or shaken in suspension at 175 rpm. For development, vegetative cells were washed twice with developmental buffer (DB：5 mM Na_2HPO_4, 5 mM KH_2PO_4, 0.2 mM $CaCl_2$, 2 mM $MgSO_4$，pH 6.5) and spread on 30 mm non-nutrient DB agarose (15 mg/ml) plates at a density of 5×10^5 cells/cm^2.

Generation of mutants and overexpression strains

All mutants were generated in the wild-type AX2 background. *gadA*- cells were generated by homologous recombination using the vector pLPBLP (Faix et al., 2004).

The 514 bp 5' homologous region and the 1071 bp 3' homologous region were amplified from genomic DNA and directionally cloned into the vector pLPBLP. The resulting construct was linearized by NotI and 2 μg linear DNA was electroporated into 5×10^6 cells. Cells were then selected with 10 μg/ml Blasticidin S for 10 days, and successful gene disruption in transformants was confirmed by PCR of genomic DNA using one primer inside the Bsr cassette and one primer outside the homologous region on the genome (Charette and Cosson, 2004). At least 2 different clones were isolated and phenotypes were confirmed.

The same strategy was used to disrupt *gadB*, *DdvGAT* (dictyBase ID: DDB_G0293074), *grlB*, and *grlE* respectively. The strategy used for disrupting *gabT* was similar as described (Anjard et al., 2009). The primers used are listed in Table 3. To generate *gadA-/gadB-* cells, the nuclear localized Cre protein from the plasmid pDEX-NLS-cre (Faix et al., 2004) was transiently expressed in *gadA-* cells to remove the Bsr cassette, and then *gadB* was subsequently disrupted. For *grlB-/grlE-* cells, *grlB-* cells were treated with Cre and *grlE* was subsequently disrupted.

gadA cDNA was amplified from cDNA prepared from AX2 cells starved for 14 hours. *gadB* genomic DNA was amplified from genomic DNA. *gabT, DdvGAT,* and *grlB* cDNA was amplified from cDNA prepared from vegetative cells. These genes were cloned into the expressing vector pDM304 and C-terminal GFP tagged vector pDM323 or N-terminal GFP tagged vector pDM317. The primers used are also listed in Table 3. These expression plasmids were transformed into 5×10^6 cells, and cells were selected with 20 μg/ml G418.

Table 3. Primers used in chapter III. Nucleotides labeled in red indicate restriction sites.

Primer name	Primer sequence (5'-3')
gadA5-F-KpnI	GGGGTACCGGTAATGCAAAACAAAACTTGG
gadA5-R-HindIII	CCCAAGCTTCTGAAATTCCTTTAACATC
gadA3-F-PstI	AACTGCAGAAGCTTGTCTAGATCATGGTATTTTC
gadA3-R-BamHI	CGGGATCCGAGTGGATGCATTCATTCAAAGTAC
gadB5-F-KpnI	GGGGTACCGGACGGTGCTGGTGGAGATGATAGTGGTGAAGATGAC
gadB5-R-HindIII	CCCAAGCTTCATATTGTAATGTAAATGTTACACCAAGAG
gadB3-F-PstI	AACTGCAGTTCATGTTGATGCAGCAAGTGGTGGATTTG
gadB3-R-BamHI	CGGGATCCCGAAGATTTAGAAACCAATAAAGATGGTAATCTCTAC
gabT-F (Anjard et al., 2009)	GTCAGATTGAAATTACCCACCCC
gabT-R (Anjard et al., 2009)	GAGGTGAGATTCCAATGTTCGTG
DdvGAT-F5-KpnI	GGGGTACCATGGCTTATAACTCAAGAAATAGTAGTAG
DdvGAT-R5-HindIII	CCCAAGCTTAAACAATCCAAATCATTGGAATGTAACC
DdvGAT-F3-PstI	AACTGCAGAAGGATAACCATGTTCATCCAC
DdvGAT-R3-BamHI	CGGGATCCCCAAGATAGTTGCCATAATACC
grlE5-F-KpnI	GGGGTACCCAGAAGTTGTTAAACCAAACCC
grlE5-R-HindIII	CCCAAGCTTGATTACGAAGTTCAGTTCTAAC
grlE3-F-BamHI	CGGGATCCTACAGGTGATAGATTGTATGG
grlE3-R-NotI	ATTTGCGGCCGCAAAGATTGGTTCAGCCAATGG
gadA-F-BglII	GAAGATCTTAAAAAATGTCACTTCATCATGTCAAAAC
gadA-R1-SpeI	GGACTAGTTTAATGATGGAATGATTGACCTTC
gadA-R2-SpeI	GGACTAGTATGATGGAATGATTGACCTTC
gadB-F-BamHI	CGGGATCCTAAAAAATGCCATTACATATTGTTGATAAAC
gadB-R1-SpeI	GGACTAGTTTAATGATGGAAATTTTCACCTTCATC
gadB-R2-SpeI	GGACTAGTATGATGGAAATTTTCACCTTCATC
gabT-F-BamHI	CGGGATCCAAACAATGTCTTCATCAAGATTAATTAAATGTTTAAGTTC
gabT-R-SpeI	GGACTAGTATTTTTATATAATTCTTTCATTGTTTGATCGAAACG
DdvGAT-F-BglII	GAAGATCTATGGCTTATAACTCAAGAAATAG
DdvGAT-R-SpeI	GGACTAGTTTAATTTGATGGATCTACAAAAGC
grlB-F-BamHI	CGGGATCCAATAAAATGAAAAATTTAATTTCAATTATTC
grlB-R1-NheI	CCGGCTAGCTTAAAGGTTATTAGAATCAATTTC
grlB-R2-NheI	CCGGCTAGCAAGGTTATTAGAATCAATTTCAAC
gadA-RT-F	GACCTTTCAGATAGAATGAG
gadA-RT-R	TGGAATGATTGACCTTCATC
gadB-RT-F	GTAAGAATTTACCCTCTGAAC
gadB-RT-R	AATCTCTAGAGAAACCATGAC
rnlA-RT-F (Nagasaki et al., 2002)	TTACATTTATTAGACCCGAAACCAAGCG
rnlA-RT-R (Nagasaki et al., 2002)	TTCCCTTTAGACCTATGGACCTTAGCG

qPCR analysis

Total RNA was prepared from axenic cells or cells starved on non-nutrient DB agarose for 4 hours using the TRIzol reagent (Invitrogen). Total RNA extracts were treated with amplification grade DNase I (Invitrogen) to remove contaminating DNA. 1 μg of total DNase I-treated RNA was reverse-transcribed into first strand cDNA using the SuperScript III First-Strand Synthesis System (Invitrogen). Quantitative PCR was performed on MyiQ Single-Color Real-Time PCR Detection System (Bio-Rad) using iQ SYBR Green Supermix (Bio-Rad) according to manufacturer's directions. All samples were prepared and run in triplicate. *rnlA* (*IG7*) was used as the reference gene, and the expression ratio was determined using the $2^{-(\Delta\Delta Ct)}$ method as described previously (Aarskog and Vedeler, 2000). The primers used are also listed in Table 3.

GABA content measurements

For extracellular GABA content, 5×10^6 cells were washed twice with DB, and then suspended in 100 μl DB. The suspension was shaken gently at 120 rpm, 22°C. At indicated time points, the suspension was centrifuged at 1,500 g for 1 minute. 40 μl supernatant was analyzed for amino acids including GABA via HPLC by the Neurochemistry Core at Vanderbilt University's Center for Molecular Neuroscience Cores. Each measurement was performed at least in triplicate.

GABA binding assays

Whole cell GABA binding assay was performed as described (Anjard and Loomis, 2006). Briefly, vegetative cells were washed three times with 10 ml MES buffer (20 mM

MES, 20 mM NaCl, 20 mM KCl, 1 mM $CaCl_2$, 1 mM $MgSO_4$, pH 6.2) and prepared at 10^7 cells/ml in ice-cold MES buffer, 500 µl cell suspension was incubated with 0.2 nM ^{3}H-GABA in the presence or absence of 200 µM CGP55845 on ice for 1 hour. Cells were then collected on GF/C glass filters (Whatman) and rinsed three times with 5 ml cold buffer before the radioactivity of bound ^{3}H-GABA was counted in a liquid scintillation counter.

For the cell lysate GABA binding assay, 5×10^7 vegetative cells were washed twice with cold MES buffer and suspended in 1 ml cold MES buffer. The cells were lysed by passing through an Acrodisc 5 µm pore size syringe filter (Pall). The identical procedure was performed for the same amount of cells in 1 ml cold MES buffer supplemented with 100 µM GTPγS. 100 µl cell lysate with or without GTPγS was incubated with 0.2 nM ^{3}H-GABA in the presence or absence of 200 µM CGP55845 on ice for 10 minutes. The crude membrane fraction was collected by centrifugation at 17,000 × g for 5 minutes at 4°C. The membrane pellet was washed three times with 1 ml MES buffer and finally dissolved in 80 µl 1% SDS solution (Snaar-Jagalska et al., 1991). The radioactivity of membrane-bound ^{3}H-GABA was then counted.

Microscopy

Images of developing cells on non-nutrient DB agarose were acquired with a Leica MZ16 stereomicroscope with a Q-Imaging Retiga 1300 camera and QCapture software. Vegetative cells were washed twice with DB and images were acquired in DB in Lab-Tek chambers (Nalge Nunc International) on a Nikon Eclipse Ti microscope with an Apo 60× objective (NA 1.49) using a Quorum WaveFX spinning disk confocal system.

Spore viability assay

1×10^7 cells were washed with KK2 buffer (16.2 mM KH_2PO_4, 4.0 mM K_2HPO_4, pH 6.1) and starved on KK2-saturated filters. After 48 hours, the filter was put in a 50 ml tube and washed repeatedly with 4 ml KK2 buffer containing 0.4% NP-40. The tube was rocked gently at 150 rpm for 10 minutes and then the filter was discarded. The density of ovoid spores was counted by a hemacytometer. 100 spores were collected and plated with *Klebsiella aerogenes* bacteria on SM plates. The number of plaques was then counted five days later.

Western blotting

5×10^6 cells were washed twice with DB and lysed with 1× NuPAGE LDS Sample Buffer (Invitrogen) and 5% (v/v) β-mercaptoethanol (Sigma) in a total volume of 50 µl. Cell lysate was incubated at 90°C for 5 minutes and 5 µl cell lysate was analyzed on 10% mini-protean TGX precast gel (Bio-Rad). After electrophoresis, proteins were transferred to a nitrocellulose membrane. The membrane was blocked with the Odyssey blocking buffer and incubated with the indicated antibodies. The rabbit anti-cAR1 antibody was pre-absorbed with 50% methanol/DB fixed cells before use. A 1:1000 dilution was used for primary antibodies and a 1:10000 dilution was used for secondary antibodies. Secondary antibodies IRDye 680LT Donkey anti-Mouse IgG (LI-COR, 926-68022) and IRDye 800CW Goat anti-Rabbit IgG (LI-COR, 926-32211) were used for 2-color detection. The nitrocellulose membrane was developed using the Odyssey Infrared Imaging System (LI-COR).

Statistical analysis

The statistical significance of differences was determined by the one-way ANOVA with Tukey's honestly significant difference using software OriginPro 8.6.0 (OriginLab Corp., Northampton, MA, USA). $P < 0.05$ was considered to be statistically significant.

RESULTS

GrlB is involved in early development

Wild-type AX2 cells usually stream at approximately 4.5 hours when plated on a non-nutrient agarose plates. At 6 hours, most wild-type cells have finished aggregation and start to form loose mounds, whereas only tiny aggregates were formed in *grlB*- cells (Fig. 6). At 8 hours, tight mounds were formed in wild-type cells but *grlB*- cells were still streaming and only a few loose mounds were formed (Fig. 6). Accordingly, *grlB*- cells exhibited a delay of about 2 hours in aggregation. Expression of full length GrlB or C-terminal GFP tagged GrlB under the control of the *act15* promoter in *grlB*- cells ameliorated the developmental postponement but could not fully rescue the delay (Fig. 6). The high expression level of GrlB in *grlB*- cells may have been responsible for the partial rescue since overexpression of GrlB in WT cells caused a more severe delay (Fig. 6). This indicates that GrlB is involved in early development. Both *grlB*- cells and GrlB overexpression cells successfully completed the life cycle without any morphological defects (data not shown).

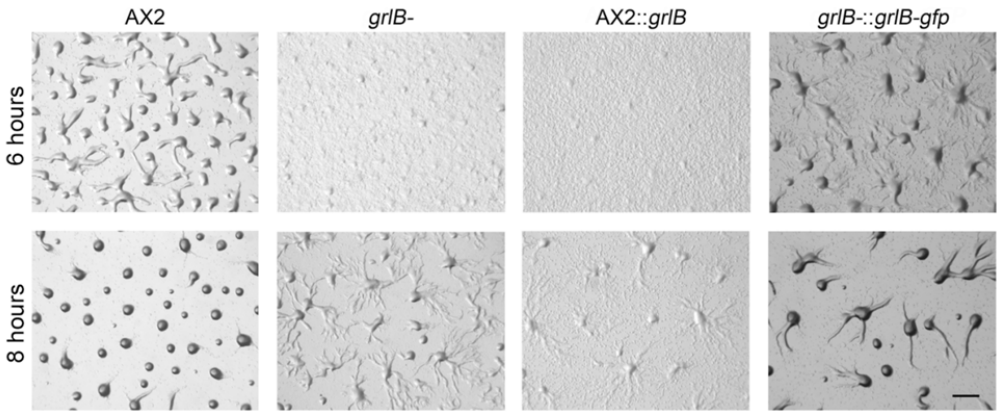

Figure 6. Early developmental phenotypes of *grlB* mutants. 5×10^6 vegetative cells were washed with DB twice and plated on non-nutrient DB agarose plates. Images were taken at indicated hours after development. *AX2::grlB*, *grlB* was over-expressed in wild-type AX2 cells; *grlB-::grlB-gfp*, *grlB-gfp* fusion was over-expressed in *grlB-* cells. Bar, 1 mm.

GABA is generated by GadB during growth and early development

GABA acts as the natural agonist for $GABA_B$ receptors, and glutamate has also been shown to bind to the $GABA_B$ receptor GrlE in the social amoeba (Anjard and Loomis, 2006). Therefore the effect of GABA and glutamate on early development was examined. Unexpectedly, direct addition of up to 1 mM GABA or glutamate to the agarose substrate barely affected aggregation (Fig. 7A), with the same results observed when cells were developed on buffer-saturated filters (data not shown). This is consistent with a previous study that reported that the presence of 1 mM GABA or glutamate had no effect on the cAMP chemotactic response (Taniura et al., 2006). I also tested the ability of cells to migrate directionally toward a wide range of GABA gradients (1 nM to 10 mM) using a micropipette assay. Vegetative cells or cells starved for 1-6 hours did not chemotax toward GABA at any of these concentration gradients, suggesting GABA is probably not a chemo-attractant (data not shown).

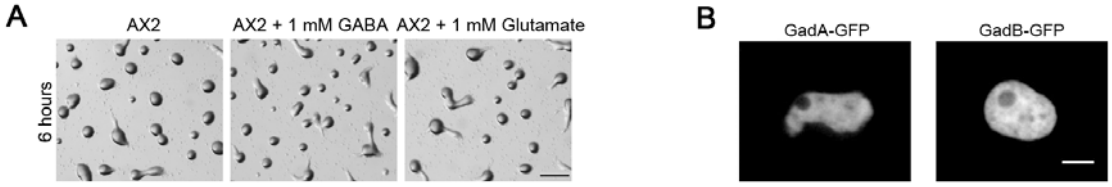

Figure 7**.** Effect of exogenous GABA on early development. (A) Development of wild-type AX2 cells with the addition of 1 mM GABA or 1 mM glutamate on DB agarose plates at 6 hours. 5×10^6 vegetative cells were developed on agarose plates. Bar, 1 mm. (B) C-terminal GFP tagged GadA and GadB were expressed in WT cells. Cells were plated in a one-well glass chamber filled with DB, and images were taken at a 60× objective on a confocal microscope. Bar, 5 μm.

I next tested whether perturbation of GABA synthesis by manipulating GAD expression would affect extracellular GABA concentration and early development. Both C-terminal GFP tagged GadA and GadB were found localized in the cytosol (Fig. 7B). To determine the extracellular GABA concentration, the secretion of GABA during development was measured. Supernatants were measured every 2 hours after starvation in control cells and in various *gad* mutants (Fig. 8). Wild-type cells expressing GFP were used as controls. The extracellular GABA concentration reached a plateau between 2-4 hours, suggesting that GABA synthesis, degradation, and uptake reached equilibrium by this time. The GABA concentration at 4 hours was used as a representative time point and analyzed. Consistent with its expression pattern, disruption of *gadB* mostly eliminated extracellular GABA with merely 2 μM remaining, and overexpression of *gadB-gfp* in WT cells showed a substantially elevated level of 60 μM extracellular GABA, as compared to a 35 μM extracellular concentration of GABA in control cells. Overexpression of *gadB-gfp* in *gadA-*/*gadB-* cells also showed a similar extracellular

GABA level when compared to *gadB-gfp* overexpression in WT cells, suggesting GadB is the main functioning glutamate decarboxylase during this period. Disruption of *gadA* showed statistically indistinguishable extracellular GABA levels as compared to control cells, which correlated with previous results that *gadA* is transcribed at basal levels during growth and early development (Iranfar et al., 2001). Interestingly, overexpression of untagged or tagged *gadA* in WT cells significantly decreased extracellular GABA level to 16 µM, and overexpression of *gadA-gfp* in *gadA-*/*gadB-* cells exhibited an even lower extracellular GABA level of 8 µM.

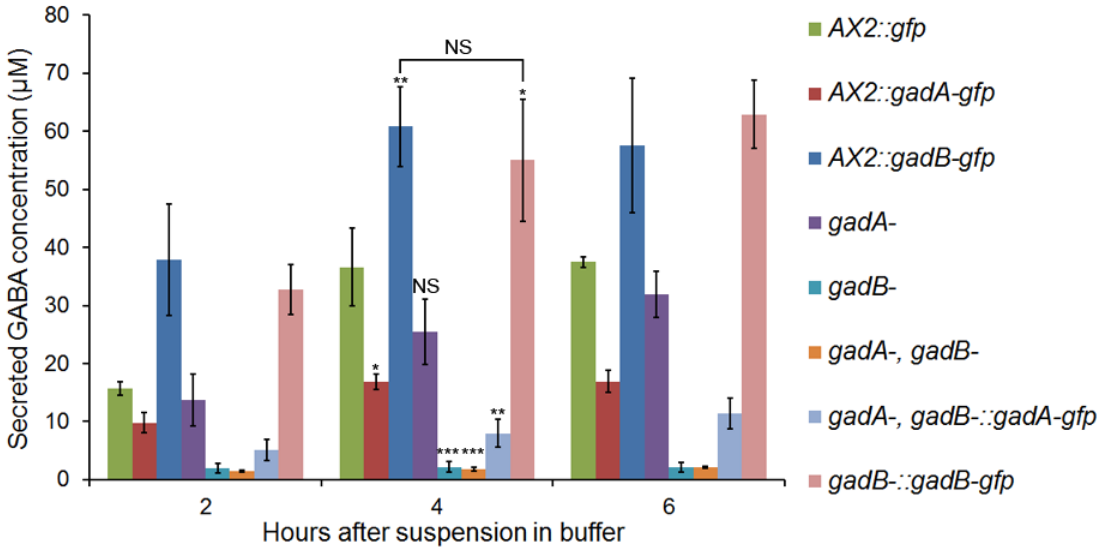

Figure 8. GABA synthesis and secretion in wild-type and mutant *D. discoideum* strains during early development. 5×10^6 vegetative cells were washed twice with DB, suspended and shaken in 100 µl DB. At indicated time points after starvation, suspensions were centrifuged. 40 µl supernatant was analyzed for amino acid content via HPLC. GABA concentrations from different genotypes at 4 hours were compared to the GABA concentration of wild type *AX2:gfp* cells. Values are means ± s.d.. NS, non-significant; *, $p<0.05$; **, $p<0.01$; ***, $p<0.001$. One-way ANOVA was used.

Secreted factors usually accumulate during growth in suspension culture. Several secreted chalones, which accumulate according to cell density, inhibit growth and promote development, have already been identified (Gomer et al., 2011). We speculated that GABA might also be accumulating during growth based on the secretion data during cell starvation. We measured GABA secretion as wild-type cells grew from a very low density of 1×10^4 cells/ml to a stationary stage in HL5 medium. The HL5 medium contained an average concentration of 20 μM GABA (Day 0 at Fig. 9). The GABA concentration in HL5 medium was tightly regulated and remained near 20 μM during all stages of growth (Fig. 9), though we had expected that the higher densities of cells would result in significant increases of extracellular GABA concentration.

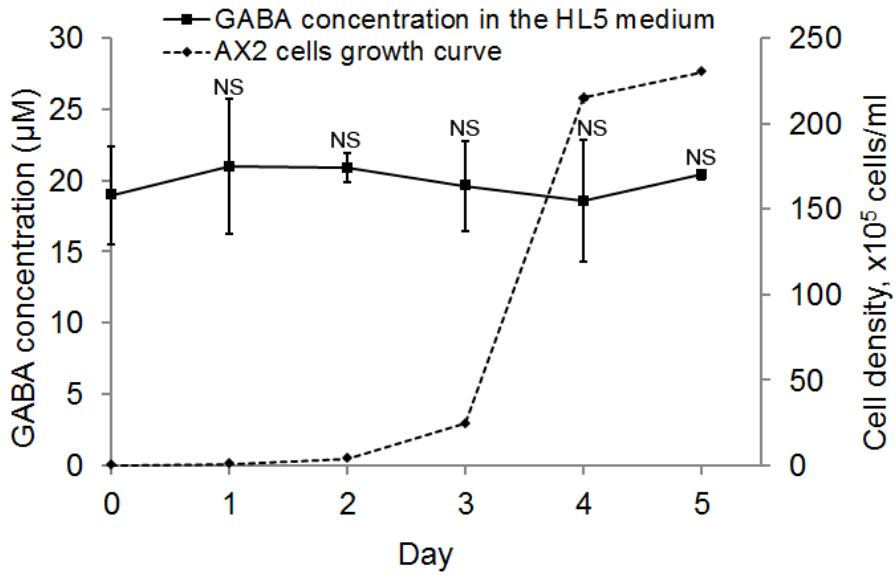

Figure 9. GABA secretion during axenic growth. WT cultures with an initial density of 1×10^4 cells/ml were shaken in HL5 medium at 175 rpm, 22°C. At indicated cell density, amino acids content in the medium was measured via HPLC and compared to values of HL5 medium. Values are means ± s.d.. NS, non-significant. One-way ANOVA was used.

Overexpression of the prespore-specific *gadA* in WT cells may compensate for the production of GABA by GadB and therefore suppress the expression of *gadB*, which leads to lower concentration of extracellular GABA. To validate this possibility, I performed qPCR to determine *gadB* mRNA expression changes when *gadA* was overexpressed (Fig. 10A). *gadB* mRNA levels were not significantly altered when *gadA* was overexpressed at either the vegetative stage or during early development, suggesting overexpression of *gadA* does not induce or suppress expression of *gadB*. Due to the extremely low expression of *gadA* at vegetative and early development stages, the overexpression of *gadA* up-regulated *gadA* mRNA level more than 2×10^4 fold (Fig. 10B). Although *gadA* was also strongly induced when overexpressed in *gadA*-/*gadB*- cells, it produced only a low level of extracellular GABA (Fig. 8). These results indicate that *gadA* and *gadB* are non-redundant.

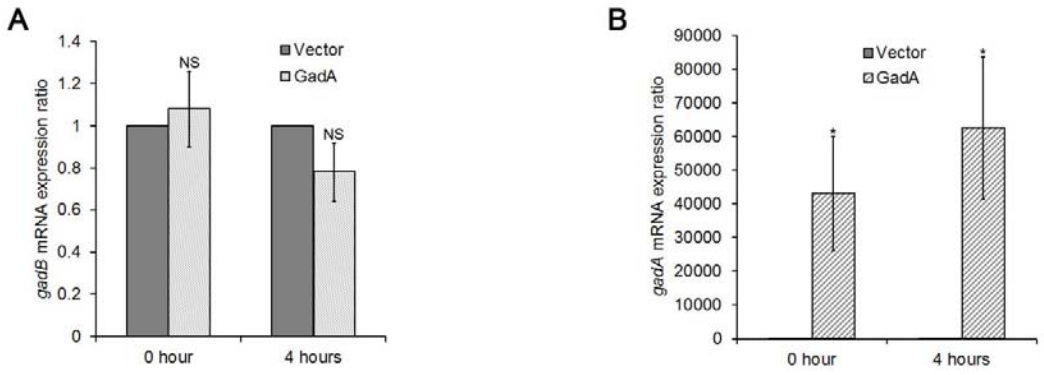

Figure 10. Transcriptional changes of *gadA* and *gadB* in different mutants. (A) qPCR analysis showing *gadB* mRNA expression change when *gadA* was overexpressed. cDNA of WT cells expressing an empty vector or *gadA* was prepared at vegetative stage (0 hours) or early development (4 hours after starvation on DB agarose). *rnlA* was used as the housekeeping gene. *gadB* transcript level in WT cells expressing *gadA* was compared to *gadB* expression level in WT cells expressing an empty vector, and *gadB* level in WT cells expressing am empty vector was normalized to 1. Ratios are means ± s.d., NS, non-significant. One-way ANOVA was used. (B) qPCR analysis showing *gadA* mRNA expression change when *gadA* was overexpressed. Same cDNA was used as in (A). Ratios are means ± s.d., *, $p<0.05$. One-way ANOVA was used.

The phenotypes of mutants with different levels of extracellular GABA during early development were then examined. *gadA*- cells aggregated normally, while disruption of *gadB* delayed aggregation about 2 hours, and *gadA*-/*gadB*- cells exhibited similar delay as *gadB*- cells (Fig. 11). WT cells overexpressing *gadA* showed a delay in aggregation (Fig. 12), which may be due to a lack of sufficient GABA, as described above. WT cells overexpressing *gadB* were similarly delayed in aggregation (Fig. 12), which was likely caused by excessive extracellular GABA. All *gad* null and overexpressing cells showed normal late development without any visible morphological defects (data not shown).

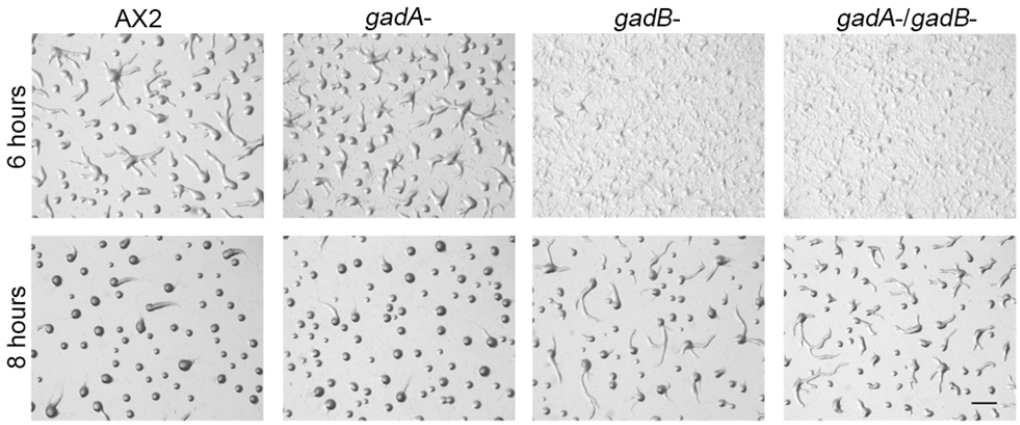

Figure 11. Early developmental phenotypes of *gad* mutants. 5×10^6 vegetative cells were developed on a non-nutrient DB agarose plates. Images were taken at indicated hours after development. Bar, 1 mm.

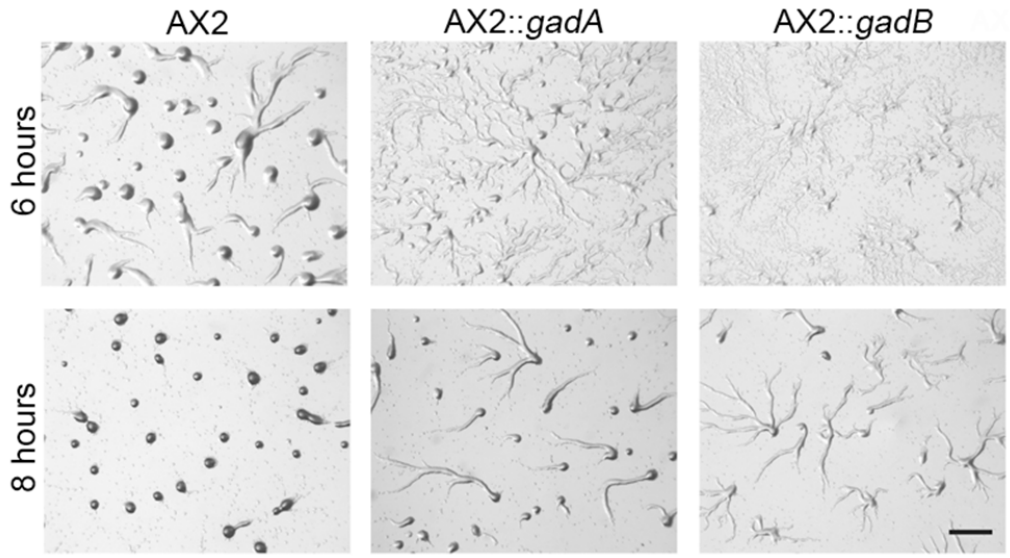

Figure 12. Early developmental phenotypes of *gad* overexpressors. 5×10^6 vegetative cells were developed on a non-nutrient DB agarose plates. Images were taken at indicated hours after development. *WT::gadA*, *gadA* was overexpressed in WT cells, *WT::gadB*, *gadB* was overexpressed in WT cells. Bar, 1 mm.

To test whether GABA is secreted as an autocrine signal, I mixed WT cells expressing GFP with WT cells overexpressing *gadB* in a 1:2 ratio and co-developed them on an agarose substrate. Unlike homogenous WT cells, which mostly formed loose mounds at 6 hours after development, a considerable number of WT cells in the mixture were still streaming at this time (Fig. 13 arrowheads). However, most WT cells still occupied the aggregation center (Fig. 13 asterisk). The aggregation delay of WT cells in the mixture implied that GABA was secreted as an autocrine signal and functioned non-autonomously.

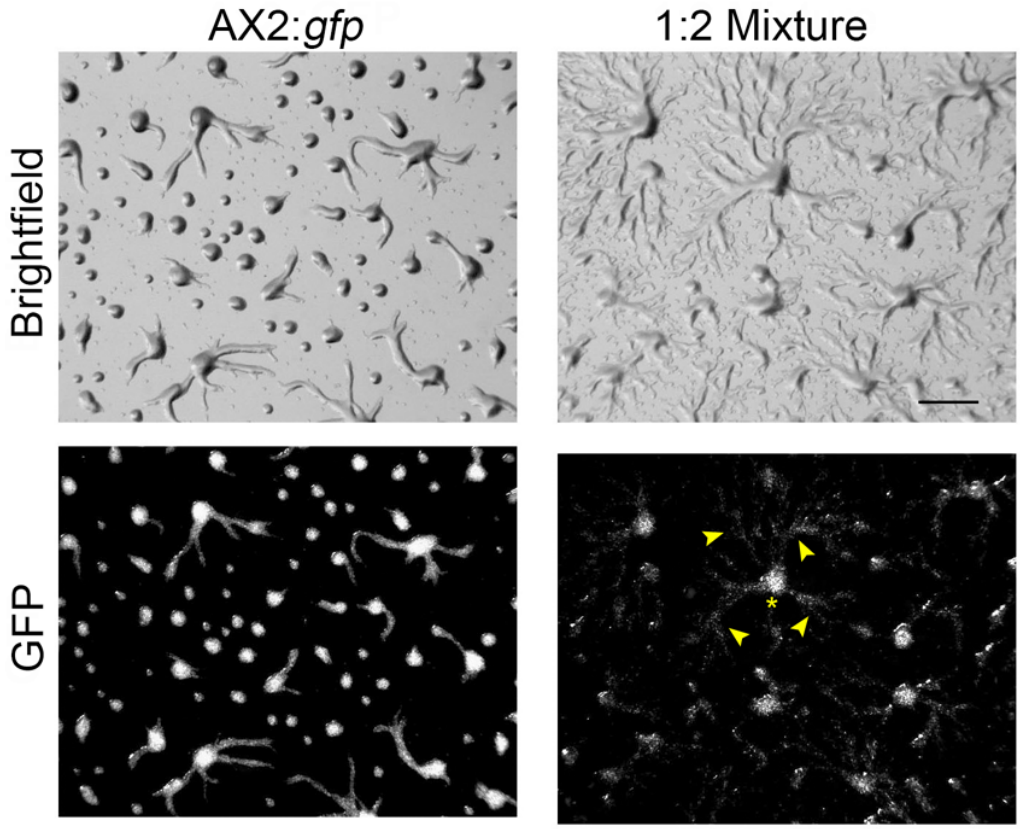

Figure 13. Co-development of WT::*gfp* and WT::*gadB* cells. 5×10^6 vegetative cells underwent development on agarose plates. For co-development, WT*::gfp* and WT*::gadB* cells were mixed in a 1:2 ratio. Images were taken at 6 hours. The asterisk denotes one aggregation center and arrowheads show streaming WT*::gfp* cells toward the aggregation center. Bar, 1 mm.

GABA is degraded in the mitochondrion

The extracellular amount of GABA is not only decided by the synthesis rate of GABA, but also by the degradation and transport of GABA out of the cell. I first studied the degradation of GABA. GABA is degraded in the mitochondria by a GABA transaminase in most eukaryotes except in yeast, which has a cytosolic GABA transaminase (Huh et al., 2003). A single GABA transaminase homologue in *D. discoideum*, *gabT*, was previously identified (Anjard et al., 2009). Here I disrupted *gabT*,

and measured extracellular GABA after starvation. Based on our previous data that extracellular GABA concentrations saturated between 2-4 hours, I measured GABA at 30 minutes intervals for 2 hours, and compared the GABA concentrations at 2 hours in the different mutants. Disruption of *gabT* significantly increased extracellular GABA levels to 18 μM, and overexpression of a C-terminal GFP tagged GabT in *gabT*- cells reduced extracellular GABA to around 5 μM (Fig. 14). However, incubation of WT cells with 5 μM of the irreversible GABA transaminase inhibitor vigabatrin didn't achieve a similar effect in increasing extracellular GABA levels (data not shown). GabT-GFP showed a punctate expression pattern, and co-localized with most of the mitotracker staining (Fig. 15). Interestingly, GabT-GFP localized in a large fraction, but not all of the mitochondria (Figure 15).

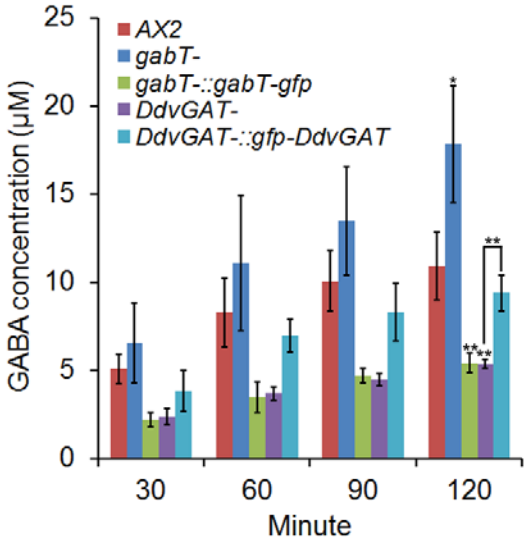

Figure 14. Regulation of GABA degradation and secretion. 5×10^6 vegetative cells were suspended and shaken in 100 µl DB. At indicated time points after starvation, the cell suspension was centrifuged. 40 µl supernatant was analyzed for amino acids content via HPLC. GABA concentrations from different genotypes at 120 minutes were compared to GABA concentration of WT cells, and GABA concentrations between *DdvGAT*- cells and *DdvGAT*- cells overexpressing GFP-DdvGAT were also compared. Values are means ± s.d.. *, $p<0.05$; **, $p<0.01$ One-way ANOVA was used.

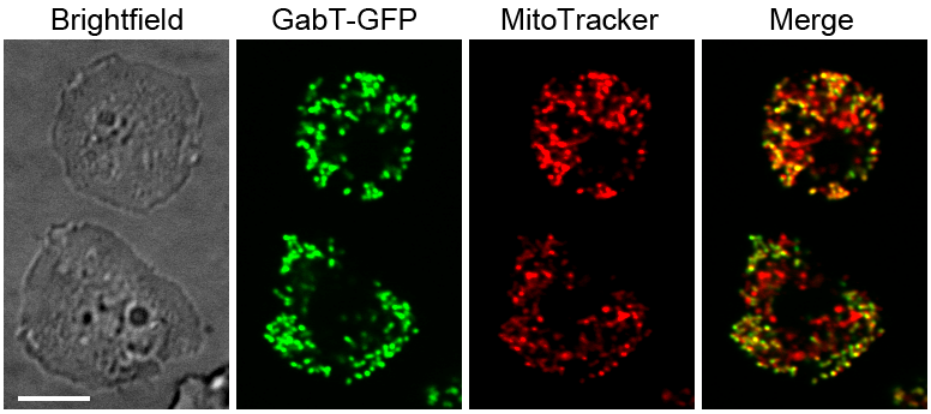

Figure 15. Localization of GabT-GFP in axenic cells. C-terminal GFP tagged GabT was expressed in *gabT*- cells. Cells were placed in a one-well glass chamber filled with DB, and stained with 100 nM Mitotracker red CMXRos (Invitrogen, M7512) for 30 minutes in DB at room temperature. Bar, 5 µm.

I also examined the early development of *gabT*- and *gabT-gfp* overexpressing cells. *gabT*- cells didn't exhibit a delay in early development, while *gabT-gfp* overexpressing cells showed delays in aggregation (Fig. 16). Both *gabT* null and overexpression cells underwent normal late development. Normal early development of *gabT*- cells suggested that only a high level of secreted GABA, as in GadB overexpressing cells, interfered with early development.

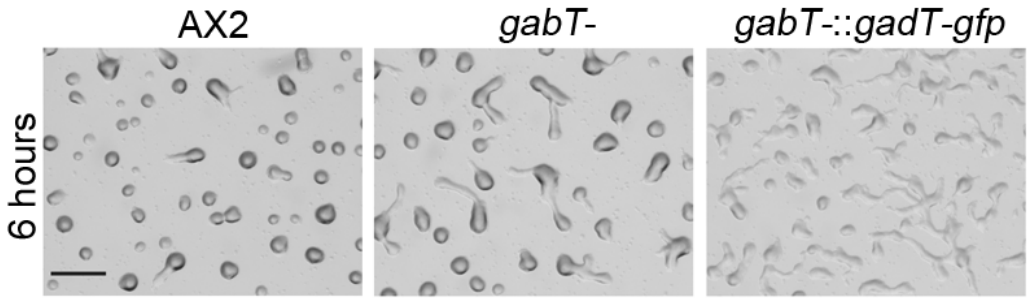

Figure 16. Early development of *gabT* mutants. 5×10^6 vegetative cells were developed on DB agarose, and images were taken at 6 hours. Bar, 1 mm

DdvGAT is partially required for GABA secretion

Since extracellular GABA levels plateau between 2-4 hours and appear to be regulated (Fig. 8), I decided to examine the uptake and secretion of GABA in *D. discoideum*. GABA is actively transported into neurons and glia by GABA transporters (GATs). All four mammalian GATs identified so far (GAT 1-3 and Betaine transporter, BGT-1 or GAT4) belong to the superfamily of sodium and chloride- dependent transporters (Liu et al., 1993; Liu et al., 1992; Lopez-Corcuera et al., 1992). A careful search of the *D. discoideum* genome did not reveal any homologues of the four GATs. Novel mechanisms may be employed for GABA uptake. Normally, GABA is packaged into synaptic vesicles by the vesicular GABA transporter (vGAT) in neurons (McIntire et

al., 1997) and released to the synaptic cleft through exocytosis. vGAT belongs to the SLC32 family (Gasnier, 2004) and shares no resemblance to the GATs. One vGAT homologue gene，*DDB_G0293074*, was identified in *D. discoideum*, and I named it *DdvGAT*. Disruption of *DdvGAT* reduced extracellular GABA levels to approximately 5 μM, and overexpression of a N-terminal GFP tagged DdvGAT restored extracellular GABA concentration to about 10 μM, which is similar to wild-type cells (Fig. 14). Previous studies revealed that the GABA transaminase inhibitor vigabatrin could also inhibit GABA transport activity of rat vGAT almost as potently as GABA (McIntire et al., 1997). This may explain why the addition of vigabatrin didn't increase the extracellular GABA level at 2 hours after development. *DdvGAT*- cells also exhibited a delay in aggregation (Fig. 17), but appeared to form normal fruiting bodies. GFP-DdvGAT was distributed on the membrane of vesicles, and these vesicles were stained with neutral red (Fig. 18), suggesting GFP-DdvGAT is localized on the membrane of lysosomes, which is consistent with a recent mass spectrometry study of the macropinocytic proteome which identified this protein from vesicles including macropinosomes and lysosomes (Journet et al., 2012). I also tested whether microtubules were required for GABA secretion. Addition of 150 μM nocodazole reduced extracellular GABA levels to 5 μM (Fig. 19), suggesting microtubules were involved in GABA secretion. Addition of 1 μM Latrunculin A had no effect on GABA secretion (Fig. 19), indicating that actin was not required for this process.

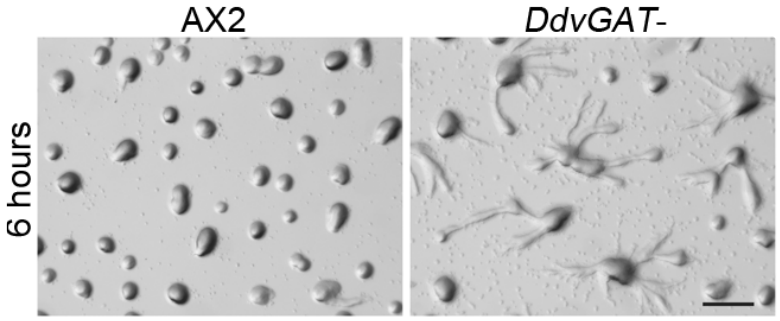

Figure 17. Early development of *DdvGAT* mutant. 5×10^6 vegetative cells were developed on DB agarose, and images were taken at 6 hours for (C) and (D). Bar, 1 mm.

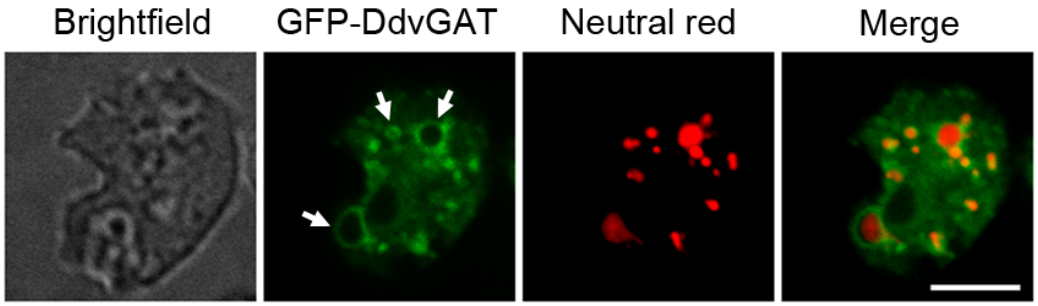

Figure 18. Localization of GFP-DdvGAT in axenic cells. *DdvGAT*- cells expressing N-terminal GFP tagged DdvGAT were placed in a glass chamber in DB, and then stained with 0.5 μM neutral red (Sigma, N4638) for 20 minutes. Arrows indicate representative lysosomes. Bar, 5 μm.

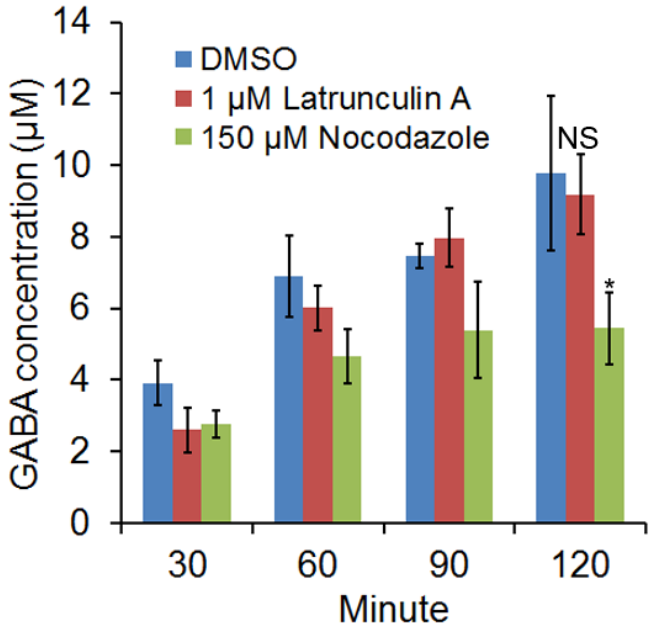

Figure 19. Effect of Latrunculin A and Nocodazole on GABA secretion. 5×10^6 vegetative cells were suspended in 100 μl DB with 1 μM Latrunculin A or 150 μM Nocodazole. Same procedure was performed as in Figure 9. Values are mean ± s.d.. NS, non-significant; *, $p<0.05$. One-way ANOVA was used.

GrlB is the major GABA receptor at the growth stage and early development

A previous study suggested that GrlE, another $GABA_B$ receptor-like family member, was the main GABA receptor during sporulation (Anjard and Loomis, 2006). Disruption of *grlE* reduced the amount of the bound GABA antagonist CGP54626 in whole cells by 90% (Anjard and Loomis, 2006). I decided to validate whether GrlB is also a GABA receptor. First I confirmed the localization of GrlB. In vegetative cells, GrlB-GFP was partially localized on the plasma membrane of cells, and strong autofluorenscence or GrlB-GFP was observed in the cytosol (Fig. 20A). Next, I tested the GABA binding capacity of GrlB. I incubated 5×10^6 axenically grown cells with 0.2 nM

tritium labeled GABA for total binding. Non-specific binding was measured by adding 1×10^6 fold excess CGP55845. I found that both *grlB*- cells and *grlB*-/*grlE*- cells showed only about 20% specifically bound GABA as compared to WT cells, whereas no significant difference was found between *grlE*- cells and WT cells (Fig. 20B). When combined with the expression profile of GrlE, whose mRNA peaks at 4 hours after development (Anjard and Loomis, 2006), the binding assay results suggest that GrlB is the major GABA receptor at growth stage and early development. To further confirm that GrlB is a G protein coupled receptor, I tested whether the non-hydrolyzable GTP analog GTPγS could desensitize GrlB and reduce GABA binding. Crude membrane fraction were prepared and treated with 0.1 mM GTPγS. The treatment of GTPγS reduced specifically bound ^{3}H-GABA to about 63% of the untreated control (Fig. 20C). This suggests that GrlB is coupled to a heterotrimeric G protein, as would be predicted from its membrane spanning topology.

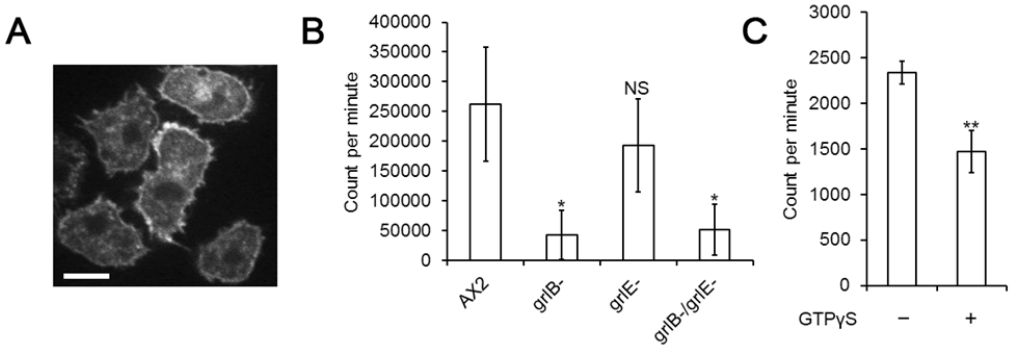

Figure 20. GABA binding in vegetative cells and early gene expression in *grlB*- cells. (A) C-terminal GFP tagged GrlB was expressed in *grlB*- cells. Cells from HL5 were washed with DB and plated in a glass chamber filled with DB before photographed. Bar, 5 μm. (B) Specific ^{3}H-GABA binding to whole vegetative cells was shown as radioactivity (Count per minute) per 5×10^{6} cells. Values are means ± s.d.. NS, non-significant; *, $p<0.05$; **, $p<0.01$. One-way ANOVA was used. (C) Specific ^{3}H-GABA binding to vegetative cell membrane fraction was shown as radioactivity (Count per minute) per membrane fraction from 5×10^{7} cells. Values are means ± s.d.. **, $p<0.01$. One-way ANOVA was used.

A previous study reported a delay of at least 2 hours in early development of *grlE*- cells, and that this delay could be rescued by overexpressing GrlE (Taniura et al., 2006). I was skeptical that GrlE functioned redundantly at the transition from growth to development and also in early development, therefore I generated our own *grlE*- cells and our *grlE*- cells exhibited a slight delay in aggregation at 6 hours after development. The *grlB*-/*grlE*- cells showed the same phenotype as the *grlB*- cells (Figs. 6 and 21A), suggesting that GrlE doesn't function redundantly with GrlB. Both *grlE*- and *grlB*-/*grlE*- cells appeared to exhibit normal morphology during late development (data not shown). I also tested whether removing GrlB and GrlE have a feedback effect on GABA production and therefore modulate the expression of GadB. qPCR showed that disruption of both *grlB* and *grlE* did not significantly change *gadB* mRNA expression (Fig. 21B).

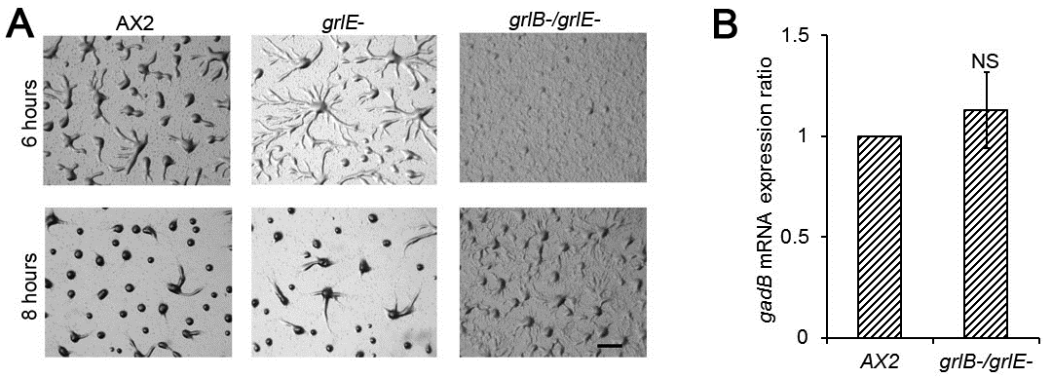

Figure 21. Early development of *grlE-* and *grlB-/grlE-* mutants. (A) 5×10^6 vegetative cells were washed with DB twice and plated on a non-nutrient DB agarose plates. Images were taken at indicated hours. Bar, 1 mm. (B) qPCR analysis showing *gadB* mRNA expression change in axenic *grlB-*/*grlE-* cells. *gadB* transcript level in wild-type AX2 cells was normalized to 1. Ratios are means ± s.d., NS, non-significant. One-way ANOVA was used.

To better explain why excess GABA also delays early development, I examined whether GABA could trigger the internalization of GrlB. 1 mM GABA was added to vegetative *grlB*-cells expressing GrlB-GFP in DB buffer, and the distribution of GrlB-GFP was recorded by time-lapse microscopy. After 20 minutes, no significant reduction of plasma membrane localization of GrlB was observed (data not shown). However, when *grlB-* cells expressing GrlB-GFP were starved on non-nutrient DB agar, GrlB-GFP began to lose its plasma membrane localization after 4 hours starvation and was clearly enriched in the cytoplasm at 6 hours (Fig. 22), suggesting GABA signaling through GrlB is down-regulated as cells polarize during aggregation.

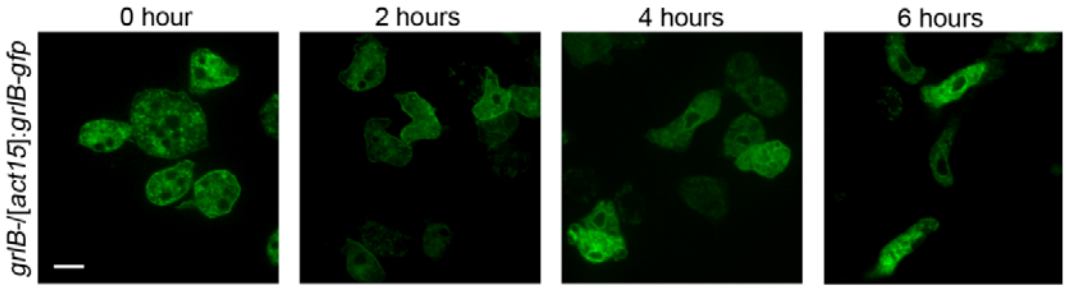

Figure 22.Distribution of GrlB-GFP during early development. *grlB*- cells expressing GrlB-GFP were collected from HL5 medium, washed twice with DB and plated on DB agarose at a density of 5×10^5 cells/cm^2. At indicated hours after starvation, cells were collected from the agarose plates and plated in glass chambers filled with DB. Images were taken at a 60× objective on a confocal microscope. Bar, 5 μm.

Dictyostelium cells exhibit a dramatic gene expression pattern shift after starvation, and necessary "early genes" start to express during early development (Iranfar et al., 2003). Thus I examined the expression profiles of early genes including *cAR1* and *csA* in *grlB*- cells. Developed cells were collected from an agarose substrate at different time points and analyzed. The cAMP receptor cAR1 was induced rapidly several hours after development and reached a peak at 4-6 hours, and then dropped drastically in WT cells. However, cAR1 was not expressed until 6 hours, and the expression tapered off at 8 hours in *grlB*- cells (Fig. 23A). Consistent with the cAR1 expression profile, *grlB*- cells were poorly polarized and showed defects in their ability to display robust chemotaxis toward cAMP at 6 hours (data not shown). The glycoprotein contact site A (CsA) mediates an EDTA-insensitive cell-cell cohesion via homophilic interaction during aggregation (Siu et al., 2011). In WT cells, csA peaked at 6 hours and decreased thereafter. While csA also peaked at 6 hours in *grlB*- cells, there was little expression at 4 hours and continued expression until 8 hours (Fig. 23B).

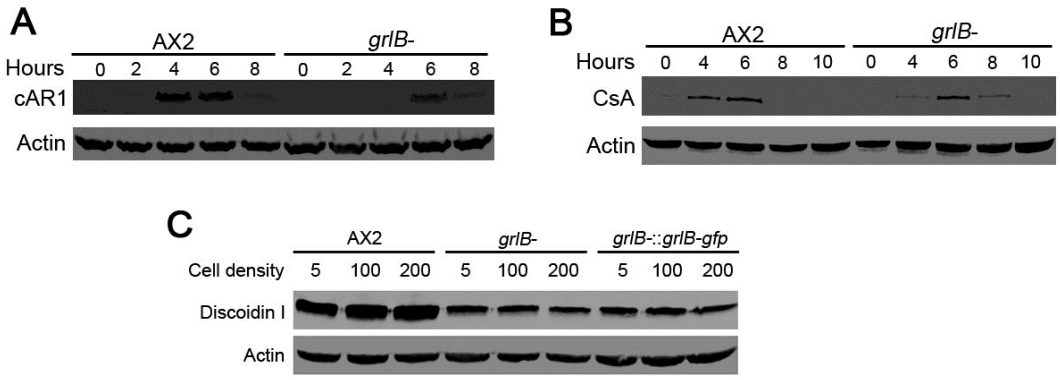

Figure 23. Expression of "early genes" during early development of *grlB*- cells. For (A) and (B) 5×10^6 vegetative cells were developed on DB agarose. At indicated hours, cells were collected and lysed for western blotting. Actin was used as the loading control. (C) 1×10^4 cells were shaken in HL5 medium at 175 rpm, 22°C. At indicated cell densities ($\times10^5$ cells/ml), equal amount of cells was collected and lysed for western blotting.

Although aggregation is affected and expression of chemotaxis and adhesion genes required for early development are delayed, it is difficult to conclude that GABA signaling interacts directly with the cAMP signaling pathway. Previous work has demonstrated that excess GABA had no effect on cAMP chemotaxis (Taniura et al., 2006). To clearly understand the function of GABA during growth and development, I examined events occurring before aggregation. The pre-starvation response is one of many cellular processes induced by nutrient depletion, and the marker protein Discoidin I is expressed in axenically grown cells and sharply induced according to cell density (Clarke et al., 1987; Maeda, 2011). Although Discoidin I was expressed at a relatively high level at low WT cell density (5×10^5 cells/ml) in our hands, it was induced to the highest level at saturation density (2×10^7 cells/ml) (Fig. 23C). However, the induction of

Discoidin I by cell density was totally abolished in *grlB-* cells and *grlB-:grlB-gfp* cells. The expression of Discoidin I remained at a low level at all densities (Fig. 23C).

Different genes required for spore formation

GABA has been suggested to induce spore formation, and GadA and GrlE were suggested as two components of GABA signaling (Anjard and Loomis, 2006). However, whether genes involved in GABA metabolism and signaling in growth and early development are also required for this process is still unknown. Therefore I examined spore formation in different mutants related to GABA metabolism (Fig. 24). Most of the wild-type spores were detergent-resistant, and only about 70% spores from *gadA-* cells were viable after NP-40 treatment as previously described (Anjard and Loomis, 2006). However, *gadB-* cells formed a similar percentage of viable spores as wild-type cells, suggesting that GadB is not required for spore formation. According to the expression pattern of *gadB*, GadB may not exist during sporulation. To test whether GadB could functionally complement GadA, I overexpressed GadB-GFP under the control of the *actin15* promoter in *gadA-*/*gadB-* cells and examined viable spores. *gadA-*/*gadB-* cells formed significantly reduced viable spores. Overexpression of GadA-GFP in *gadA-*/*gadB-* cells successfully recovered the reduced viable spores number to normal level as compared to wild-type cells, whereas *gadA-*/*gadB-* cells overexpressing GadB-GFP still exhibited reduced viable spores, suggesting GadB could not functionally complement GadA during sporulation.

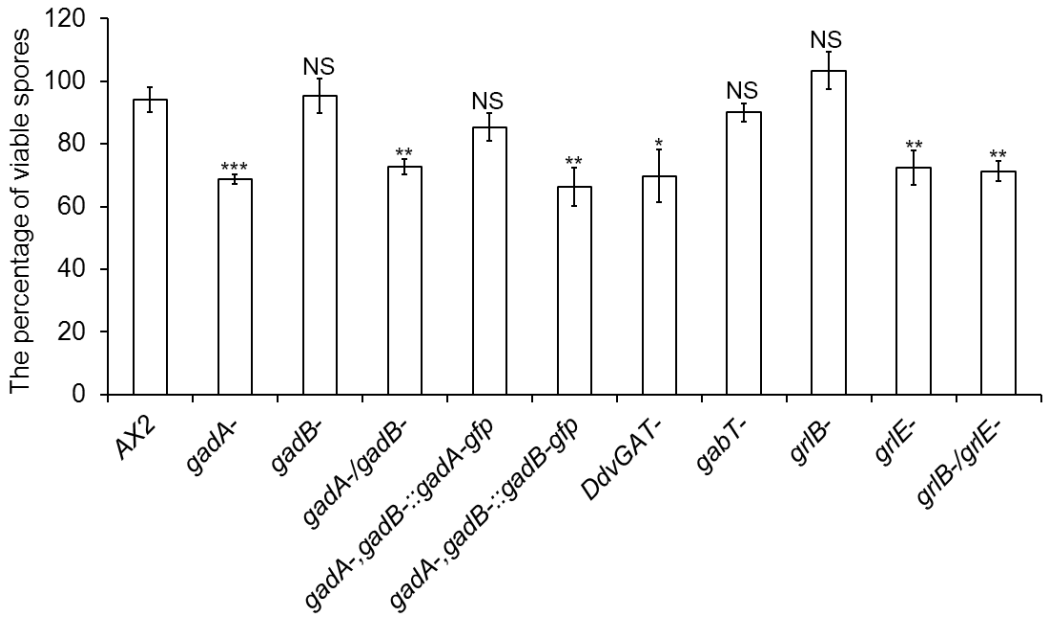

Figure 24. The percentage of detergent-resistant spores in different GABA mutants. 1×10^7 cells were developed on buffer-saturated filters. After 48 hours, spores were collected and treated with 0.4% NP-40 for 10 minutes. 100 spores were then counted and cultured with bacteria. The plaques formed from detergent-resistant spores were counted after 5 days. Values are means ± s.d.. NS, non-significant; *, $p<0.05$; **, $p<0.01$; ***, $p<0.001$. One-way ANOVA was used.

grlE- cells only formed about 70% viable spores, whereas *grlB*- cells formed a similar percentage of viable spores as wild-type cells (Fig. 24), suggesting GrlB is not required for spore formation. *grlB*-/*grlE*- cells generated similar viable spores as *grlE*- cells. As expected, *gabT*- cells generated similar viable spores as wild-type cells. Interestingly, *DdvGAT*- cells generated significantly reduced viable spores, suggesting that DdvGAT is likely responsible for GABA secretion in prespore cells.

GPCRs transduce extracellular stimuli by coupling to heterotrimeric G proteins, and addition of GTPγS reduced GABA binding (Fig. 20C). 14 Gα subunits have been identified in the *Dictyostelium* genome and most of them have been fairly well

characterized (Heidel et al., 2011). To determine which Gα subunit is coupled to GrlB, *gadB* was overexpressed in all available Gα subunit null mutants except Gα2 and Gα3 mutants which fail to undergo development. Phenotypes of these strains were analyzed (Fig. 25). Only *gadB* overexpression in the Gα8 null mutant exhibited similar developmental progress as the Gα8 null mutant, strongly suggesting that GrlB is coupled to the Gα8 subunit.

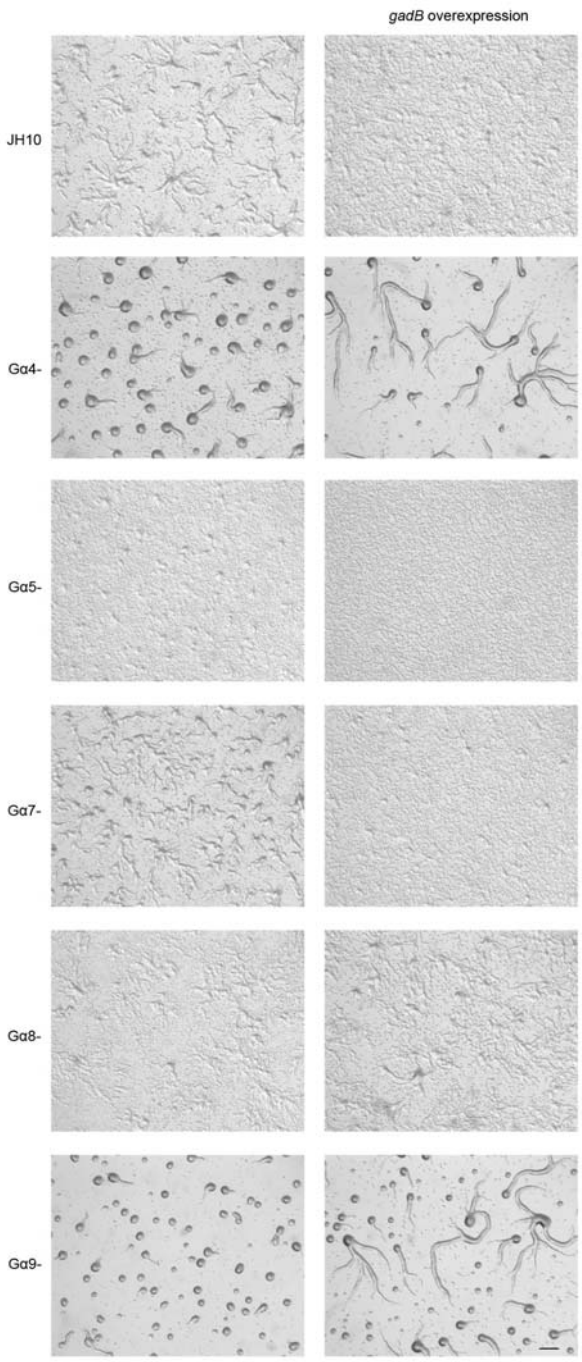

Figure 25. Overexpression of *gadB* in different Gα subunit null mutants. 5×10^6 axenic cells were washed with DB twice and plated on a non-nutrient DB agarose plates. Images were taken 6 hours after development. JH10 is the parental cell strain of Gα5-, Gα7-, and Gα8-. Bar, 1mm

DISCUSSION

The evolutionary history of glutamate decarboxylase appears to be quite complicated. In *Escherichia coli*, two isozymes of GadA and GadB show identical biochemical properties (De Biase et al., 1996). However, two human isoforms of GADs, GAD65 and GAD67, differ in many aspects including subcellular localization, enzymatic activity, expression region, and level (Erlander et al., 1991; Soghomonian and Martin, 1998). These divergences indicate that GAD65 and GAD67 are both spatially and temporally regulated. In *D. discoideum*, two isozymes, GadA and GadB, are most similar to their homologues in *E. coli.*, but are temporally regulated. GadB is expressed in vegetative and early development stages, and decreases before the rising expression of GadA. This mutually-exclusive expression pattern of GadA and GadB could be explained by our data. Disruption of *gadB* eliminates production of GABA, and *gadA* is not up-regulated to compensate the loss of *gadB*. A previous study reported that the disruption of *gadA* alone leads to the sporulation defect (Anjard and Loomis, 2006), and our data suggests that GadB is not required for sporulation. Besides, GadB could not functionally complement GadA when overexpressed in the sporulation stage, possibly because GadB is inactive during this stage. These results suggest that GadA and GadB are differently regulated. In addition, as I show here, co-expression of GadA and GadB reduced the production of extracellular GABA. Since overexpression of GadA does not alter the transcript levels of GadB, one plausible explanation for reduced GABA production in wild-type cells expressing *gadA* is that GadA has a much stronger affinity for the enzyme cofactor pyridoxal phosphate (PLP) than GadB and sequesters the cofactor when overexpressed, therefore GadB is devoid of pyridoxal phosphate and remains as an

apoenzyme. Recombinant GAD65 has been reported to be more preferable to the enzyme cofactor than GAD67 (Erlander et al., 1991).

It seems that the enzymatic activity of GadA and GadB are not identical, although they are highly similar to each other. Overexpressing GadA alone drastically induces *gadA* mRNA level in *gadA*-/*gadB*- cells but still results in low extracellular GABA levels during early development, suggesting the activity of GadA is extremely low and/or the environment is optimal for GadB but not GadA. On the basis of weak activity of GadA, it can be inferred that only a small amount of GABA is required for spore formation. It has been shown that GadA expression is enriched in pre-spore cells and GABA generated from pre-spore cells can induce sporulation (Anjard and Loomis, 2006; Iranfar et al., 2001). 1 nM GABA is sufficient to maximally induce spore formation (Anjard and Loomis, 2006). The weak enzymatic activity of GadA could also explain why a huge amount of *gadA* mRNA is enriched in pre-spore cells for generating enough GABA to induce cell differentiation (Anjard and Loomis, 2006; Maruo et al., 2004). Our data supports the idea that the GadB is responsible for GABA shunt in vegetative stage and regulation of early development, and GadA is specific for sporulation.

In mammalian systems, GABA is actively transported into the cell in favor of the ionic gradient by GABA transporters (GATs), while amoebae lack most of the counterpart homologues. However, there are still several putative amino acid transporters in the *D. discoideum* genome, including tmem104, ctrA-C, DDB_G0287423, DDB_G0267504, and DDB_G0287303. The functions of these proteins remain largely unknown. Another possible way for GABA absorption is through pinocytosis. Axenic

cells acquire nutrients from liquid medium through pinosomes, and it is likely that GABA in the medium can also be absorbed.

vGAT is responsible for synaptic GABA release only in neurons. However, DdvGAT is responsible for GABA secretion in the social amoeba, implying that it is an ancient mechanism for GABA secretion. The disruption of *DdvGAT* reduced secreted GABA to 50% of normal levels at 2 hours after starvation, which suggests the existence of other mechanisms for GABA secretion. Loss of DdvGAT causes the similar defect in sporulation as loss of GadA, indicating this mechanism likely exists in pre-spore cells to release GABA.

Extracellular GABA levels need to be tightly regulated, with low and high levels both leading to a delay in early development. When WT cells were mixed with GadB overexpressing cells, the increased extracellular levels of GABA presumably also delayed the development of the WT cells. Moreover, it seems that only very high levels of GABA have these effects. WT cells secrete about 11 μM GABA at 2 hours after starvation, and WT cells expressing *gadB* secrete about 38 μM at the same time and exhibit a significant delay in aggregation, whereas *gabT*- cells, which increase GABA level to about 18 μM, aggregate normally. Compared to wild-type cells, *gabT*- cells don't show very high extracellular GABA, suggesting that newly synthesized GABA is partially degraded in the mitochondria.

Two confusing questions still remain unanswered. First, why does exogenous addition of GABA not delay aggregation? The GABA secretion data I collected were from cells in suspension, and they may not reflect the real GABA secretion when cells develop on a solid surface, which is very difficult to measure. Crawling cells on a surface

may only sense GABA from their surrounding cells and respond to it, and they might also secrete an unknown enzyme to clear GABA in their environment. This enzyme is probably not the GabT, which I found is localized in the mitochondria. If a gradient in the microenvironment surrounding a cell is required for the function of GABA, the uniform application of GABA would not exhibit any effects. One well known secreted factor in early development of *Dictyostelium* is cAMP. During streaming toward an aggregation center, rearguard localized Adenylate Cyclase of Aggregation stage (ACA) secrets cAMP guiding chemotaxis of subsequent cells, and cells secrete cAMP phosphodiesterase (PDE) to remove surrounding cAMP (Kriebel et al., 2003; Sucgang et al., 1997). Another possibility is that intracellular GABA causes the phenotypes and also controls the levels of external GABA. GABA is generated in the GABA shunt, which is required for energy metabolism. Thus intracellular GABA levels might represent the nutritional or energy state of a cell. These metabolic states clearly specify whether a cell would start to develop. If this is the case, direct addition of GABA would also have no effect.

Second, why do deficient and excess extracellular GABA levels both generate the delay in aggregation? It is easy to understand that insufficient extracellular GABA could lead to the abolishment of the pre-starvation response and result in the delay in early genes expression, and the aggregation process. However, the mechanism by which excess extracellular GABA works is unclear. Maybe high GABA levels down-regulate the GABA receptor. I tested the internalization of GFP labeled GrlB when excess GABA is provided, but the plasma membrane localization of GrlB-GFP was barely changed after 20 minutes treatment, strongly suggesting the receptor internalization is not the reason to explain the *gadB* overexpression phenotype.

GABA signaling during early development is also regulated through the regulation of the localization of GABA receptor GrlB. The GrlB-GFP fusion showed internalization when cells start to become polarized. Although most highly polarized cells lose the plasma membrane localization of GrlB-GFP, overexpression of GrlB might still leave trace amounts of receptor at the membrane and continuing GABA signaling might jeopardize the onset of aggregation. This could explain why overexpression of GrlB in WT cell shows a more severe delay in aggregation than in *grlB*- cells. In vegetative cells, both co-culture with bacteria and periodic folic acid pulsing greatly increase transcript levels of *grlB*. These two treatments sharply up-regulate the capacity of axenic cells to chemotax toward folic acid, indicating that folic acid signaling somehow interacts with GABA signaling and regulates expression of GrlB. It is possible that there is crossover at the level of the heterotrimeric G proteins. Given that many G protein mutants are available, it may be worth examining GABA signaling in the various Gα subunit nulls, including Gα4, which is coupled to the folic acid receptor(s) (Hadwiger et al., 1991).

In summary, I have investigated the homeostasis of GABA and explored its function during early development of *D. discoideum* for the first time. GABA is converted from glutamate mainly by the cytosolic glutamic acid decarboxylase GadB. Due to its trace expression level, the glutamic acid decarboxylase GadA generates little or no GABA at this time. However, elevated expression of GadA suppresses production of GABA possibly by sequestering the cofactor pyridoxal phosphate. Newly synthesized GABA is secreted through two potential pathways. DdvGAT, the only homologue of vGAT, is expressed on the membrane of lysosomes and likely transports GABA into the lysosomes. GABA is then released through exocytosis. It is also possible that GABA is

transported directly by an unknown plasma membrane bound transporter(s). GABA is degraded in the mitochondria by the GABA transaminase GabT. Secreted GABA binds to the G protein coupled receptor GrlB of surrounding cells, which in turn triggers the pre-starvation response and regulates early development.

CHAPTER IV

THE G ALPHA SUBUNIT GA8 INHIBITS PROLIFERATION, PROMOTES ADHESION AND REGULATES CELL DIFFERENTIATION

ABSTRACT

In the previous chapter, the G protein alpha subunit Gα8 was suggested to regulate GABA signaling. Unexpectedly, overexpression of Gα8 induced cytokinesis defects in wild-type cells. In this chapter the functions of the G protein alpha subunit Gα8 are characterized during vegetative and development stages. Gα8 is expressed at low levels during vegetative growth. Loss of Gα8 promotes cell proliferation, whereas excess Gα8 expression dramatically inhibits growth and induces aberrant cytokinesis on substrates in a Gβ-dependent manner. Overexpression of Gα8 also leads to increased cell-cell cohesion and cell-substrate adhesion. I demonstrate that the increased cell-cell cohesion is mainly caused by induced CadA expression, and the induced cell-substrate adhesion is responsible for the cytokinesis defects. However, the expression of several putative constitutively active mutants of Gα8 does not augment the phenotypes caused by intact Gα8. Gα8 is strongly induced after starvation, and loss of Gα8 results in decreased expression of certain adhesion molecules including CsA and tgrC1. Interestingly, Gα8 is preferentially distributed in the basal disc, the upper and lower cup of the fruiting body. Lack of Gα8 decreases the expression of the specific marker of the anterior-like cells, suggesting that Gα8 is required for anterior-like cell differentiation. The work in this chapter has also been published (Wu and Janetopoulos, 2013a).

INTRODUCTION

Heterotrimeric G proteins are central mediators in signal transduction pathways, with cells utilizing them to respond to the environment and communicate with each other. Heterotrimeric G proteins consist of an α subunit and an obligate βγ dimer, and localize to the cytosolic face of the plasma membrane. G proteins typically transduce extracellular stimuli from G protein-coupled receptors (GPCRs) to downstream effectors. Ligand binding to the GPCR activates the G protein heterotrimer by facilitating GDP/GTP exchange on the Gα subunit which leads to the dissociation of the Gα and Gβγ dimer (Oldham and Hamm, 2008). The activated GTP bound Gα and free Gβγ interact with their downstream effectors respectively, including adenylyl cyclases (Pierre et al., 2009), phospholipases (Mizuno and Itoh, 2009) and ion channels (Padgett and Slesinger, 2010). GPCR-mediated signaling has been implicated in numerous physiological and pathological processes and represents 50-60% of current drug targets (Overington et al., 2006).

The social amoeba *Dictyostelium discoideum* has been employed as a model system to study G protein signaling. The amoeba has a relatively short life cycle, a haploid genome and is amenable to numerous biochemical and genetic techniques (Schaap, 2011b). The *D. discoideum* genome contains 14 Gα subunits, 2 Gβ subunits and a single Gγ subunit (Eichinger et al., 2005; Heidel et al., 2011). The Gα2-mediated cAMP chemotaxis pathway has been intensively studied in this organism. The amoeba usually lives in the soil feeding on bacteria. Once the food source is depleted, cells start a developmental process that leads to the secretion of propagating waves of cAMP (Schaap, 2011a). Gradients of cAMP are formed and can be sensed by other cells through the

cAMP receptor cAR1 (Klein et al., 1988). Binding of cAMP to cAR1 in turn activates Gα2 and leads to the dissociation of Gα2 from the Gβγ subunit (Elzie et al., 2009; Janetopoulos et al., 2001; Kesbeke et al., 1988; Kumagai et al., 1989). The activated Gα2 and Gβγ elicit a plethora of cellular responses which allow thousands of cells to stream toward the aggregation center, undergo morphological changes and finally form environmental-resistant spores (Franca-Koh et al., 2006). Another Gα subunit, Gα9, has been suggested as an inhibitor of the cAMP pathway (Brzostowski et al., 2002; Brzostowski et al., 2004).

Vegetative *D. discoideum* cells can sense the bacterial metabolite folic acid to help track down bacteria. This process has also been shown to be G protein-mediated. Cells lacking the Gβ subunit form tiny plaques on bacterial lawns (Wu et al., 1995), and Gα4 likely couples to the folic acid receptor (Hadwiger et al., 1994), although the folic acid receptor itself has remained elusive and is still not identified. A recent study shows that several elements thought to be required for cAMP chemotaxis are quite dispensable for folic acid chemotaxis (Srinivasan et al., 2012).

One of the Gα subunits, Gα8, has been investigated previously and no obvious function was revealed (Wu et al., 1994). Recently, Gα8 has been suggested to regulate the proliferation inhibition and chemorepellant activity of AprA (Bakthavatsalam et al., 2009; Phillips and Gomer, 2012). In this chapter I generated *gα8*- cells in a new background and confirmed that the disruption of *gα8* leads to rapid proliferation. On the other hand, overexpression of *gα8* not only represses proliferation but also induces cytokinesis defects. I also found that overexpression of *gα8* promotes both cell-cell cohesion and cell-substrate adhesion, with the induced cell-substrate adhesion largely

contributing to the cytokinesis deficiency. In addition, I present evidence showing that Gα8 modulates stalk cell fate determination and affects spore viability.

MATERIALS AND METHODS

Materials

Wild-type strains including Ax2, JH10, DH1, Ax3, KAx3, and the mutant strains summarized in Table 4 were obtained from dictyBase (http://dictybase.org/). Plasmids pLPBLP (Faix et al., 2004), pDM series (pDM304, pDM323, pDM326, and pDM358) (Veltman et al., 2009), GFP-Gβ (Jin et al., 2000), pDdGal-17 (Harwood and Drury, 1990), pVS (Zhang et al., 1999), pEcmAO-i-α-gal (Rafols et al., 2001), pEcmO-i-α-gal, pEcmB-i-α-gal, and pPsA-i-α-gal (Detterbeck et al., 1994) were also obtained from dictyBase. Polyclonal rabbit anti-Gα8 (Wu et al., 1994) and anti-Gα1 (Johnson et al., 1989) antisera were kindly provided by Dr. Peter Devreotes at John Hopkins University. Polyclonal rabbit anti-CadA antiserum (R851) (Knecht et al., 1987) and monoclonal mouse anti-CadA antibody (mLJ11) (Knecht et al., 1987) were kindly gifted by Dr. William Loomis at University of California San Diego. Rabbit anti-tgrC1 antiserum (Geltosky et al., 1979) was kindly provided by Dr. Charles Singleton at Vanderbilt University. Monoclonal mouse anti-CsA antibody (33-294-17) (Bertholdt et al., 1985) was obtained from the Developmental Studies Hybridoma Bank at the University of Iowa. Monoclonal mouse anti-Actin antibody (MAB1501R) was purchased from Millipore. Monoclonal mouse anti-c-myc antibody (46-0603) was purchased from Invitrogen. Monoclonal mouse anti-GFP antibody (11814460001) was purchased from Roche.

Table 4. Summary of mutants obtained from dictybase.

Strain	DictyBase ID	Background	Phenotype mentioned in this study	References
gα8-	DBS0236107	JH10	Rapid proliferation	Bakthavatsalam et al., 2009
gβ-	DBS0236530	JH10	Rapid proliferation	Bakthavatsalam et al., 2009
paxB-	DBS0236728	Ax2	Reduced cell-substrate adhesion	Bukharova et al., 2005
sadA-	DBS0236921	Ax3	Abolished cell-substrate adhesion	Fey et al., 2002
cadA-	DBS0237013	KAx3	Loss of Ca^{2+}-dependent cell-cell cohesion	Wong et al., 2002

Cell culture, growth and development

Cells were axenically maintained in HL-5 medium or grown with *Klebsiella aerogenes* bacteria on SM plates at 22°C. 100 μg/ml thymidine was supplemented in HL-5 medium for JH10 cells. Wild-type background used in each experiment was indicated in the figure legends. For proliferation measurements of suspension cultures, axenic cells were harvested from plastic petri-dishes, diluted in 50 ml HL-5 medium to 5×10^4 cells/ml, and shaken at 175 rpm, 22°C. Cell density was measured by a hemacytometer. To measure adherent cell proliferation, cells were spread on 35 mm petri-dishes at a density of 1×10^4 cells/cm^2. At indicated time points, cells were removed thoroughly from the dish bottom by repeatedly pipetting, and the cell number was determined by a hemacytometer. The cell density was defined as cell number divided by petri-dish bottom area. To examine the developmental process, cells were collected from dishes or suspension culture, washed twice with developmental buffer (DB: 5 mM Na_2HPO_4, 5 mM KH_2PO_4, 0.2 mM $CaCl_2$, 2 mM $MgSO_4$，pH 6.5), and then plated on 1.5% non-nutrient DB agar at a density of 5×10^5 cells/cm^2.

Generation of mutant and overexpression strains

All primers used for molecular cloning are listed in Table 5. To disrupt *gα8* in wild-type Ax2 cells, a 677 bp 5' homologous region and a 726 bp 3' homologous region were amplified from genomic DNA and directionally cloned into the vector pLPBLP. The resulting construct replaced a small region on exon 2 of *gα8* (genomic DNA fragment bp 690-721, beginning with the start codon ATG) with the Bsr cassette. The knockout construct was linearized by NotI and 2 μg linear DNA was then electroporated into 5×10^6 Ax2 cells. 20 hours after transformation, cells were selected with 10 μg/ml Blasticidin S for 10 days. The clones were isolated, diluted and then clonally spread on a *K. aerogenes* lawn for 5 days. Successful gene disruption in plaques was confirmed by PCR of genomic DNA using one primer inside the Bsr cassette and one primer outside the homologous region on the genome (Charette and Cosson, 2004) .

The coding region of *gα8* was amplified from the first strand cDNA prepared from Ax2 cells starved for 5 hours and cloned into the pDM304, pDM358 and pDM326 expression vectors respectively. To generate the Gα8-GFP fusion, a SpeI restriction site was first introduced after the amino acid 110 of Gα8 by PCR and then *gα8* was inserted back into pDM304. *gfp* flanked by three glycine codons encoding "-GGG-GFP-GGG-" was amplified from the pEGFP-C1 vector and inserted into the SpeI site of *gα8*. For the inducible expression of Gα8-GFP fusion, the *gα8-gfp* fragment was amplified and cloned into the pVS vector. The point mutations G41V, S46C and Q203L of Gα8 were introduced by PCR and the resulting gα8 mutants were cloned into the pDM304 vector. The truncated $G\alpha8^{\Delta Tail}$ was generated by removing the 51 amino acids at the COOH-terminus through PCR and cloning into the pDM304 vector. The DNA fragment

“gaacaaaaactcatttcagaagaagattta” encoding the c-myc epitope “EQKLISEEDL” was fused to the NH_2-terminus of the Gγ gene, and the fusion protein was cloned into the pDM358 vector. The coding region of *gα1* was also amplified from the cDNA and cloned into the pDM304 vector. Cells transformed with these expression plasmids were selected with 20 μg/ml G418 or 50 μg/ml Hygromycin B or 10 μg/ml Blasticidin S as required until single colonies emerged. To reduce the expression level of Gα8-GFP, *gα8*- cells carrying *gα8-gfp* driven by the *discoidin I* promoter were either supplemented with 1 mM folate in HL-5 medium or co-cultured with *K. aerogenes* bacteria.

Table 5. Primer sequences used in chapter IV. Restriction sites and mutated codons are highlighted in red.

Primer name	Primer sequence (5'-3')
Gα8-F5-KpnI	**GGGGTACC**CAATCACGTGTTCAAGTAGAAG
Gα8-R5-HindIII	**CCCAAGCTT**TCAGTTACAGAGATACCTGTAG
Gα8-F3-PstI	**AACTGCAG**TTGTTGATGTTGGTGGTCAAAG
Gα8-R3-BamHI	**CGGGATCC**TGCACCATCAATTGTAGTTTGG
Gα8-F-BglII	**GAAGATCT**ATAAAATGGGTTGCTATCAATCACGTGTTC
Gα8-R-XbaI	**GCTCTAGA**TTAAGAATTAATTTTGGCGGTTGCACC
Gα8^{I10}-F-SpeI	GTTAAATCATTCCAA**ACTAGT**TTTGAACCAGAAGTTAAAC AAATG
Gα8^{I10}-R-SpeI	CATTTGTTTAACTTCTGGTTCAAA**ACTAGT**TTGGAATGATT TAAC
EGFP-F-SpeI	**GGACTAGTGGTGGAGGT**ATGGTGAGCAAGGGCGAGGAG
EGFP-R-SpeI	**GGACTAGTACCTCCACC**CTTGTACAGCTCGTCCATGCC
Ga8-F-KpnI	**GGGGTACC**ATAAAATGGGTTGCTATCAATCACGTGTTC
Ga8-R-BamHI	**CGGGATCC**TTAAGAATTAATTTTGGCGGTTGCACC
Gα8^{G41V}-F	GTTGGGTGCT**GTT**GAAAGTGG
Gα8^{G41V}-R	CCACTTTCAACAGCACCCAAC
Gα8^{S46C}-F	GAAAGTGGTAAA**TGC**ACTGTTG
Gα8^{S46C}-R	CAACAGTGCATTTACCACTTTC
Gα8^{Q203L}-F	GATGTTGGTGGT**CTA**AGAAATG
Gα8^{Q203L}-R	CATTTCTTAGACCACCAACATC
Gα8$^{\Delta Tail}$-R	**GGACTAGT**TTATGTTGCTTTCATTAAAACC

Immunocytochemistry

Cells were grown on coverslips in HL-5 medium overnight, and then washed with phosphate buffered saline (PBS: 10 mM Na_2HPO4, 1.8 mM KH_2PO_4, 2.7 mM KCl, 137 mM NaCl, pH 7.4) twice. Cells were then fixed in 4% formaldehyde for 20 minutes, washed with PBS, and blocked in PBS containing 0.1% Triton X-100, 1% normal goat serum (NGS) and 1% bovine albumin serum (BSA) for 30 minutes. Primary rabbit anti-Gα8 was used at 1:200, and secondary FITC-labeled goat anti-rabbit IgG was used at

1:750. Images were taken on a Quorum WaveFX spinning disk confocal system running Metamorph software.

Microscopy

Images of developing structures on DB agarose were acquired with a Leica MZ16 stereomicroscope with a Q-Imaging Retiga 1300 camera and QCapture software. Live cells were photographed on coverslips or in Lab-Tek II chambers (Nalge Nunc International). Cells were imaged in DB for epifluorescence or confocal. For DAPI (4′, 6-diamidino-2-phenylindole) stain, cells were first fixed with 4% formaldehyde in DB for 20 minutes, and then incubated with 1 μg/ml DAPI in DB for 5 minutes. To examine the cytokinesis process, cells were incubated with *K. aerogenes* bacteria overnight, collected and allowed to settle in Lab-Tek II chambers (Janetopoulos et al., 2005). The chambers were rinsed with DB three times to remove residual bacteria. Cells at the onset of cytokinesis were identified by their round shape, and imaged at 15 second intervals. Images were acquired on a Zeiss Axiovert Marianas Workstation from Intelligent Imaging and Innovations running Slidebook software. A 40× PlanNeofluar (NA 1.3) wide-field lens was used. Confocal images were obtained by using a Quorum WaveFX spinning disk confocal system on a Nikon Eclipse Ti microscope with a PlanApo 60× TIRF objective (NA 1.49) (Figures 35B, 37 and 39C).

Cell-substrate adhesion and cell-cell cohesion assays

Cell-substrate adhesion assay was performed as described (Fey et al., 2002). 5×10^5 cells were plated in 35 mm petri-dishes in a total volume of 1 ml HL-5, and settled

for 4 hours to allow them to completely adhere to the substrate. The dishes were then set on a platform shaker and shaken at 125 rpm. At indicated time points, the number of floating cells in the medium was immediately scored by a hemacytometer. The total cell number was also counted in control dishes, which were not shaken. The number of floating cells divided by total cell number is the percentage of detached cells. For the cell-cell cohesion assay in vegetative cells, cells were shaken in suspension starting at 1×10^4 cells/ml. After 2 days, cell cultures were dropped on coverslips and immediately photographed using the 40× PlanNeofluar (NA 1.3) wide-field lens. Cells in the field of view were then counted. Triplets and clumps containing more than three cells were defined as "cell clusters", while singlet and doublets were not. To confirm the accuracy of cell number counting in large cell clusters as seen in *gα8* overexpression cells, another photograph was taken after cells dissociated from each other, which usually happened a few minutes after the cell culture was plated. The dissociation process was also recorded to examine whether cells in the medium adhere to the coverslip and whether a cytoplasmic bridge between cells was formed during the separation, which indicates the existence of cytokinesis defects in the cluster. To test whether the cohesion was EDTA or EGTA sensitive, EDTA or EGTA was added to a final concentration of 10 mM and cells continued to shake for 3 hours before they were counted. To test the effect of anti-CadA blocking, a final concentration of 20 μg/ml normal rabbit IgG or rabbit anti-CadA antiserum (R851) was added and continued to shake for 3 hours before counting. The cell cohesion assay in starving cells was performed as described (Wong et al., 2002). Cells from petri-dishes were developed in DB suspension at 5×10^6 cells/ml, and cell aggregates were photographed after 3 hours. Cell aggregates in 500 μl were dispersed by rigorously

vortexing for 15 seconds and then examined under a microscope. The cells were then allowed to re-aggregate while shaking at 180 rpm. At indicated time intervals, only single cells were scored by a hemacytometer as non-aggregated cells. The percentage of cell-cell cohesion was defined as [(total number of cells minus non-aggregated cells)/total number of cells] × 100.

Western blots

To prepare crude membrane-enriched fractions, 5×10^7 vegetative cells were washed twice with cold DB and suspended in cold DB containing 1× EDTA-free protease inhibitor cocktail (Roche). The cells were lysed by passing through an Acrodisc 5 μm pore size syringe filter (Pall). The crude membrane and cytosolic fraction were separated by centrifugation at 17,000 × g for 5 minutes at 4°C. The membrane pellet was washed twice with DB containing protease inhibitor cocktail before dissolved in 1× NuPAGE LDS Sample Buffer (Invitrogen) and 5% (v/v) β-mercaptoethanol (Sigma). For whole cells, 5×106 cells were washed twice with DB and lysed with 1× LDS Sample Buffer and 5% (v/v) β-mercaptoethanol in a total volume of 20-50 μl. The cell lysate was incubated at 90°C for 5 minutes and 3-10 μl was analyzed on 4-10% mini-protean TGX precast gel (Bio-Rad). After electrophoresis, proteins were transferred to a nitrocellulose membrane. The membrane was blocked with the Odyssey blocking buffer and incubated with the indicated antibodies. Unless otherwise mentioned, a 1:1000 dilution was used for primary antibodies and a 1:10000 dilution was used for secondary antibodies. Secondary antibodies IRDye 680LT Donkey anti-Mouse IgG (LI-COR, 926-68022) and IRDye 800CW Goat anti-Rabbit IgG (LI-COR, 926-32211) were used for 2-color detection. The

nitrocellulose membrane was developed using the Odyssey Infrared Imaging System (LI-COR，Lincoln, Nebraska).

β-galactosidase stain and activity assay

The 1681 bp 5' *gα8* region between position -1630 and position +51 was amplified from genomic DNA and inserted into the pDdGal-17, which resulted in a fusion of the first 17 codons of *gα8* in frame with *lacZ*. After transformation in wild-type Ax2 cells, β-galactosidase activity was stained with X-gal in developmental structures as described (Richardson et al., 1994). To visualize staining of structures, cells were starved on a 5 μm filter which was set on top of absorbent pads saturated with KK2 buffer (16.2 mM KH_2PO_4, 4.0 mM K_2HPO_4, pH 6.1). At different developmental stages, the filters were sprayed gently with 1% glutaraldehyde in Z buffer (60 mM Na_2HPO_4, 40 mM NaH_2PO_4, 10 mM KCl, 1 mM $MgSO_4$, pH 7.0) to fix developing structures for 10 minutes, permeabilized with 0.1% NP-40 in Z buffer for 10 minutes. Filters were washed twice with Z buffer, and then incubated with X-gal stain solution (5 mM $K_3[Fe(CN)_6]$, 5 mM $K_4[Fe(CN)_6]$, 1 mM X-gal, 1 mM EGTA in Z buffer) for 5 minutes to 24 hours. The developing of blue staining was examined under a stereomicroscope, and the filters were rinsed three times with Z buffer to remove X-gal stain solution before being photographed. Wild-type cells expressing lacZ driven by the endogenous gα8 promoter were also cultured in suspension starting at 5×10^4 cells/ml, and cell density was measured by a hemacytometer. At indicated cell density, 5×10^7 cells were collected, washed twice with KK2 buffer, and lysed with 1 ml reporter lysis buffer. The β-galactosidase activity was measured using β-Galactosidase enzyme assay system (Promega, Madison, WI).

Specific enzyme activities are given as milliunit per mg total protein. One unit is defined as the enzymatic activity that hydrolyses 1 μM of o-nitrophenyl-β-D-galactopyranoside (ONPG) per minute at pH 7.5 and 37°C.

Spore viability assay

The spore viability assay was performed as described (Brock and Gomer, 2005) with some modifications. All procedures were performed at room temperature. Cells were collected from dishes, washed twice with KK2 buffer, and suspended at 1×10^7 cells/ml. 1 ml of cells were then starved on KK2-saturated filters. After 4 days, the filter was put in a 50 ml tube and washed repeatedly with 2 ml KK2 buffer. 2 ml KK2 buffer with 0.8% NP-40 was then added to the tube. The tube was rocked gently for 10 minutes and then the filter was discarded. 11 ml KK2 buffer was added and thoroughly mixed to make a final 15 ml suspension. The density of ovoid spores was counted by a hemacytometer. 1 μl from the 15 ml suspension was diluted in 1 ml KK2 buffer, and a 100 μl dilution was plated with *K. aerogenes* bacteria on SM plates. The number of plaques was counted a week later.

Statistical analysis

The statistical significance of differences was determined by the two-tailed Student's t test or two-way ANOVA using software OriginPro 8.6.0 (OriginLab Corp., Northampton, MA, USA). $P < 0.05$ was considered to be statistically significant.

RESULTS

Gα8 elicits aberrant cytokinesis and inhibits proliferation in a Gβ-dependent manner

The function of Gα8 was first investigated almost twenty years ago and no evident phenotypes were observed for either *gα8* null mutant or *gα8* overexpression strains (Wu et al., 1994). Recently we revisited this study and explored Gα8 function further in development. Surprisingly, wild-type cells (Ax2 background) expressing *gα8* under the control of the *act15* promoter were substantially larger than control cells when grown on solid substrates such as plastic or glass (Fig. 26A). When stained with DAPI, the large cells frequently harbored multiple nuclei. In control cells, the vast majority of them had a single nucleus, and only about 5% had two nuclei. No cells with three or more nuclei were identified (Fig. 26B). In contrast, only 40%-50% of the cells overexpressing gα8 had a single nucleus, about 30% of the cells have two nuclei, and more than 20% of the cells had four nuclei or more (Fig. 26B), suggesting cells overexpressing *gα8* divide abnormally on substrates. This phenotype was also confirmed in several other wild-type background strains including JH10, DH1, Ax3 and KAx3 cells (data not shown).

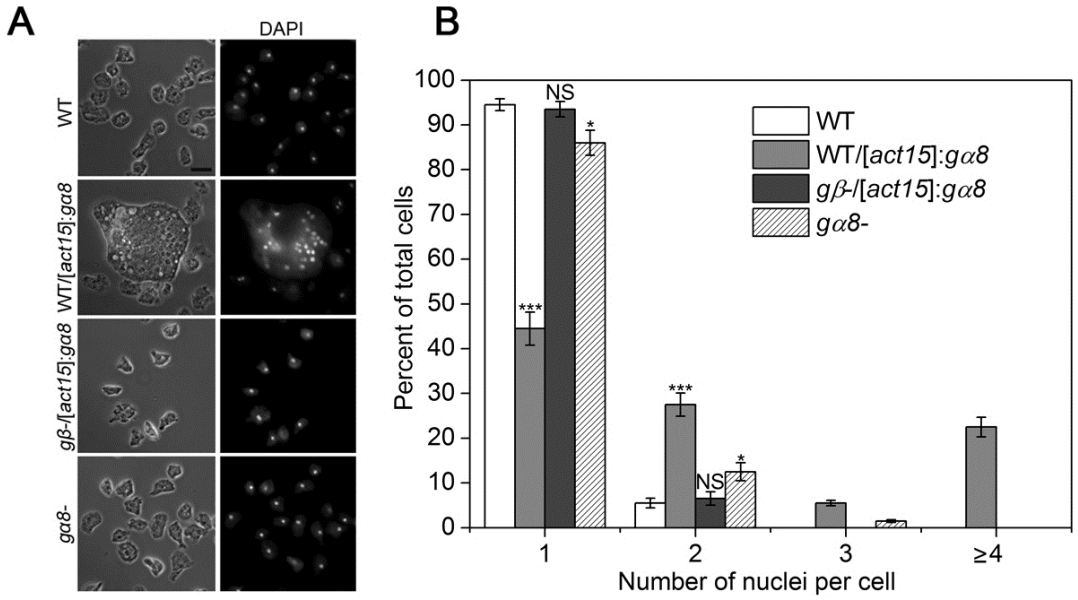

Figure 26. Characterization of nuclei per cell and cell proliferation in adherent cells lacking or overexpressing Gα8. (A) Cells were cultured in glass chambers, fixed in 4% formaldehyde and stained with DAPI. Ax2 cells were used as the wild-type (WT) cells. Images on the left panel were taken using phase microscopy. Bar, 10 µm. (B) Number of nuclei in cells from (A) was quantified. 200-300 cells were counted per sample in triplicates. Values are means ± s.e.m., and values are compared with WT values. *, $p<0.05$; ***, $p<0.001$; NS, non-significant (two-tailed Student's t test).

To test whether the deficient division of cells expressing Gα8 could be recapitulated when no adhesive force between the cell and substrate is present, cells were cultured in suspension and nuclei number was quantified. Cells grown in axenic medium usually divide faster in suspension than on a substrate (Novak et al., 1995). This contributes to the increase in double-nucleated cells observed when cells are shifted from dishes to suspension cultures (Fig. 27A and 27B). When *gα8* overexpressing cells were grown in shaking culture, less than 2% of the cells with three or more nuclei were identified, which is comparable to control cells. This suggests that the adhesive force provided by the substrate contributes to the cytokinesis failure or that shaking shears the multinucleated cells. Interestingly, *gα8* overexpressing cells had a significantly higher

percentage of single-nucleated cells and a significantly lower percentage of double-nucleated cells than untransformed cells (Fig. 27A and 27B). The expression level of Gα8 was revealed by western blots (Fig. 28A). Gα8 was expressed at relatively low levels in vegetative cells, and at least 20-fold higher in *gα8* overexpressing cells.

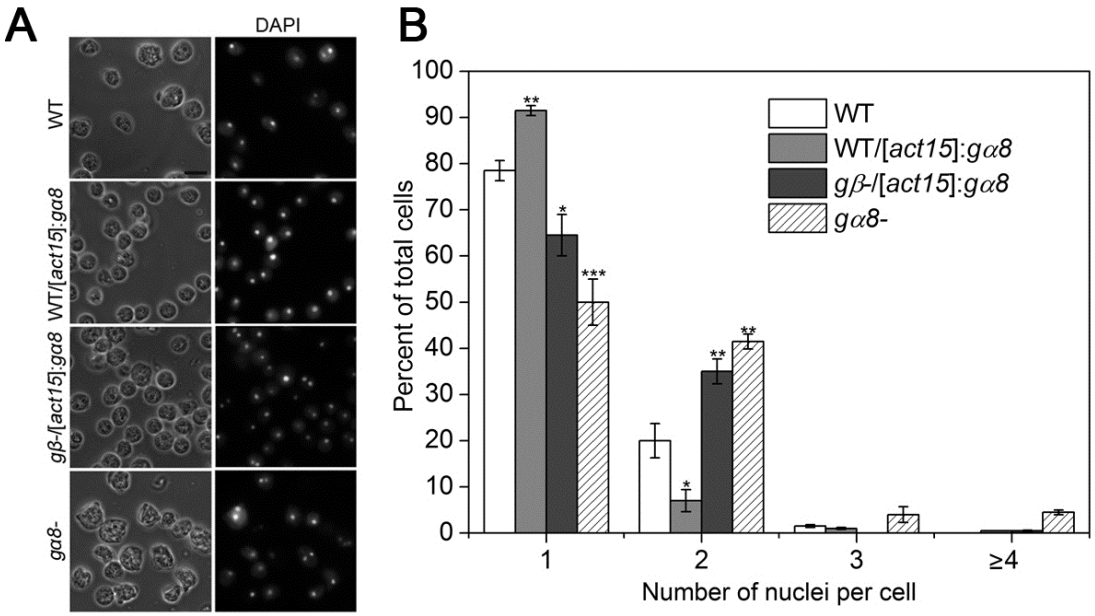

Figure 27. Characterization of nuclei per cell and cell proliferation in shaking cells lacking or overexpressing Gα8. (A) Cells from suspension culture were fixed and stained with DAPI as in Figure 26A. Cells were then spread in glass chambers. WT cells and WT cells expressing *gα8* were pretreated with 10 mM EDTA to dissociate cell clusters before fixation. Bar, 10 µm. (B) Number of nuclei in cells from (A) was quantified as in Figure 26B. Values are means ± s.e.m.. *, $p<0.05$; **, $p<0.01$; ***, $p<0.001$ (two-tailed Student's t test).

Figure 28. Expression of Gα8 in different mutants. (A) Gα8 level was probed with anti-Gα8 serum in the parental WT cells, *gα8*- cells and WT cells expressing *gα8*. Actin was used as a loading control. (B) The Gα8 level was also probed in the parental JH10 cells, *gβ*- cells and *gβ*- cells expressing *gα8*. Actin was used as a loading control.

To test whether the Gβ subunit is required for the function of Gα8, *gα8* was overexpressed in *gβ*- cells (Lilly et al., 1993). *gβ*- cells overexpressing *gα8* were indistinguishable from wild-type cells in the number of nuclei when grown on substrates (Fig. 26A and 26B). When *gβ*- cells overexpressing gα8 were grown in shaking culture, less single-nucleated cells and more double-nucleated cells were formed, as compared to control cells (Fig. 27A and 27B). The expression level of Gα8 was also examined in wild-type, *gβ*- cells and *gβ*- cells overexpressing *gα8* (Fig. 28B). The expression level of Gα8 was lower in *gβ*- cells than wild-type cells, consistent with previous studies reporting that loss of its binding partner Gβ results in a decreased amount of the Gα subunit (Marrari et al., 2007). Overexpression of *gα8* in *gβ*- cells led to at least a 20-fold increase in Gα8 expression level (Fig. 28B).

gα8- cells created in the JH10 background have been reported to proliferate rapidly (Bakthavatsalam et al., 2009). This phenotype was reproduced when *gα8* was disrupted in the Ax2 background. The successful disruption of *gα8* was confirmed by western blots (Fig. 28A). When grown in glass chambers, *gα8*- cells formed significantly

less single-nucleated cells and more double-nucleated cells as compared to wild-type cells (Fig. 26A and 26B). A very small portion of cells (about 1.5%) had three nuclei and no cell had more than four nuclei. In suspension, about 54% *gα8*- cells had a single nucleus, comparing to about 79% in wild-type cells (Fig. 27A and 27B) and about 42% cells had double nuclei, twice as many as in wild-type cells, which is consistent with a previous report (Bakthavatsalam et al., 2009). In addition, about 4.5% cells had more than four nuclei, which was attributed to the rapid proliferation of *gα8*- cells previously (Bakthavatsalam et al., 2009). The increased proportion of cells with double nuclei suggests a higher proliferation rate in *gα8*- cells as compared to wild-type cells. To confirm this is the case, the proliferation rates of *gα8*- cells, as well as *gα8* overexpressing cells, were directly measured in suspension. *gα8*- cells proliferated faster than wild-type cells as previously described (Bakthavatsalam et al., 2009), whereas overexpression of *gα8* drastically inhibited proliferation (Fig. 29). gβ- cells have been shown to proliferate faster than wild-type cells (Bakthavatsalam et al., 2009), and gβ- cells expressing *gα8* still exhibited a rapid proliferation rate (Fig. 29) which is comparable to gβ- cells transformed with an empty pDM304 vector (data not shown), and suggests that the function of Gα8 is dependent on Gβ.

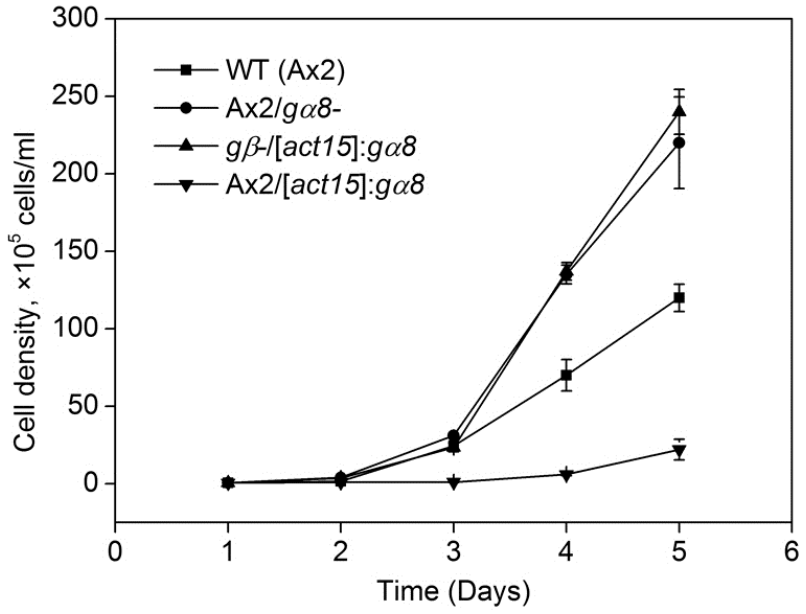

Figure 29. Proliferation of different *gα8* mutants in suspension. Cells were diluted to 5 × 10^4 cells/ml in HL-5 medium and the cell density was measured daily. The graph shows means ± s.e.m. from three independent experiments. The differences between each strain are as follows: *gα8*- cells versus WT cells, $p<0.01$; *gβ*- cells expressing *gα8* versus WT cells, $p<0.01$; WT cells expressing gα8 versus WT cells, $p<0.001$ (Two-way ANOVA).

The overexpression of another Gα subunit, Gα1, has a similar multinucleated phenotype (Kumagai et al., 1989). Therefore I attempted to reproduce this data in a wild-type Ax2 background. Although overexpression of *gα1* in wild-type cells induced multinucleated cells on substrates (Fig. 30A), only about 2% of the cells had three or more nuclei, and the difference in the percentage of single-nucleus and double-nuclei cells between wild-type cells transformed with an empty vector and wild-type cells overexpressing *gα1* was insignificant (Fig. 30B). Gα1 was expressed at an extremely low level in axenic cells, and was strongly induced when overexpressed (Fig. 30C). Interestingly, overexpression of *gα1* did not significantly inhibit cell proliferation (Fig. 30D), suggesting that Gα1 functions differently than Gα8.

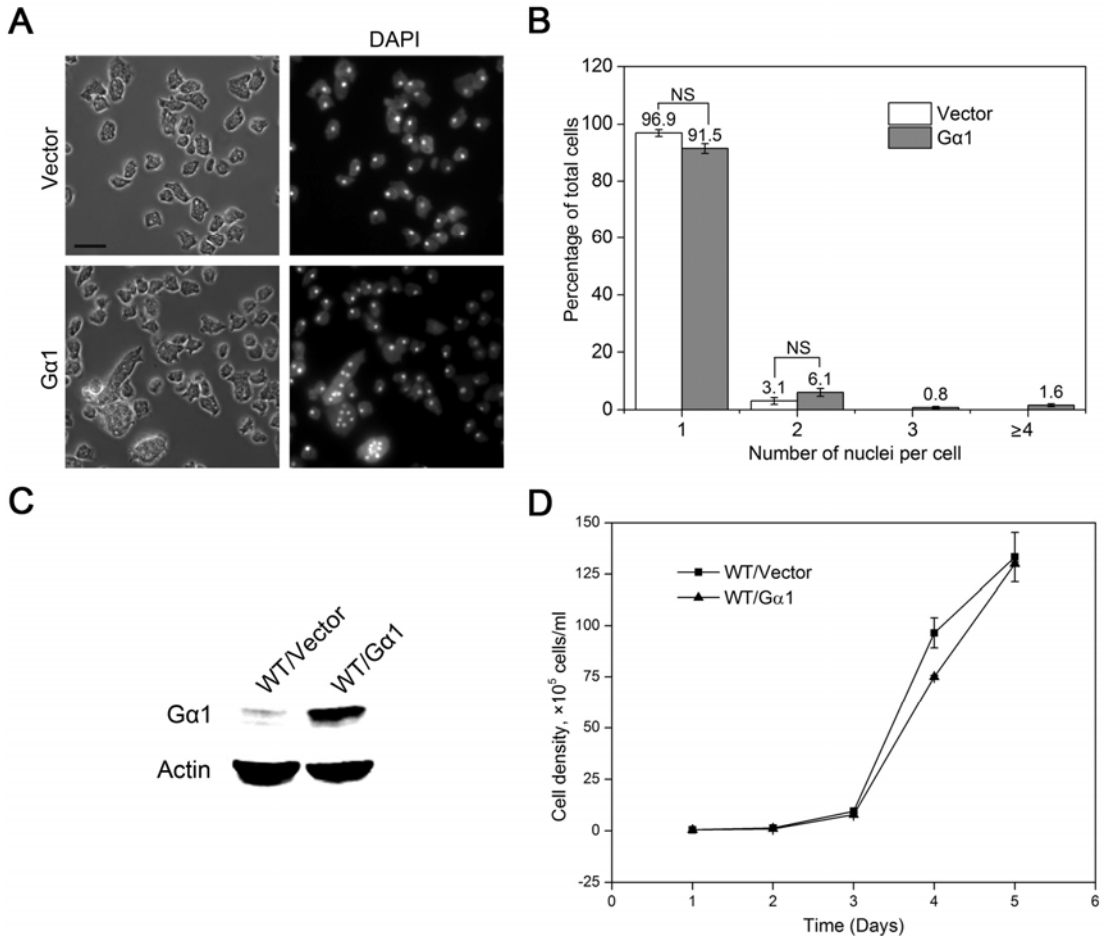

Figure 30. Phenotypic characterization of Gα1 overexpression in wild-type Ax2 cells. (A) The pDM304 vector and *gα1* were transformed in WT cells. Cells were fixed and stained with DAPI. Bar, 10 µm. (B) Number of nuclei in cells from (A) was quantified. 200-300 cells were counted per sample in triplicates. Values are means ± s.e.m.. NS, non-significant (two-tailed Student's t test). (C) The Gα1 expression levels were examined in cells from (A) using anti-Gα1. (D) Cells were shaken starting at 5×10^4 cells/ml and cell density was measured daily. The graph shows means ± s.e.m. from three independent experiments. The differences between each strain are as follow: WT cells expressing *gα1* versus WT cells expressing the pDM304 vector, p=0.23 (Two-way ANOVA).

Gα8 promotes both cell-cell cohesion and cell-substrate adhesion

When grown in suspension, more than 80% of cells overexpressing *gα8* tended to form large clusters with other cells, whereas about 35% of control cells formed clusters (Fig. 31A and 31B). The natural dissociation of the clusters was carefully examined on a coverslip and with the addition of 10 mM EDTA or EGTA, which completely dissociated the clusters (Fig. 31A and 31B). This suggests that Ca^{2+}-dependent cell-cell interaction facilitates the formation of the clusters. In *D. discoideum*, CadA (Gp24) is the major cell adhesion molecule mediating Ca^{2+}-dependent cell-cell interaction (Siu et al., 2011). Therefore, I tested whether anti-CadA serum blocks the formation of the clusters. A final concentration of 20 μg/ml anti-CadA serum successfully reduced clusters to 25% of total cells, which is in stark contrast to more than 70% in normal IgG treated cells (Fig. 31A and 31B). This suggests that CadA is responsible for the cluster formation. In addition, cells overexpressing *gα8* at a low density of 1.5×10^5 cells/ml (cells from Fig. 31A) showed an increased CadA expression level (Fig. 31C), indicating that overexpression of *gα8* promotes expression of CadA in suspensions with low densities. However, both *gα8*- cells and cells overexpressing *gα8* were indistinguishable in their CadA expression levels from wild-type cells collected from petri-dishes (Fig. 32A) or from high density suspension cultures (data not shown). Since the CadA levels are positively correlated with cell density and CadA is expressed at a high level in petri-dishes and in dense suspensions (Fig. 32A and 32B), overexpression of *gα8* may not significantly induce the amount of CadA at these stages. *gα8*- cells had a similar percentage of cells in clusters as wild-type cells, and comparable CadA levels at the low density of 1.5×10^5 cells/ml (data

not shown). These results suggest that disruption of *gα8* is not sufficient to suppress the expression of CadA and inhibit adhesion in vegetatively growing cells.

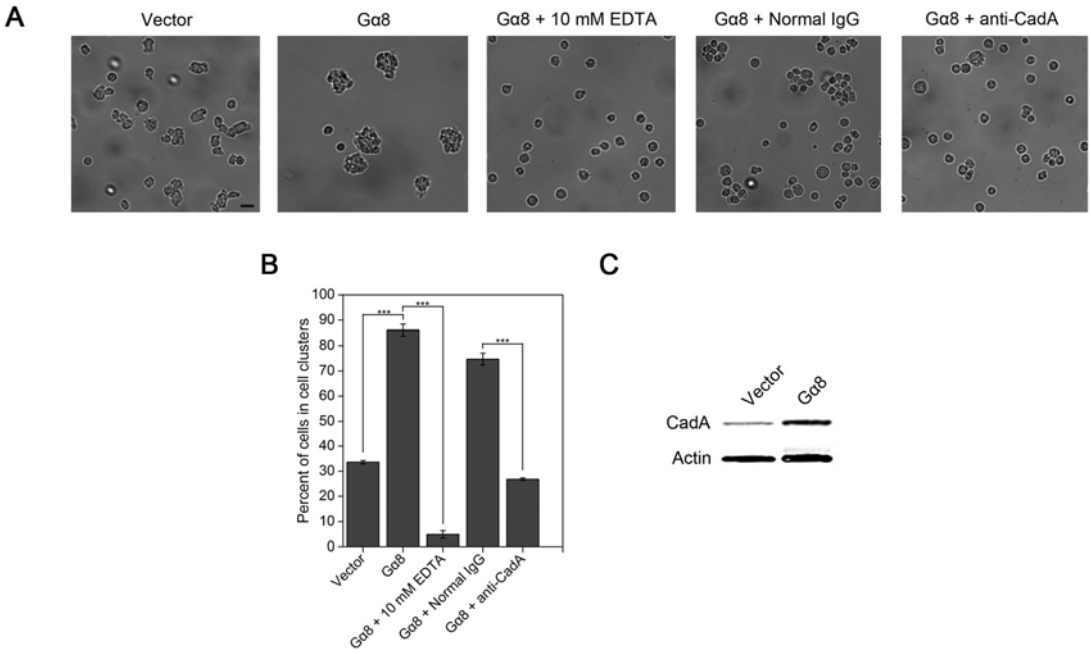

Figure 31. Induction of adhesion in response to Gα8 overexpression. (A) WT cells expressing an empty vector or *gα8* were shaken in suspension starting at 5×10^4 cells/ml. After two days, cells were allowed to settle in glass chambers and photographed immediately. For EDTA and anti-serum treatment, 10 mM EDTA and 20 μg/ml normal IgG or anti-CadA serum were added to the suspension during 3 hours continuous shaking. Bar, 10 μm. (B) The percentage of cells in clusters from (A) was quantified. 150-200 cells were counted per sample in triplicates. Values are means ± s.e.m.. ***, $p<0.001$ (two-tailed Student's t test). (C) CadA levels were examined in cells expressing an empty vector or *gα8* from (A) using monoclonal anti-CadA antibody.

CadA has been shown to initiate homophilic interactions between cells after starvation (Siu et al., 2011). Therefore, I tested whether overexpression of *gα8* could promote cell-cell aggregation after development. A large portion of control cells existed as small clumps or single cells after shaking for three hours in DB. By contrast, cells

expressing *gα8* formed large clumps, and single cells were seldom observed (Fig. 33A). Examination of the re-aggregation of dispersed cells showed that cells expressing *gα8* rapidly aggregated, but could not aggregate in the presence of 10 mM EDTA (Fig. 33B). This suggests that overexpression of Gα8 promotes cell-cell aggregation after the onset of development, even though it does not substantially induce the expression of CadA when grown on petri-dishes (Fig. 32A).

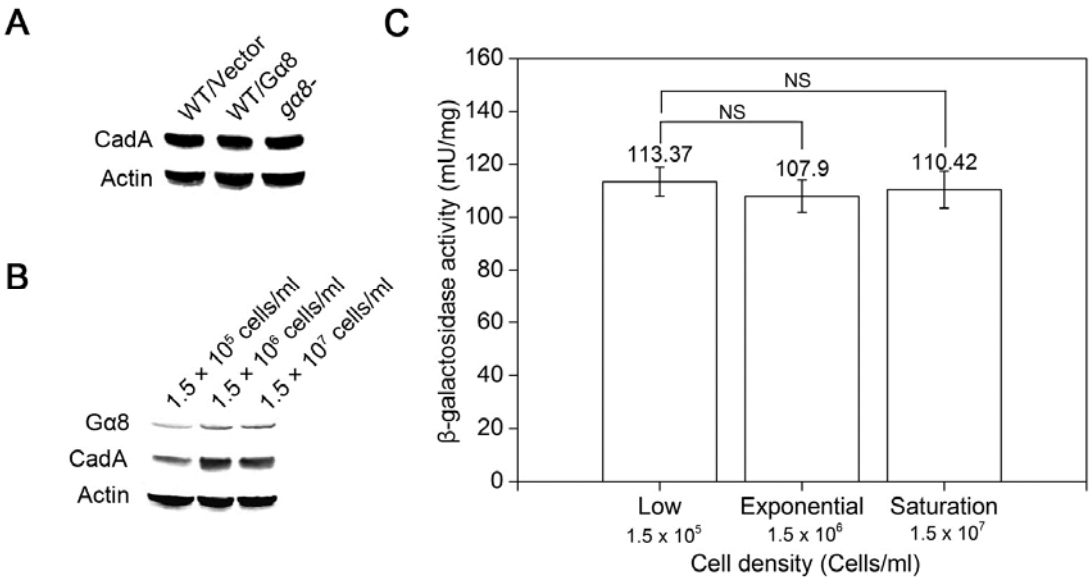

Figure 32. Expression of CadA and Gα8 in vegetative growing cells. (A) Same amount of cells were collected from dishes and lysed for probing the CadA expression level using anti-CadA antibody. (B) WT cells were diluted to 5×10^4 cells/ml, and shaken in suspension. At indicated cell density, same amount of cells were collected and examined for expression level of CadA and Gα8. (C) WT cells expressing *lacZ* driven by the endogenous *gα8* promoter were shaken in suspension starting at 5×10^4 cells/ml. At indicated cell density, cells were collected and the β-galactosidase activity was assayed.

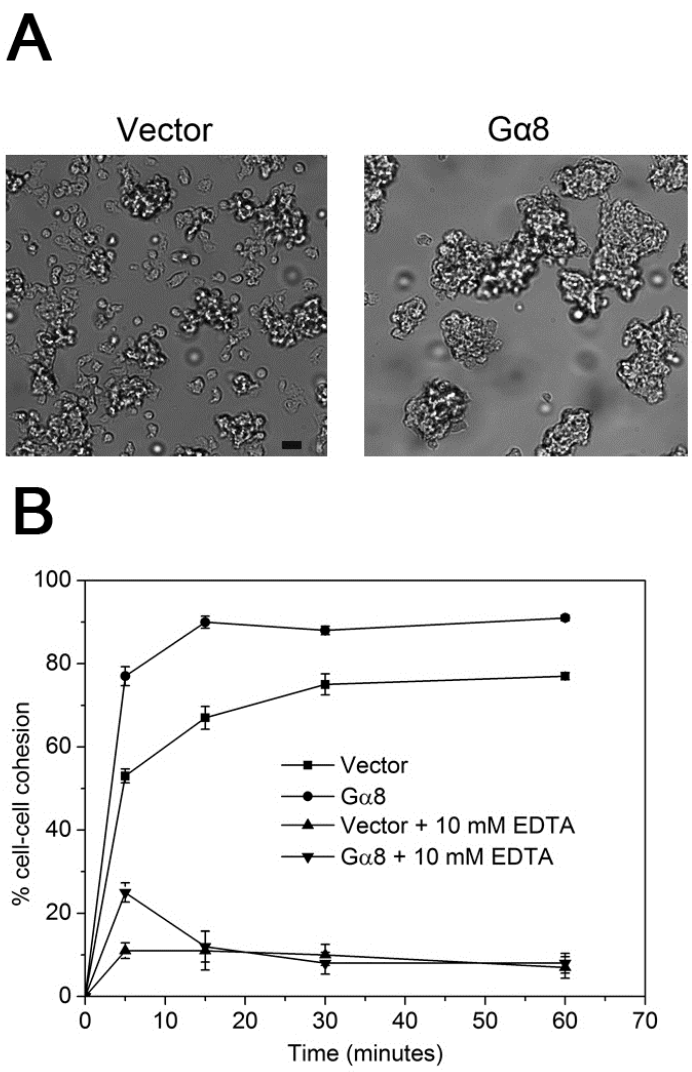

Figure 33. Effect of Gα8 overexpression on cell-cell cohesion. (A) Cells expressing an empty vector or *gα8* were starved in DB while in shaking suspension for 3 hours. Cells were then plated in chambers and photographed. Bar, 10 μm. (B) Cells from (A) were dissociated by rigorous vortexing and cell reassociation was monitored over time in the absence or presence of 10 mM EDTA. Data represent means ± s.e.m. of three independent experiments. WT cells expressing *gα8* versus WT cells expressing empty vector without EDTA, $p<0.001$; with EDTA, $p=0.17$ (Two-way ANOVA).

Cells utilize cell-cell adhesion to communicate and form multicellular structures, and they require adhesive forces to move on a substrate. Different components are

employed in cell-cell adhesion and cell-substrate adhesion in the social amoeba (Cornillon et al., 2006; Fey et al., 2002; Niewohner et al., 1997; Siu et al., 2011). Since overexpression of Gα8 induces cell-cell cohesion, the cell-substrate adhesion level was also examined. After 2 hours in shaking suspension, only about 30% of cells expressing *gα8* were released from the dishes, whereas about 80% of wild-type cells were detached (Fig. 34A). No significant difference was observed in the percentage of detached cells between wild-type cells and *gα8*- cells (Fig. 34A). These results suggest that overexpression of Gα8 promotes cell-substrate adhesion. However, loss of Gα8 does not result in adhesion loss. Overexpression of Gα8 suppresses proliferation when grown in suspension (Fig. 29), and it also substantially reduces proliferation when grown on substrates (Fig. 34B).

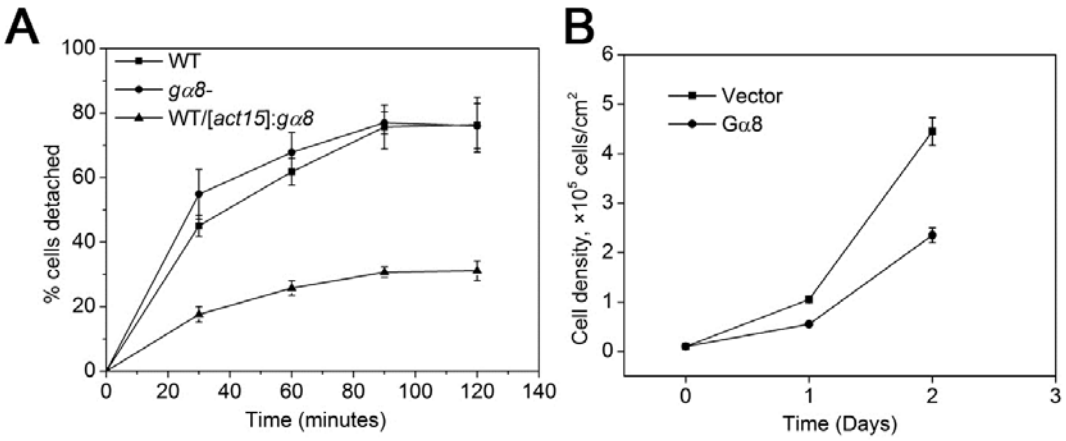

Figure 34. Effect of Gα8 on cell-substrate adhesion. (A) 5×10^5 cells were plated in dishes and the dishes were set on a rotary shaker to detach cells. Cells floating in the medium were scored at indicated time. Data represent means ± s.e.m. of three independent experiments. *gα8*- cells versus WT cells, p=0.32; WT cells expressing *gα8* versus WT cells, p<0.001 (Two-way ANOVA). (B) Cells were plated in dishes at 1×10^4 cells/cm^2, and cell density was measured daily. Data represent means ± s.e.m. of three independent experiments. WT cells expressing *gα8* versus WT cells harboring an empty vector, p<0.001 (Two-way ANOVA).

Previous studies have suggested that Gα8 is indispensable for the proliferation-inhibiting and chemorepellant activity of the autocrine signal AprA (Bakthavatsalam et al., 2009; Phillips and Gomer, 2012). AprA accumulation corresponds to cell density and reaches the highest level when density saturates (Choe et al., 2009). However, Gα8 was expressed at a very low level in suspension, and was only slightly induced when density increased (Fig. 32B). In addition, the reporter activity of lacZ driven by the *gα8* promoter did not change when grown in suspension (Fig. 32C).

GDP-bound Gα8 associated with Gβγ is essential for the aberrant cytokinesis induced by Gα8

The G protein heterotrimer is usually localized and functions at the plasma membrane, and efficient plasma membrane targeting requires the interaction of Gα with Gβγ (Fishburn et al., 2000; Hepler et al., 1993; Marrari et al., 2007). In *D. discoideum*, Gα2 failed to localize to the plasma membrane but instead was enriched in the cytoplasm in the absence of the Gβ subunit (unpublished data, Gus Wright). To verify the localization of Gα8 and examine whether loss of Gβ alters the localization of Gα8, crude membrane and cytosolic fractions were separated and examined by western blot analysis to determine Gα8 levels. Gα8 was enriched in the membrane fraction in both wild-type cells and in *gβ*- cells (Fig. 35A). In addition, the Gα8-GFP fusion was localized to the plasma membrane of both wild-type and *gβ*- cells (Fig. 35B). The fusion induced large multinucleated cells in wild-type cells (Fig. 35B), though the percentage of multinucleated cells was lower as compared to cells overexpressing untagged Gα8 (data not shown). It is worth noting that Gα8 was sometimes not uniformly enriched in the entire cell periphery of the extremely large multi-nucleated cells. Like untagged Gα8, the fusion did not induce cytokinesis failure in gβ- cells (Fig. 35B). Therefore, in addition to showing that an intact heterotrimer is involved in the cytokinesis failure, these results suggest that the plasma membrane localization of Gα8 is independent of Gβ.

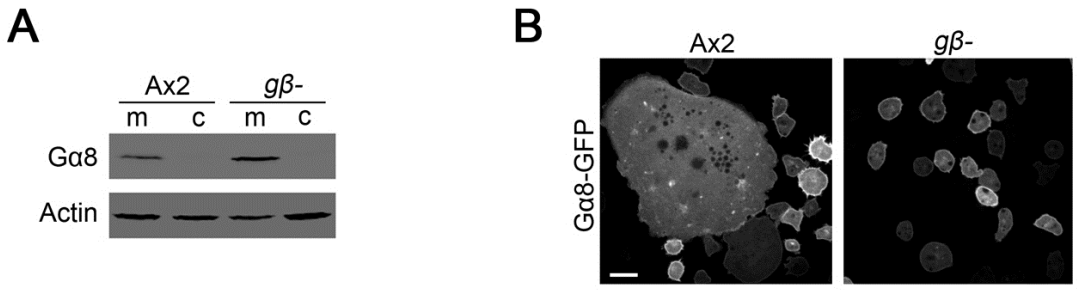

Figure 35. Localization of Gα8 in wild-type Ax2 and *gβ*- cells. (A) For western blot analysis, the crude membrane fraction and cytosol fraction were separated by filtering cells through 5 μm filters. Gα8 level in each fraction was examined using anti-Gα8 serum. m, membrane fraction; c, cytosol fraction. (B) The Gα8-GFP fusion was expressed in WT and *gβ*- cells. Images were taken on a spinning disk confocal microscope. Bar, 10 μm.

I next tried to recapitulate the cytokinesis defect using putative constitutively active mutants of Gα8. Two different mutants were generated by replacing glycine with valine at position 41 ($G\alpha8^{G41V}$), or by replacing glutamate with leucine at position 203 ($G\alpha8^{Q203L}$) to theoretically ablate GTPase activity as described (Conklin and Bourne, 1993; Rens-Domiano and Hamm, 1995). If the function of Gα8 required activation, these mutations should augment the cytokinesis defect. To our surprise, none of these mutations induced any cytokinesis defects (Fig. 36A). I also generated a dominant negative Gα8 mutant by mutating the serine residue of the G1 motif ($G\alpha8^{S46C}$), which is essential for binding the phosphate moieties of guanine nucleotides and Mg^{2+} (Noel et al., 1993). This mutation leads to reduced affinity for GDP and Gβγ sequestration in Gα subunits (Natochin et al., 2006; Slepak et al., 1993), thereby inhibiting signaling by the wild-type G protein. The dominant negative $G\alpha8^{S46C}$ (Fig. 11A) did not lead to cytokinesis defects, consistent with *gα8*- cells, which also grow quite normally when grown on substrates (Fig. 26A and 26B). Interestingly, a truncated Gα8 with the removal

of the last 51 amino acids ($G\alpha8^{\Delta Tail}$) led to cytokinesis failure (Fig. 36A), although the defect was less severe than that induced by intact Gα8. These data suggest that proper cycling of Gα8 between the GDP and GTP bound state is required to induce cytokinesis defects. With the exception of cells expressing $G\alpha8^{\Delta Tail}$, which lacks the antigen region where the anti-serum was raised, the levels of Gα8 in various strains shown in Fig. 36A were confirmed by western blot analysis (Fig. 36B).

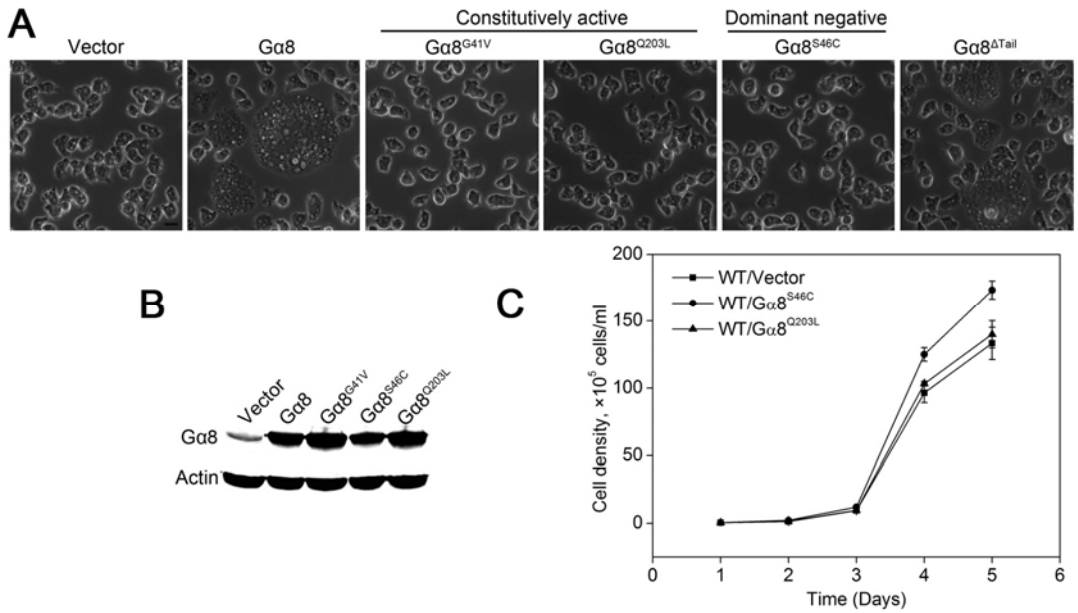

Figure 36. Effect of different mutant forms of Gα8 on cell division. (A) The empty vector pDM 304 or Gα8 forms with different acitvity were expressed in WT cells. Images were taken using phase microscopy. Bar, 10 μm. (B) Gα8 level in cells from (A) was confirmed using anti-Gα8 serum. (C) Cells were cultured in shaking suspension starting at 5×10^4 cells/ml and the cell density was measured daily. The graph shows means ± s.e.m. from three independent experiments. The differences between each strain are as follow: WT cells expressing dominant negative $G\alpha8^{S46C}$ versus WT cells expressing empty vector, $p<0.01$; WT cells expressing constitutively active $G\alpha8^{Q203L}$ versus WT cells expressing empty vector, $p=0.39$ (Two-way ANOVA).

In addition to displaying regular cytokinesis, cells expressing constitutively active Gα8^{Q203L} proliferated normally in suspension (Fig. 36C). As expected, cells expressing dominant negative Gα8^{S46C} grew significantly faster than control cells (Fig. 36C). One possible explanation for why constitutively active Gα8 mutants show no phenotypes when overexpressed is that these mutations modulate the G protein conformation and trigger the internalization of Gα8. To test this possibility, the Gα8 mutants were expressed in *gα8*- cells and stained with the anti-Gα8 serum. Intact Gα8, constitutively active Gα8^{Q203L}, and dominant negative Gα8^{S46C} were all enriched on the plasma membrane, which demonstrate that these mutations do not alter the localization of Gα8 (Fig. 37).

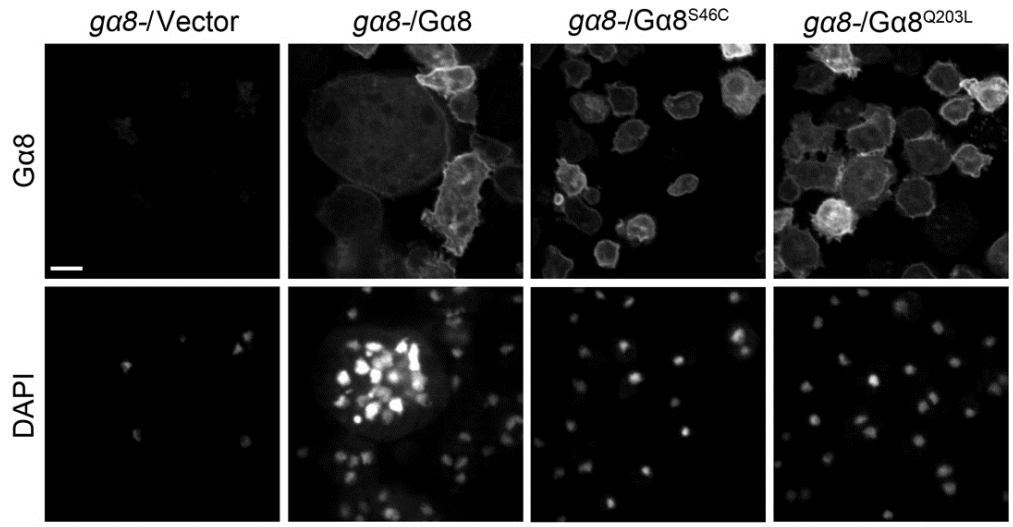

Figure 37. Subcellular localization of Gα8 mutants. Different forms of Gα8 were expressed in *gα8*- cells. Cells were then fixed and labeled with anti-Gα8 serum and DAPI and again images were taken by confocal microscopy. Bar, 10 μm.

Another possibility is that Gα8 sequesters the Gβγ subunit. Overexpression of Gα8 might limit the amount of free Gβγ that could interact with other Gα subunits, therefore the phenotypes observed in cells overexpressing Gα8 might be from a lack of Gα signaling in general. To examine this possibility, Gβγ was co-overexpressed with Gα8 to see whether the cytokinesis defect could be rescued. Overexpression of Gβγ alone in wild-type cells did not induce any cytokinesis abnormalities (Fig. 38A). Overexpression of Gα8 in cells overexpressing Gβγ still exhibited a similar cytokinesis defect when compared to cells expressing Gα8 alone (Fig. 38A), indicating Gα8 does not function by sequestering Gβγ to induce cytokinesis defects. The induced level of Gβ and Gγ were confirmed by western blots (Fig. 38B), as were the amounts of Gα8 in cells coexpressing Gβγ (Fig. 38C).

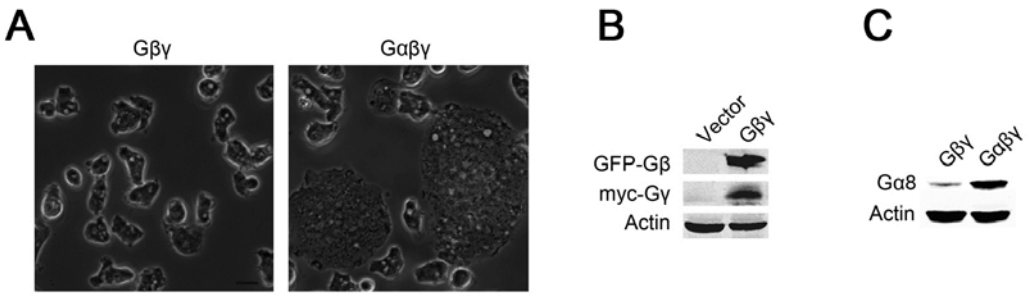

Figure 38. The induction of cytokinesis defects by the heterotrimer Gα8βγ. (A) myc-Gγ was cloned into pDM358 and co-transformed with GFP-Gβ into WT cells to generate cells expressing Gβγ. Gα8 was cloned into pDM328 and expressed in cells expressing Gβγ. Images were taken using phase microscopy. Bar, 10 μm. (B) Gβ and Gγ levels were examined in cells expressing Gβγ using anti-GFP antibody and anti-myc antibody. (C) Gα8 level was confirmed in cells expressing Gα8βγ using anti-Gα8 serum.

I also examined the localization of Gα8 during cytokinesis. An inducible expression system of Gα8-GFP was generated using the *discoidin I* promoter. Expression

of Gα8-GFP under the control of the *discoidin I* promoter in *gα8*- cells significantly increased the number of multinucleated cells, whereas repression of Gα8-GFP by adding 1 mM folate rescued the cytokinesis defect (Fig. 39A), suggesting that the cytokinesis defect depends on the amount of Gα8. The reduction of Gα8-GFP by addition of folate was confirmed by western blot (Fig. 39B). When cells with reduced Gα8-GFP level undergo cytokinesis, Gα8-GFP appears to be localized uniformly across the plasma membrane (Fig. 39C). GFP-Gβ is also localized uniformly across the plasma membrane during cytokinesis (Fig. 39D).

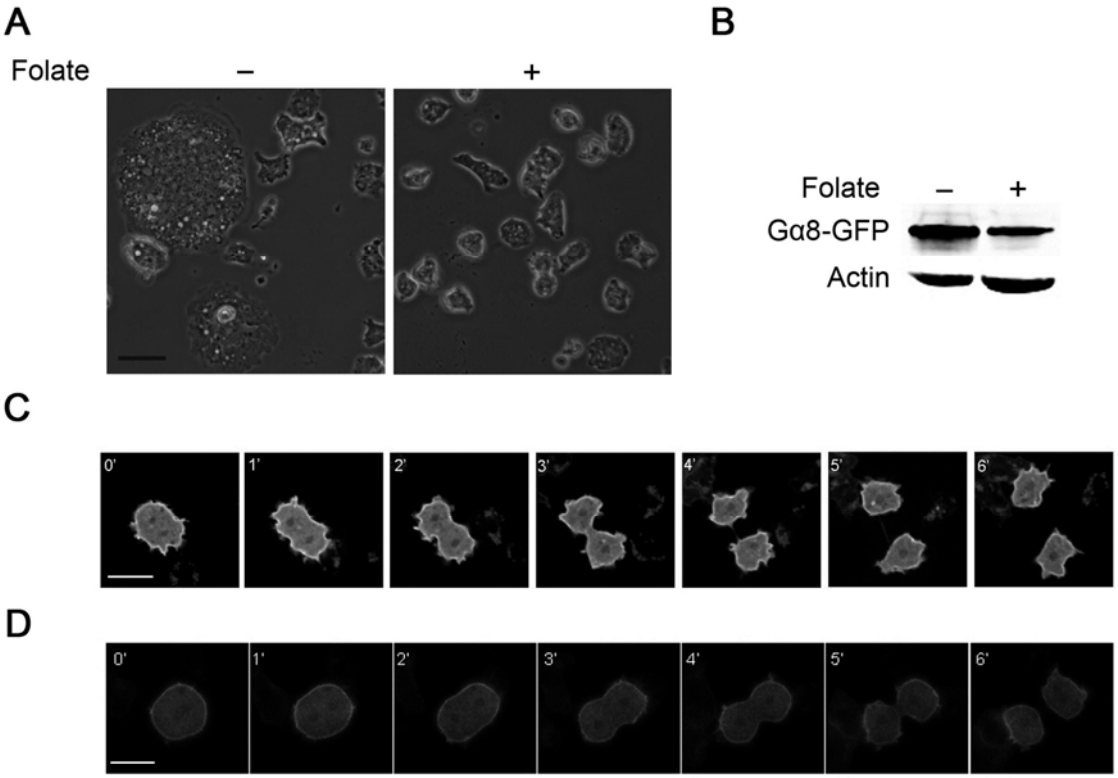

Figure 39. Distribution of Gα8 and Gβ during cytokinesis. (A) *gα8*- cells expressing *gα8-gfp* driven by *discoidin I* promoter were cultured in glass chambers in HL-5 medium, and 1 mM folate was added to repress Gα8 expression. After three days, images were taken using phase microscopy. Bar, 10 μm. (B) Gα8 level in cells with or without folate was examined using anti-Gα8 serum. (C) *gα8*- cells expressing *gα8-gfp* driven by the *discoidin I* promoter were cultured with bacteria overnight. Cells were collected, washed with DB and plated in glass chambers. Cells about to divide were identified by their round shape, and the cytokinesis process was captured every 15 seconds. The experiment was repeated three times and at least 5 dividing cells were observed each time. A typical cytokinesis is shown here at a 1 minute interval. Bar, 10 μm. (D) Wild-type Ax2 cells expressing GFP-Gβ and myc-Gγ (Same cell line as in Fig. 38A left panel) were cultured with bacteria overnight and the cytokinesis process was captured as in (C). Bar, 10 μm.

The cytokinesis defect induced by Gα8 is caused by increased cell-substrate adhesion

Since Gα8 induces CadA expression and promotes cell-cell cohesion, I examined whether loss of CadA might attenuate the cytokinesis defect caused by Gα8 overexpression. *cadA*- cells were previously generated and they exhibited very mild

cytokinesis defects (Kim et al., 2011; Wong et al., 2002). Overexpression of *gα8* in *cadA*- cells resulted in a similar cytokinesis defect as seen for *gα8* overexpression in wild-type cells (Fig. 40A and 40B). This indicates that reducing CadA level could not rescue the cytokinesis defect induced by Gα8. Western blot showed that Gα8 was significantly induced by overexpression both in wild-type and *cadA*- background (Fig. 40B inset).

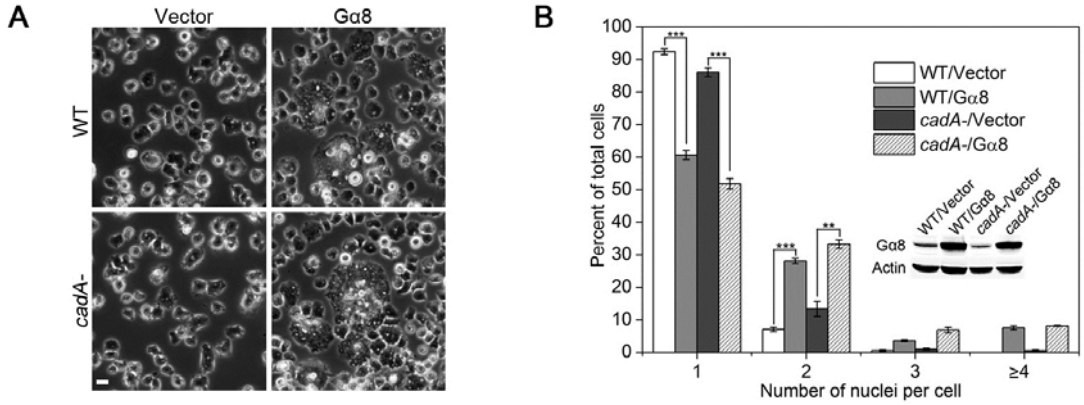

Figure 40. Overexpression of *gα8* in *cadA*- cells. (A) The empty vector pDM304 and Gα8 were expressed in the parental KAx3 cells (WT) and *cadA*- cells. Images were taken using phase microscopy. Bar, 10 μm. (B) Cells from (A) were fixed and stained with DAPI. 200-300 cells were counted per sample in at least triplicates. Values are means ± s.e.m.. **,$p<0.01$; ***, $p<0.001$ (two-tailed Student's t test). Inset, the Gα8 levels were examined in cells from (A) using anti-Gα8 serum.

Since Gα8 also promotes cell-substrate adhesion, I next postulated that the increased cell-substrate adhesion may cause the cytokinesis defect. If this is true, low cell-substrate adhesion might rescue the defect, and the extent of rescue would depend on the level of cell-substrate adhesion. I used two mutants to test our hypothesis, *paxB*- and *sadA*- cells. It has been previously shown by two independent studies that loss of Paxillin results in decreased cell-substrate adhesion (Bukharova et al., 2005; Nagasaki et al.,

2009). About 0.5% of *paxB*- cells transformed with an empty vector had four nuclei and had normal or slightly large morphology as (Fig. 41A arrow) and very few cells have five or more nuclei. Overexpression of Gα8 in *paxB*- cells still induced large multinucleated cells as shown in Fig. 41A (arrow head), however, only about 1.5% of the cells were evidently large and had more than four nuclei (Fig. 41B), significantly lower than gα8 overexpression in wild-type background. Moreover, the percentage of cells with one or two nuclei was indistinguishable between control *paxB*- cells and *paxB*- cells expressing *gα8* (Fig. 41B). The induced Gα8 level in *paxB*- cells overexpressing gα8 was confirmed by western blotting (Fig. 41B inset). Although overexpression of *gα8* in *paxB*- cells had no significant cytokinesis defect, it dramatically reduced the proliferation of *paxB*- cells in suspension (Fig. 41C). This suggests that the cytokinesis defect, but not the proliferation defect, as induced by *gα8* overexpression, is suppressed by loss of Paxillin.

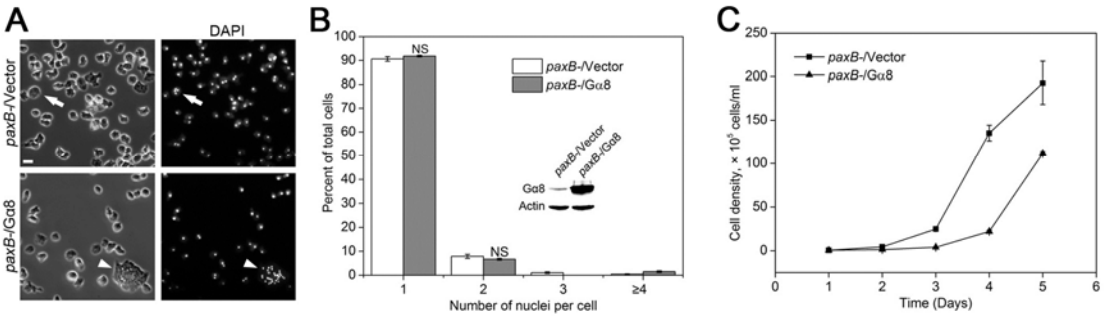

Figure 41. Overexpression of Gα8 in *paxB*- cells. (A) The pDM304 vector and Gα8 were expressed in *paxB*- cells. Cells were fixed and stained with DAPI. Bar, 10 μm. (B) Number of nuclei in cells from (A) was quantified. 200-300 cells were counted per sample in at least triplicates. Values are means ± s.e.m.. NS, non-significant (two-tailed Student's t test). Inset, the Gα8 levels were examined in cells from (A) using anti-Gα8 serum. (C) *paxB*- cells expressing pDM304 vector or Gα8 were diluted to 5×10^4 cells/ml, and cell density was measured daily. *paxB*- cells expressing *gα8* versus *paxB*- cells expressing pDM304 vector, $p<0.001$ (two-way ANOVA).

The second mutant examined was *sadA* nulls, which have severely impaired cell-substrate adhesion, can barely attach to the substrate, and have cytokinesis defects (Fey et al., 2002). *sadA*- cells exhibited strong cytokinesis defects with 7% having three or more nuclei and more than 20% having double-nuclei (Fig. 42A and 42B). Interestingly, overexpression of gα8 in *sadA*- cells significantly increased the percentage of cells with a single nucleus, and reduced the percentage of cells with two or more nuclei (Fig. 42A and 42B). This indicates the cytokinesis defect caused by loss of adhesion in *sadA*- cells was partially rescued. The induced Gα8 level by overexpression was also confirmed by western blotting (Fig. 42B inset). Similar to *paxB*- cells expressing *gα8*, *sadA*- cells expressing *gα8* exhibited extremely slow proliferation (Fig. 42C). This suggests the proliferation-inhibiting activity of Gα8 is independent of induced cell-substrate adhesion. Taking these data together, the Gα8-induced cytokinesis defect can be rescued by reducing cell-substrate adhesion.

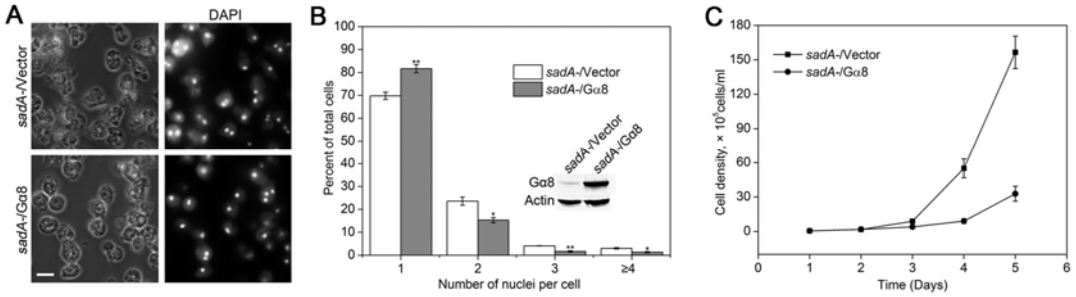

Figure 42. Overexpression of Gα8 in *sadA*- cells. (A) The pDM304 vector and Gα8 were expressed in *sadA*- cells. Cells were fixed and stained with DAPI. Bar, 10 μm. (B) Number of nuclei in cells from (A) was quantified. 200-300 cells were counted per sample in at least triplicates. Values are means ± s.e.m.. *, $p<0.05$; **. $p<0.01$ (two-tailed Student's t test). Inset, the Gα8 levels were examined in cells from (A) using anti-Gα8 serum. (C) Proliferation of *sadA*- expressing pDMA304 or Gα8 in suspension was measured as in Fig. 16C. *paxB*- cells expressing *gα8* versus *paxB*- cells expressing pDM304 vector, $p<0.01$ (two-way ANOVA).

Gα8 is enriched in stalk cells and required for the differentiation of anterior-like cells

Gα8 levels rise after starvation (Wu et al., 1994), and disruption of *gα8* does not cause any dramatic phenotypes except rapid proliferation (Bakthavatsalam et al., 2009) (Fig. 29). To address the functions of Gα8 during development, I examined the life cycle of *gα8*- cells and cells overexpressing *gα8*. Wild-type cells or those carrying the pDM304 vector exhibited a similar life cycle, with aggregation and mounds forming at 6 hours after the onset of starvation (Fig. 43). At 24 hours, most of the cells form fruiting bodies (Fig. 43). However, *gα8*- cells showed a slight delay (about 1-2 hours) in aggregation, but were able to finish the life cycle in 24 hours (Fig. 43). In contrast, *gα8* overexpressing cells only formed small aggregates on the cell lawn (Fig. 43). At 24 hours, only a small portion of cells formed tiny fruit bodies, whereas most cells were culminating or still solitary (Fig. 43). Cells expressing constitutively active $G\alpha8^{Q203L}$ developed normally (Fig. 43). This is not surprising, as $G\alpha8^{Q203L}$ also did not display cytokinesis defects. I

also confirmed the expression pattern of Gα8 after starvation. Consistent with a previous study (Wu et al., 1994), Gα8 protein levels gradually increase after starvation and peak at 4 hours (Fig. 44A).

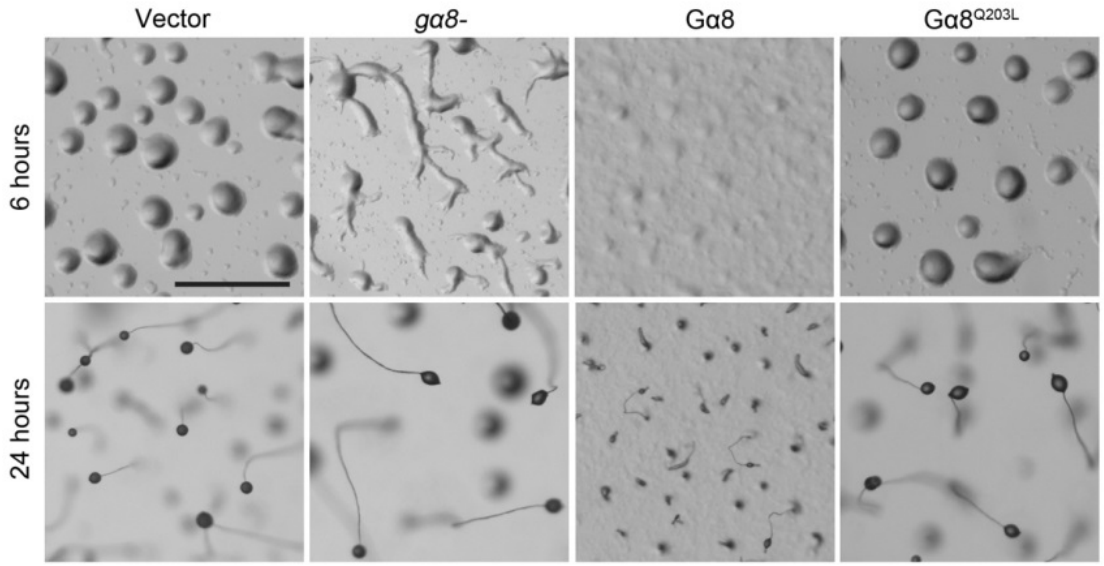

Figure 43. Early development of Gα8 mutants. 5×10^6 vegetative cells were washed with DB twice and plated on non-nutrient DB agarose. Images were taken at indicated hours after development. Bar, 1 mm.

Overexpression of Gα8 promotes adhesion in vegetative cells. However, disruption of *gα8* barely reduces adhesion. When taken together with the temporal expression pattern of Gα8, I hypothesized that the adhesion loss of *gα8*- cells might happen in later development. To investigate this possibility, the expression of three adhesion molecules CadA, CsA (Gp80) and tgrC1 (Gp150) were examined during the development of *gα8*- cells. In wild-type cells, CadA expression decreased concomitantly with the increase of CsA. Interestingly, CsA was only weakly induced and CadA

remained unchanged in *gα8*- cells (Fig. 44B). A previous study showed that the CsA level is increased to compensate the loss of CadA (Wong et al., 2002), therefore our data suggest that CadA compensates for low levels of CsA in *gα8*- cells. It has been reported that loss of CsA expression induces the precocious expression of TgrC1 (Wang et al., 2000). However, TgrC1 was still expressed at a relatively low level in *gα8*- cells when compared to wild-type cells (Fig. 44B). These data suggest that disruption of *gα8* inhibits expression of certain adhesion molecules.

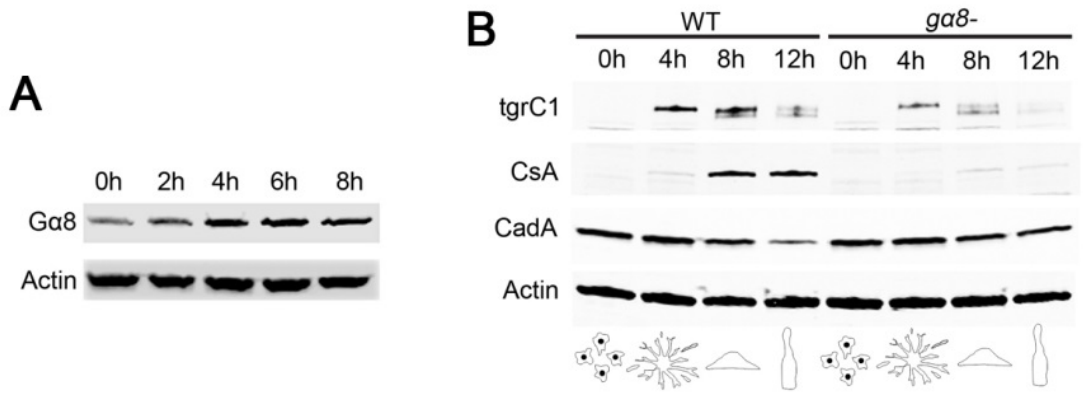

Figure 44. Expression of Gα8 and adhesion molecules during early development. (A) 5×10^6 WT cells were starved on non-nutrient agarose. At indicated hours cells were collected, lysed and examined for Gα8 expression. (B) Same as in (A), WT cells and *gα8*- cells were starved on non-nutrient agarose and collected at indicated hours. The expression levels of adhesion molecules tgrC1, CsA and CadA were then examined. The cartoon at the bottom shows developmental stages at indicated hours.

To better understand the role Gα8 plays during development, I examined the spatial pattern of *gα8* expression using a *lacZ* reporter driven under the control of the endogenous *gα8* promoter. The gene fusion was transformed into wild-type cells and the developing structures were stained with X-gal and examined at different stages.

Interestingly, *gα8* is strongly expressed throughout the slug and enriched in the anterior and rearguard of the slugs. Typical staining patterns are shown in Fig. 45A left panel, and the arrows indicate intensive staining. In fruiting bodies, Gα8 is specifically distributed in the upper cup, lower cup and basal disc but not in the stalk tube, similar to the distribution of anterior-like cells (ALCs) (Sternfeld and David, 1982) (Fig. 45A, right panel). The *ecmO* promoter is the distal portion of the full promoter for the *ecmA* gene, and it is the specific marker for ALCs (Jermyn et al., 1989). Therefore the lacZ reporter under the control of the *ecmO* promoter was examined in *gα8*- cells. The *ecmO* expression was significantly suppressed in *gα8*- cells (Fig. 45B), suggesting that Gα8 is required for the differentiation of ALCs.

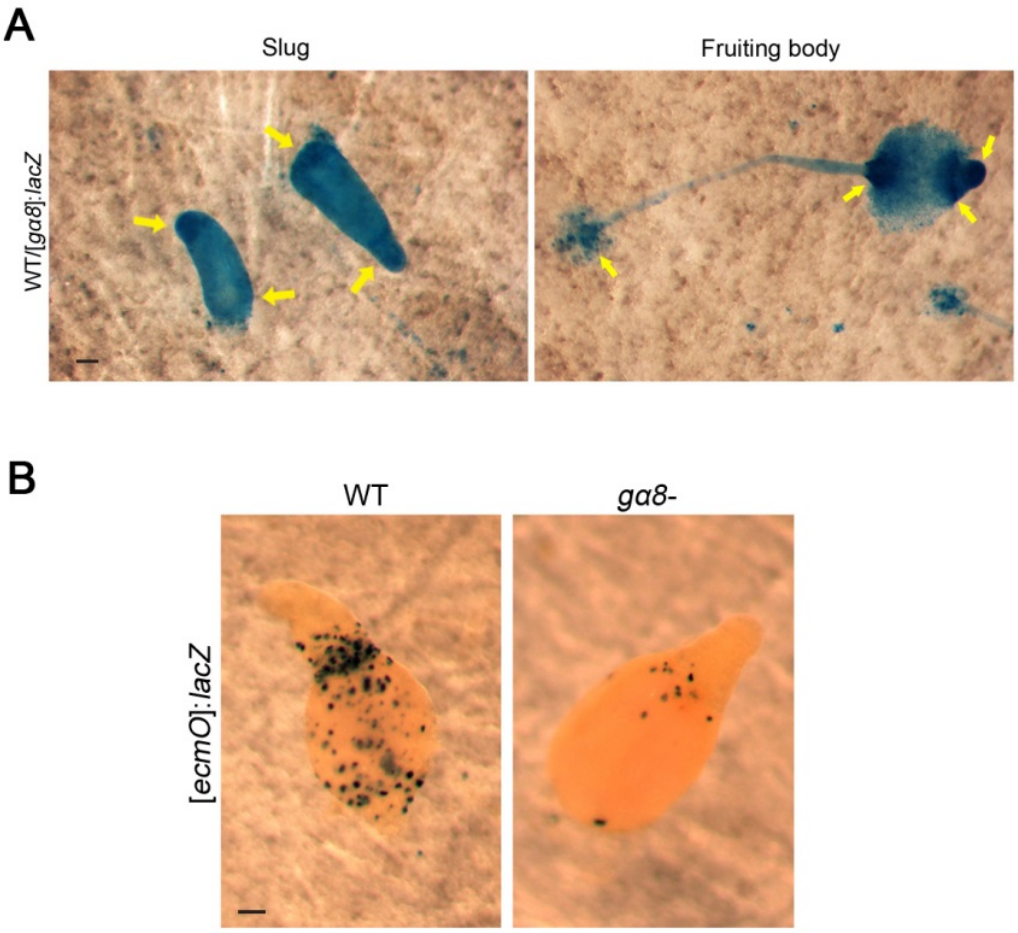

Figure 45. Distribution of Gα8 in multi-cellular structures. (A) WT cells expressing *lacZ* driven by the *gα8* promoter were developed on KK2 buffer-saturated filters. At 16 hours (Slug stage) and 24 hours (Fruiting body stage) after starvation, developing structures were fixed in 1% glutaraldehyde solution and stained with X-gal. Arrows indicates intensive blue staining. Bar, 50 µm. (B) *β-galactosidase* gene driven by the *ecmO* promoter was transformed in WT cells and *gα8*- cells. Cells were then developed on KK2-saturated filters. 20 hours after development, developing structures were fixed and stained with X-gal. Typical stainings are shown. Bar, 50 µm.

Since Gα8 appears to be preferentially expressed in stalk cells, I examined whether Gα8 regulates cell fate. *gα8*- cells and cells overexpressing *gα8* were labeled with GFP and mixed with control wild-type cells to generate chimeras. At 6 hours after the chimeras were starved on non-nutrient agarose, mounds were formed and wild-type

cells were distributed throughout the mound (Fig. 46A and 46B). The *gα8*- cells exhibited a similar distribution pattern as compared to wild-type cells (Fig. 46C and 46D). However, cells overexpressing Gα8 were primarily distributed in the periphery of the mound (Fig. 46E and 46F), suggesting they were unable to populate the aggregation center. In early culminates, wild-type cells were distributed evenly in both the stalk and spore cells regions (Fig. 46G and 46H). The *gα8*- cells were predominantly localized in the spore cells region (Fig. 46I and 46J), whereas cells overexpressing Gα8 were primarily found in the tip, upper and lower cup regions (Fig. 46K and 46L). The above results suggest that loss of Gα8 biased cells towards the spore cell fate and excess Gα8 biased cells towards the stalk cell fate.

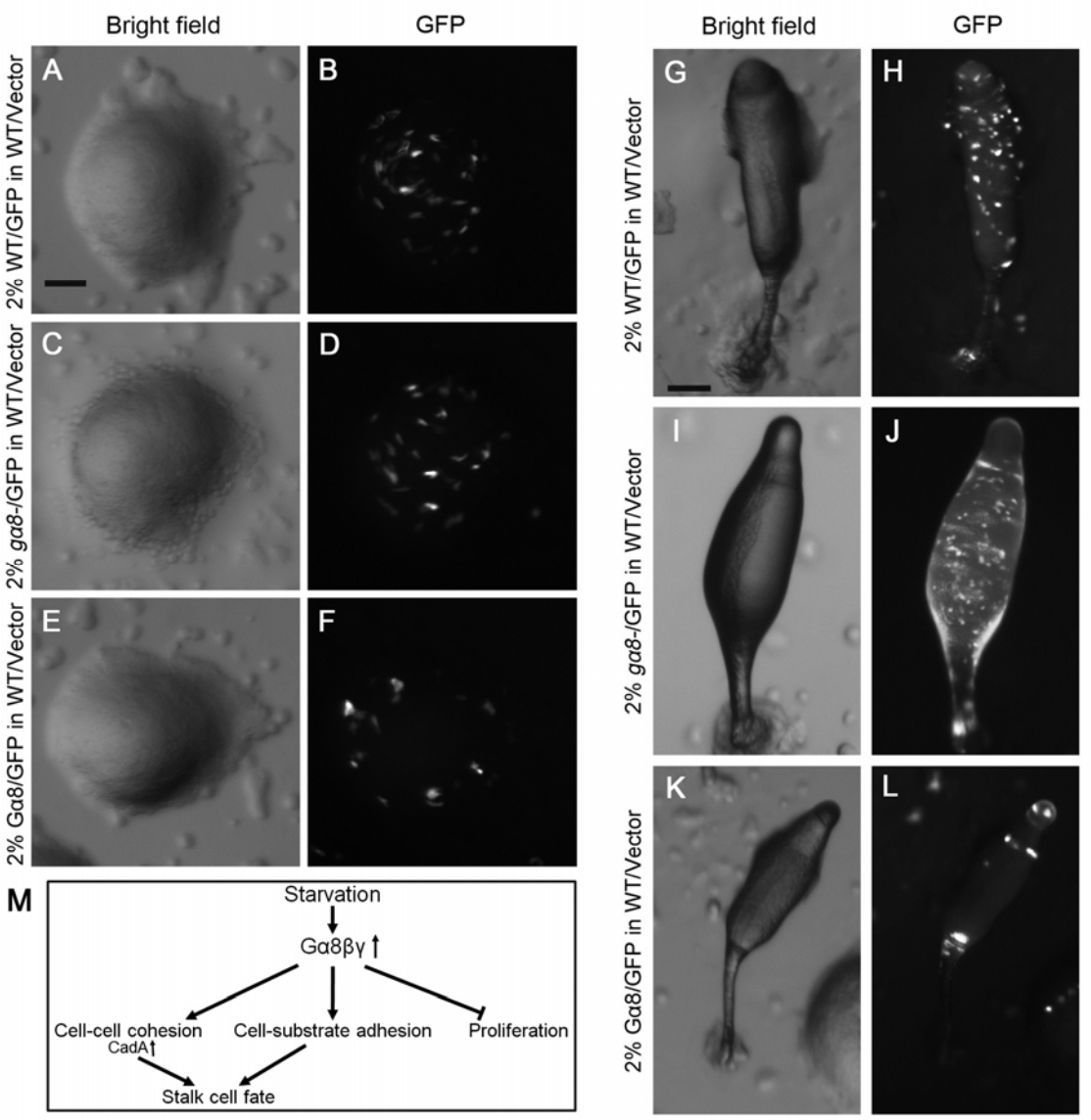

Figure 46. Distribution of *gα8*- and *gα8* overexpression cells in chimeras. 2% wild-type Ax2 cells expressing GFP (Using pDM323 vector), *gα8*- cells expressing GFP (Using pDM323 vector), WT cells expressing *gα8* and GFP (Using *gα8* in pDM358 and pDM323 vector) were mixed with WT cells expressing pDM304 vector. 5×10^6 mixture cells were developed on non-nutrient agarose, and representative images were taken at mound stage (6 hours after starvation, A-F) and culmination stage (20 hours after starvation, G-L). Bar, 100 μm. Diagram showing proposed functions of the Gα8βγ heterotrimer is presented in panel M. The heterotrimer is increased in response to starvation. The heterotrimer thereby inhibits proliferation and promotes adhesion. The induced adhesion facilitates cell differentiation.

The percentage of spores was also examined in *gα8*- cells. Consistent with a previous report (Bakthavatsalam et al., 2009), *gα8*- cells have a reduced percentage of spores in contrast to wild-type cells, and these spores have significantly impaired viability when treated with the detergent NP-40 (Fig. 47A). In addition, overexpression of Gα8 also dramatically decreased the number and viability of spores (Fig. 47A). Since the Gα8 regulates cell fate, I further examined whether any particular cell type, other than the ALCs, would show a disproportionate localization in the *gα8*- cells. To examine this, the *lacZ* reporter gene driven by cell type-specific promoters (*ecmAO*, *ecmA*, *ecmB*, and *pspA*) was used to label different types of cells. The resulting structures were stained at 20 hours of development. None of these specific markers showed significant changes in *gα8*- cells (Fig. 47B), suggesting that only the ALCs are affected by loss of Gα8.

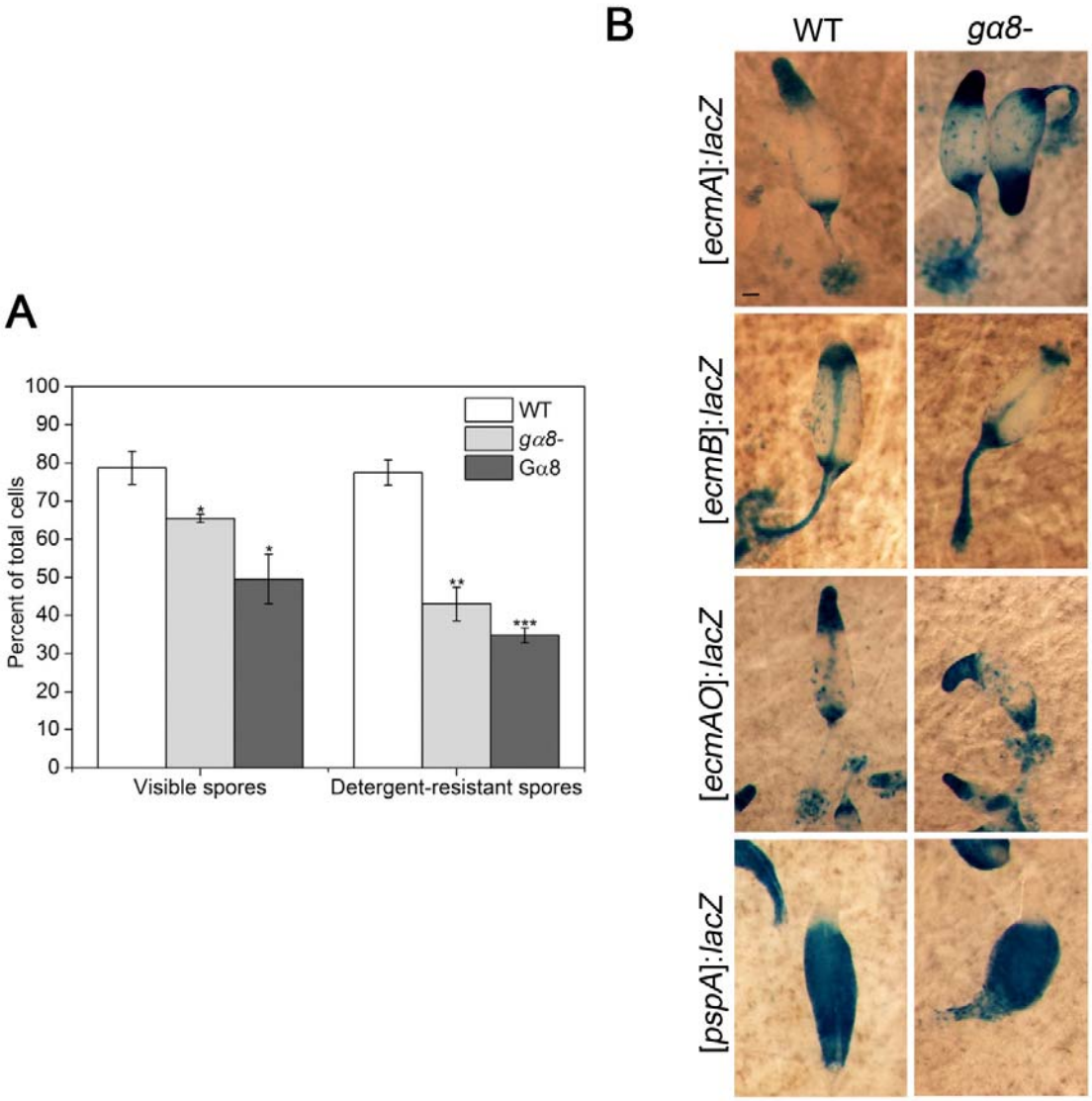

Figure 47. Spore formation and spatial patterning during culmination. (A) 1×10^7 cells were starved on KK2 buffer-saturated filters. After 4 days spores were collected and treated with 0.1% NP-40. Visible spores were counted by a hemacytometer. Detergent-resistant spores were counted by allowing NP-40 treated spores to germinate on bacterial lawn. Data represent means ± s.e.m. of three independent experiments, and values are compared with WT values. *, $p<0.05$; **, $p<0.01$; ***, $p<0.001$ (two-tailed Student's t test). (B) β-galactosidase gene driven by different cell-type specific promoters was transformed in WT cells and *gα8*- cells. Developing structures were stained and imaged as in Fig. 45B. Typical stainings are shown. Bar, 50 μm.

DISCUSSION

In this chapter, I characterized the functions of a G protein alpha subunit Gα8 during vegetative growth and development. Gα8 is induced after starvation, and distributed in the prestalk/stalk region during development.

Gα8 inhibits cells proliferation

Gα8 has been previously suggested to be part of the signal transduction pathway used by AprA to inhibit proliferation (Bakthavatsalam et al., 2009). Here I confirmed that loss of Gα8 leads to rapid proliferation. When over-expressed, excess Gα8 dramatically reduced the proliferation rate. Unlike the secreted chalone AprA, Gα8 remains at a low level during vegetative growth, and does not accumulate according to cell density. Upon starvation, Gα8 is promptly induced and probably functions through the accumulated AprA activated pathway to inhibit proliferation and facilitate development. Although excess Gα8 also promotes cell adhesion, it is likely that this effect of proliferation inhibition is independent of the high adhesion level since Gα8 still inhibits proliferation in several adhesion mutants. Cells without Gβ subunit also exhibit rapid proliferation (Bakthavatsalam et al., 2009), and loss of Gβ suppresses Gα8-induced proliferation inhibition, suggesting Gβ is an indispensable component for the activity of Gα8. In mammalian systems, it was shown years ago that the inhibitory Gαi subunits likely regulate proliferation (Bloch et al., 1989; Hermouet et al., 1991). Gα8 is most similar to the $G\alpha_i$ subunit family of vertebrates (Brzostowski et al., 2002), suggesting this function of regulating proliferation in the inhibitory $G\alpha_i$ subunits is conserved.

Gα8 promotes cell adhesion

In addition to reduced proliferation, overexpression of Gα8 also causes cytokinesis deficiency on substrates. Subsequent results indicate excess Gα8 leads to both induced cell-cell cohesion and induced cell-substrate adhesion. This induced cell-cell cohesion was sensitive to the treatment of EDTA or EGTA, which indicates the cohesion is Ca^{2+}-dependent. Treatment with CadA antibody and analysis of CadA expression further suggest that the cell-cell cohesion is induced through up-regulating expression levels of CadA in cells overexpressing Gα8. Reducing cell-cell cohesion by removing CadA did not rescue the cytokinesis defect. However, reducing cell-substrate adhesion using different adhesion mutants including *paxB*- and *sadA*- successfully rescued the cytokinesis defect. These data also explained why no significant amount of multi-nucleated cells was observed when cells were grown in suspension since no cell-substrate adhesion is present in suspension. It is surprising that adhesion loss was not observed in *gα8*- cells. The low expression level of Gα8 in vegetative cells may explain this finding.

Although *paxB*- and *sadA*- rescued the cytokinesis defect, both Paxillin and SadA are not necessary components of the Gα8 signaling pathway. I showed that the cell-adhesion level governs the severity of the cytokinesis defect. Many proteins including Paxillin and SadA regulate cell-substrate adhesion in *D. discoideum* (Benghezal et al., 2003; Bukharova et al., 2005; Cornillon et al., 2006; Fey et al., 2002; Niewohner et al., 1997). The Gα8 signaling pathway might act through some of these proteins to induce cell-substrate adhesion, which causes more pulling force required for proper division. These data suggest that other adhesion mutants might also rescue the cytokinesis defect induced by excess Gα8. Interestingly, *sadA*- cells overexpressing Gα8 slightly increase

adhesion toward substrates but are still severely impaired in cell-substrate adhesion. This suggests that SadA is the major substrate adhesion receptor and overexpression of Gα8 might promote expression of other minor substrate adhesion receptors in the absence of SadA.

The C terminus of Gα subunit has been recognized as a crucial receptor G protein interaction region (Bourne, 1997), and the truncated Gα8 lacking the C-terminal 51 amino acids causes similar cytokinesis failure as intact Gα8, suggesting Gα8 might induce the cytokinesis defect without the involvement of a GPCR, though the requirement for a GPCR is not absolutely ruled out. It is surprising to find that cells overexpressing two theoretically persistently activated Gα8 mutants failed to augment the overexpression phenotypes and instead grew and developed normally. The dominant negative Gα8 mutant theoretically binds to Gβγ but loses affinity for GDP, and overexpression of the heterotrimer with low affinity for guanine nucleotides does not induce cytokinesis defects. Since native Gα8 still induces cytokinesis defects when excess Gβγ exists, it is unlikely that overexpression Gα8 sequesters Gβγ from other Gα subunits. While it is possible that our Gα8 point mutations do not function as would be predicted and simply cause a loss of function, these data suggest that the activity of Gα8 requires the cycling of Gα8 between a GDP-bound and GTP-bound state.

Gα8 regulates cell differentiation

The expression pattern of Gα8 suggests that it functions after starvation. Moreover, the specified distribution of Gα8 in multi-cellular developing structures, the reduced EcmO marker and the decreased percentage of spores all suggest Gα8 regulates

cell differentiation. I have shown that Gα8 inhibits proliferation, promotes cell-cell cohesion and cell-substrate adhesion. All three of these factors have been proposed to control cell fate determination when cells are shifted from the vegetative stage to starvation conditions. Cells that are starved at S phase or early or late G2 phase differentiate mostly into prestalk cells, whereas cells at middle G2 phase tend to differentiate into prespore cells (Gomer and Firtel, 1987; Weijer et al., 1984; Zimmerman and Weijer, 1993). Gα8 apparently regulates cell proliferation. However, it is still unclear whether the proportion of cell-cycle phase is altered with deficient or excess Gα8. D. discoideum cells have a prolonged G2 phase that accounts for over 90% of the cell cycle (Muramoto and Chubb, 2008). To explain the altered rate of proliferation, I speculate that gα8- cells have a shortened G2 phase and the proportion of G2 phase cells is lower, whereas cells overexpressing Gα8 have a prolonged G2 phase and the proportion of G2 phase cells is higher. However, our results showing differentiation of different cells in chimeras are contradictory to this cell cycle position theory. Cell-type specific alterations in adhesion have also been proposed in cell sorting. Cells with greater adhesiveness tend to differentiate into prestalk cells (Nicol et al., 1999; Sriskanthadevan et al., 2011). Our results are consistent with adhesion-dependent differentiation during development and suggest that cell adhesion likely precedes cell cycle position in determining cell differentiation.

In chimeras, cells expressing Gα8 are primarily located in the periphery of the mound. However, cells that show greater cohesiveness for one another usually stay in the center and the less cohesive ones typically sort to the periphery in chimeric mounds (Steinberg and Takeichi, 1994). One possible explanation is that cells overexpressing

Gα8 have an impaired capacity for cAMP firing. This would explain why cells expressing Gα8 are seldom observed at aggregation centers. The strong cell-substrate adhesion of cells expressing Gα8 might also reduce cAMP chemotactic speed, which causes cells to reach the aggregates later than wild-type cells. Previous studies have suggested that spatial position in aggregates affects cell type differentiation (Krefft et al., 1984; Sriskanthadevan et al., 2011). Cells in the periphery differentiate mostly into prestalk cells and our results are consistent with position-dependent differentiation during development.

About 20% of prestalk cells populate the anterior region of the slug, and anterior-like cells with the prestalk features are scattered in the prespore zone (Sternfeld and David, 1982). Anterior-like cells could re-differentiate into prespore cells and form the upper cup and the lower cup which cradle the spore sorus (Jermyn et al., 1989), which possibly suggests that the decreased ratio of spores in *gα8*- cells is caused by the reduced number of anterior-like cells. A previous study revealed that the Gα4 subunit is distributed in anterior-like cells and disruption of *gα4* results in biased cell fate (Hadwiger and Firtel, 1992), which further suggests that the G protein is involved in anterior-like cell differentiation.

My results provide evidence for novel functions of Gα8 during vegetative growth and development. These functions are summarized in Fig. 46M. Upon starvation, the expression levels of Gα8 and Gβγ are strongly induced. Based on the inhibition of proliferation inhibition effect that Gα8 has on vegetative cells, the increased Gα8βγ heterotrimer likely also inhibit proliferation in starving cells. This heterotrimer may induce cell-cell cohesion in starving cells, as shown in Gα8 overexpressing cells.

Overexpression of Gα8 promotes cell-substrate adhesion in vegetative cells, therefore I postulate that the heterotrimer may also increase cell adhesiveness in early development. An adequate adhesion level is required for efficient cAMP chemotaxis and proper cell sorting. Further studies on the downstream targets of Gα8 will provide a better understanding of the mechanisms underlying this heterotrimeric G protein signaling cascade.

CHAPTER V

SUMMARY AND PERSPECTIVE

In this thesis, I explored the functions of several GPCRs and G proteins during growth and development of the social amoeba *D. discoideum*. The area that has gained the most interest in this model organism is determining the mechanism underlying directional cell movement (chemotaxis), including gradient sensing, polarity establishment and cytoskeleton re-organization. The cAR1 family, G protein alpha subunit Gα2 and Gα4 play vital roles in chemotaxis and have been intensively studied. My research provides an understanding of the functions of other somewhat neglected GPCRs and G proteins.

Folic acid receptor(s)

Due to unknown factors, my screening for the folic acid receptor(s) through transcriptional change did not successfully isolate a candidate folic acid receptor. However, many alternative methods are available to identify this receptor in the future. Reverse-transcriptase PCR described in chapter II is currently an outdated and inaccurate method to measure transcriptional changes, whereas high through-put microarrays or RNA-seq are powerful and popular for measuring gene expression nowadays. A previous study investigated the transcriptional difference between axenic cells and cells feeding on bacteria using microarrays, and showed that the transcriptional levels of two putative GPCRs, GrlB and GrlJ, were up-regulated when cells were cultured with bacteria (Sillo et al., 2008). However, subsequent disruptions of these two genes did not lead to loss of folic acid response (Prabhu et al., 2007b; Wu and Janetopoulos, 2013b). Moreover, none

of the published single GPCR mutants exhibited defective folic acid chemotaxis. These data strongly suggest that, either the folic acid receptor is redundant or the transcriptional level of a folic acid receptor(s) barely changes upon folic acid stimulation.

Recently Gα4 was used as bait to pull-down proteins interacting with Gα4, and a nonreceptor guanine exchange factor (GEF) was identified (Kataria et al., 2013). During this screening, a protein containing seven trans-membrane domains was isolated. This protein does not belong to any of the identified putative GPCRs, and whether this protein is required for folic acid sensing is currently being investigated.

GABA metabolism

Characterization of GABA metabolism indicates GABA is not only utilized as an inhibitory neurotransmitter but also is employed as an ancient signal for cell-cell communication in this lower eukaryote. Distinct genes are found to regulate GABA metabolism and signaling in different stages. Due to its separated life stages with distinct characteristics, solitary versus social, it is a quite common phenomenon in this organism. For instance, cAMP is synthesized by different adenylyl cyclases in different developmental stages (Schaap, 2011).

The study of GABA metabolism in *D. discoideum* may provide insight into our understanding of neurodegenerative diseases in human. The GABA enzymes, including Gad65 and Gad67, and $GABA_B$ receptors are mis-regulated in brains affected with Huntington's disease, as has been shown by the examination of postmortem brains from patients with Huntington's chorea and in studies performed in mammalian model systems (Gajcy et al., 2010; McGeer and McGeer, 1976; Perry et al., 1973; Rekik et al., 2011;

Walker et al., 1984). The *D. discoideum* genome contains an orthologue of the mammalian Huntingtin gene (*htt*). The genetic disruption of *htt* has a wide range of effects on the morphology of the cell including negative consequences on their ability to divide, undergo proper chemotactic cAMP relay, and differentiate (Myre et al., 2011; Wang et al., 2011). Interestingly, when *htt* is disrupted, microarray analysis suggests that the GABA pathway components have significant transcriptional changes (personal communication, Michael Myre). In *htt*- cells, *gadB* and *grlB* transcriptional level were increased about 4 fold while *grlE* level was up about 10 fold. *gadA* expression was down about 10 fold. This is consistent with my results described in chapter III. *gadA* and *gadB* expression are somehow inversely regulated.

In addition, the mis-regulated GABA metabolism might account for the developmental phenotypes seen in *htt*- cells (Myre et al., 2011). The *htt*- cells exhibited a mild delay in aggregation and reduced viable spores, which were also observed in GABA signaling mutants. Recently *gadB* was disrupted in *htt*- cells, and I am testing whether loss of GABA can rescue the developmental phenotypes of *htt*- cells. The *htt*- cells exhibited hyper-sensitivity to hypo-osmotic stress (Myre et al., 2011), however, none of the GABA signaling mutants exhibited this defect (data not shown). Moreover, the *gadB*-/*htt*- cells were still sensitive to hypo-osmotic stress (data not shown). These data indicate that GABA is not required for the HTT function in osmotic regulation. In plants, GABA is quickly accumulated as an osmolyte for adapting to hyper-osmotic stress (Shelp et al., 1999). Whether GABA is also utilized as an osmolyte in amoeba adaptation to hyper-osmotic stress induced by sorbitol is also being tested. Overall, these strikingly similar findings in the regulation of GABA in *D. discoideum* and humans suggest that this simple

eukaryote may be a valuable tool to further our understanding of the HTT protein and its role in cellular function (Myre, 2012).

Gα8 and adhesion

The Gα8 expression level is significantly induced after development. The elevated Gα8 increases the adhesiveness of the cells and inhibits cells proliferation. This likely facilitates cell-cell communication required for development. Since overexpression of Gα8 still reduces cell proliferation in adhesion mutants, the proliferation inhibition is likely independent of increased cell adhesion. Gα8 probably plays these distinct roles through two different pathways. Previous studies suggested that Gα8 is required for both the proliferation inhibition effect and the chemo-repellent effect of the chalone AprA (Bakthavatsalam et al., 2009; Phillips and Gomer, 2012). These results indicate that Gα8 probably functions through the AprA pathway to inhibit proliferation.

The classic G protein activation cycle suggests that GTP-bound Gα subunit separates from Gβγ and these separated G protein subunits interact with their downstream effectors. Based on my data that putative constitutively active Gα8 does not induce the cytokinesis defect and C-terminal truncated Gα8 still induce the defect, I propose a non-canonical model for the relationship between Gα8 and adhesion. First, GDP-bound Gα8 remains as a heterotrimer with Gβγ. This "inactive" heterotrimer could interact with effectors which eventually increase cell adhesiveness, probably by inducing plasma membrane-bound adhesion molecules, including CadA and CsA. The interaction site is probably on Gα8. This interaction does not require the replacement of GDP by GTP, that is, no requirement for the function of GEFs, including GPCRs. However, the activation

and separation of Gα8 may prevent the interaction of the heterotrimer with its effector. The activated Gα8 may then activate other pathways, for example, the AprA pathway to inhibit proliferation. Although I am still lacking strong evidence to support this model, it is still a possibility to explain the data I obtained.

Recently the mammalian Gα13 subunit was revealed to directly bind to the cytoplasmic domain of integrin β3 subunit which activates protein kinase Src and inhibits the activation of the small GTPase RhoA (Gong et al., 2010). This interaction prevents cell spreading and accelerates cell retraction, suggesting that the Gα subunit regulates integrin-mediated cell adhesion. Integrins act as major metazoan adhesion receptors in mediating cell adhesion to the extracellular matrix (Hynes, 2002), however, no protein homologous to the integrin α or β subunit has been identified in the *D. discoideum* genome. An adhesion molecule SibA was found to share conserved extracellular domains with integrin β subunit in *D. discoideum*, and loss of SibA significantly reduces cell-substrate adhesion (Cornillon et al., 2006). Considering Gα8 dramatically promotes cell-substrate adhesion, it would be intriguing to determine any potential interactions between Gα8 and SibA. SadA is thought to be an important substrate adhesion receptor (Fey et al., 2002), and SadA controls the cell surface expression and stability of SibA (Froquet et al., 2012). Though overexpression of Gα8 in *sadA*- cells partially rescues the cytokinesis defect, *sadA*- cells expressing Gα8 only slightly increase adhesion toward substrates and are still severely impaired in cell-substrate adhesion. This suggests SadA is the major substrate adhesion receptor and overexpression of Gα8 might promote expression of other minor substrate adhesion receptors in the absence of SadA.

Though excess Gα8 strongly induces adhesion and alters the developmental process, loss of Gα8 only has a minimal affect on the developmental process. These data indicate that the physiological Gα8 level may be the minor regulator of adhesion or plays a role in the fine tuning of adhesion. Therefore, the next step is to identify the potential downstream effector of Gα8 that regulates adhesion. I found that the Gα8 labeled with a small epitope tag at the COOH terminus functions was similarly to intact Gα8 by examining the overexpression phenotypes. The Gα8-His tag fusion was used to perform pull-down experiments, and the pull-down products have been analyzed by mass spectrometry. The analysis of potential targets is still ongoing.

REFERENCES

Anjard, C., Loomis, W. F., 2006. GABA induces terminal differentiation of Dictyostelium through a GABAB receptor. Development. 133**,** 2253-61.

Anjard, C., Su, Y., Loomis, W. F., 2009. Steroids initiate a signaling cascade that triggers rapid sporulation in Dictyostelium. Development. 136**,** 803-12.

Bakthavatsalam, D., Choe, J. M., Hanson, N. E., Gomer, R. H., 2009. A Dictyostelium chalone uses G proteins to regulate proliferation. BMC Biol. 7**,** 44.

Bouche, N., Fromm, H., 2004. GABA in plants: just a metabolite? Trends Plant Sci. 9**,** 110-5.

Brandon, M. A., Podgorski, G. J., 1997. G alpha 3 regulates the cAMP signaling system in Dictyostelium. Mol Biol Cell. 8**,** 1677-85.

Brzostowski, J. A., Johnson, C., Kimmel, A. R., 2002. Galpha-mediated inhibition of developmental signal response. Curr Biol. 12**,** 1199-208.

Charette, S. J., Cosson, P., 2004. Preparation of genomic DNA from Dictyostelium discoideum for PCR analysis. Biotechniques. 36**,** 574-5.

Chisholm, R. L., Firtel, R. A., 2004. Insights into morphogenesis from a simple developmental system. Nat Rev Mol Cell Biol. 5**,** 531-41.

Clarke, M., Kayman, S. C., Riley, K., 1987. Density-dependent induction of discoidin-I synthesis in exponentially growing cells of Dictyostelium discoideum. Differentiation. 34**,** 79-87.

Cornillon, S., Gebbie, L., Benghezal, M., Nair, P., Keller, S., Wehrle-Haller, B., Charette, S. J., Bruckert, F., Letourneur, F., Cosson, P., 2006. An adhesion molecule in free-living Dictyostelium amoebae with integrin beta features. EMBO Rep. 7**,** 617-21.

De Biase, D., Tramonti, A., John, R. A., Bossa, F., 1996. Isolation, overexpression, and biochemical characterization of the two isoforms of glutamic acid decarboxylase from Escherichia coli. Protein Expr Purif. 8**,** 430-8.

Doherty, G. J., McMahon, H. T., 2009. Mechanisms of endocytosis. Annu Rev Biochem. 78**,** 857-902.

Ehrenman, K., Yang, G., Hong, W. P., Gao, T., Jang, W., Brock, D. A., Hatton, R. D., Shoemaker, J. D., Gomer, R. H., 2004. Disruption of aldehyde reductase increases group size in dictyostelium. J Biol Chem. 279**,** 837-47.

Eichinger, L., Pachebat, J. A., Glockner, G., Rajandream, M. A., Sucgang, R., Berriman, M., Song, J., Olsen, R., Szafranski, K., Xu, Q., Tunggal, B., Kummerfeld, S., Madera, M., Konfortov, B. A., Rivero, F., Bankier, A. T., Lehmann, R., Hamlin, N., Davies, R., Gaudet, P., Fey, P., Pilcher, K., Chen, G., Saunders, D., Sodergren, E., Davis, P., Kerhornou, A., Nie, X., Hall, N., Anjard, C., Hemphill, L., Bason, N., Farbrother, P., Desany, B., Just, E., Morio, T., Rost, R., Churcher, C., Cooper, J., Haydock, S., van Driessche, N., Cronin, A., Goodhead, I., Muzny, D., Mourier, T., Pain, A., Lu, M., Harper, D., Lindsay, R., Hauser, H., James, K., Quiles, M., Madan Babu, M., Saito, T., Buchrieser, C., Wardroper, A., Felder, M., Thangavelu, M., Johnson, D., Knights, A., Loulseged, H., Mungall, K., Oliver, K., Price, C., Quail, M. A., Urushihara, H., Hernandez, J., Rabbinowitsch, E., Steffen, D., Sanders, M., Ma, J., Kohara, Y., Sharp, S., Simmonds, M., Spiegler, S., Tivey, A., Sugano, S., White, B., Walker, D., Woodward, J., Winckler, T., Tanaka, Y., Shaulsky, G., Schleicher, M., Weinstock, G., Rosenthal, A., Cox, E. C., Chisholm, R. L., Gibbs, R., Loomis, W. F., Platzer, M., Kay, R. R., Williams, J., Dear, P. H., Noegel, A. A., Barrell, B., Kuspa, A., 2005. The genome of the social amoeba Dictyostelium discoideum. Nature. 435**,** 43-57.

Elzie, C. A., Colby, J., Sammons, M. A., Janetopoulos, C., 2009. Dynamic localization of G proteins in Dictyostelium discoideum. J Cell Sci. 122**,** 2597-603.

Erlander, M. G., Tillakaratne, N. J., Feldblum, S., Patel, N., Tobin, A. J., 1991. Two genes encode distinct glutamate decarboxylases. Neuron. 7**,** 91-100.

Faix, J., Kreppel, L., Shaulsky, G., Schleicher, M., Kimmel, A. R., 2004. A rapid and efficient method to generate multiple gene disruptions in Dictyostelium discoideum using a single selectable marker and the Cre-loxP system. Nucleic Acids Res. 32**,** e143.

Fey, P., Stephens, S., Titus, M. A., Chisholm, R. L., 2002. SadA, a novel adhesion receptor in Dictyostelium. J Cell Biol. 159**,** 1109-19.

Fredriksson, R., Lagerstrom, M. C., Lundin, L. G., Schioth, H. B., 2003. The G-protein-coupled receptors in the human genome form five main families. Phylogenetic analysis, paralogon groups, and fingerprints. Mol Pharmacol. 63**,** 1256-72.

Froquet, R., le Coadic, M., Perrin, J., Cherix, N., Cornillon, S., Cosson, P., 2012. TM9/Phg1 and SadA proteins control surface expression and stability of SibA adhesion molecules in Dictyostelium. Mol Biol Cell. 23**,** 679-86.

Gajcy, K., Lochynski, S., Librowski, T., 2010. A role of GABA analogues in the treatment of neurological diseases. Curr Med Chem. 17**,** 2338-47.

Gasnier, B., 2004. The SLC32 transporter, a key protein for the synaptic release of inhibitory amino acids. Pflugers Arch. 447**,** 756-9.

Gomer, R. H., Jang, W., Brazill, D., 2011. Cell density sensing and size determination. Dev Growth Differ. 53**,** 482-94.

Gong, H., Shen, B., Flevaris, P., Chow, C., Lam, S. C., Voyno-Yasenetskaya, T. A., Kozasa, T., Du, X., 2010. G protein subunit Galpha13 binds to integrin alphaIIbbeta3 and mediates integrin "outside-in" signaling. Science. 327**,** 340-3.

Hadwiger, J. A., Firtel, R. A., 1992. Analysis of G alpha 4, a G-protein subunit required for multicellular development in Dictyostelium. Genes Dev. 6**,** 38-49.

Hadwiger, J. A., Lee, S., Firtel, R. A., 1994. The G alpha subunit G alpha 4 couples to pterin receptors and identifies a signaling pathway that is essential for multicellular development in Dictyostelium. Proc Natl Acad Sci U S A. 91**,** 10566-70.

Hadwiger, J. A., Natarajan, K., Firtel, R. A., 1996. Mutations in the Dictyostelium heterotrimeric G protein alpha subunit G alpha5 alter the kinetics of tip morphogenesis. Development. 122**,** 1215-24.

Hadwiger, J. A., Wilkie, T. M., Strathmann, M., Firtel, R. A., 1991. Identification of Dictyostelium G alpha genes expressed during multicellular development. Proc Natl Acad Sci U S A. 88**,** 8213-7.

Heidel, A. J., Lawal, H. M., Felder, M., Schilde, C., Helps, N. R., Tunggal, B., Rivero, F., John, U., Schleicher, M., Eichinger, L., Platzer, M., Noegel, A. A., Schaap, P., Glockner, G., 2011. Phylogeny-wide analysis of social amoeba genomes highlights ancient origins for complex intercellular communication. Genome Res. 21**,** 1882-91.

Howard, A. D., McAllister, G., Feighner, S. D., Liu, Q., Nargund, R. P., Van der Ploeg, L. H., Patchett, A. A., 2001. Orphan G-protein-coupled receptors and natural ligand discovery. Trends Pharmacol Sci. 22**,** 132-40.

Huh, W. K., Falvo, J. V., Gerke, L. C., Carroll, A. S., Howson, R. W., Weissman, J. S., O'Shea, E. K., 2003. Global analysis of protein localization in budding yeast. Nature. 425**,** 686-91.

Hynes, R. O., 2002. Integrins: bidirectional, allosteric signaling machines. Cell. 110**,** 673-87.

Iranfar, N., Fuller, D., Loomis, W. F., 2003. Genome-wide expression analyses of gene regulation during early development of Dictyostelium discoideum. Eukaryot Cell. 2**,** 664-70.

Iranfar, N., Fuller, D., Sasik, R., Hwa, T., Laub, M., Loomis, W. F., 2001. Expression patterns of cell-type-specific genes in Dictyostelium. Mol Biol Cell. 12**,** 2590-600.

Jakoby, W. B., Fredericks, J., 1959. Pyrrolidine and putrescine metabolism: gamma-aminobutyraldehyde dehydrogenase. J Biol Chem. 234**,** 2145-50.

Janetopoulos, C., Jin, T., Devreotes, P., 2001. Receptor-mediated activation of heterotrimeric G-proteins in living cells. Science. 291**,** 2408-11.

Johnson, R. L., Saxe, C. L., 3rd, Gollop, R., Kimmel, A. R., Devreotes, P. N., 1993. Identification and targeted gene disruption of cAR3, a cAMP receptor subtype expressed during multicellular stages of Dictyostelium development. Genes Dev. 7**,** 273-82.

Journet, A., Klein, G., Brugiere, S., Vandenbrouck, Y., Chapel, A., Kieffer, S., Bruley, C., Masselon, C., Aubry, L., 2012. Investigating the macropinocytic proteome of Dictyostelium amoebae by high-resolution mass spectrometry. Proteomics. 12**,** 241-5.

Kataria, R., Xu, X., Fusetti, F., Keizer-Gunnink, I., Jin, T., van Haastert, P. J., Kortholt, A., 2013. Dictyostelium Ric8 is a nonreceptor guanine exchange factor for heterotrimeric G proteins and is important for development and chemotaxis. Proc Natl Acad Sci U S A. 110**,** 6424-9.

Kessin, R. H., 2001. Dictyostelium: The Evolution, Cell Biology, and Development of a Social Organism. Cambridge University Press, Cambridge

Klein, P. S., Sun, T. J., Saxe, C. L., 3rd, Kimmel, A. R., Johnson, R. L., Devreotes, P. N., 1988. A chemoattractant receptor controls development in Dictyostelium discoideum. Science. 241**,** 1467-72.

Kleppner, S. R., Tobin, A. J., GABA. In: V. S. Ramachandran, (Ed.), Encyclopedia of the human brain, 2002, pp. 353-367.

Kriebel, P. W., Barr, V. A., Parent, C. A., 2003. Adenylyl cyclase localization regulates streaming during chemotaxis. Cell. 112**,** 549-60.

Kumagai, A., Hadwiger, J. A., Pupillo, M., Firtel, R. A., 1991. Molecular genetic analysis of two G alpha protein subunits in Dictyostelium. J Biol Chem. 266**,** 1220-8.

Lilly, P., Wu, L., Welker, D. L., Devreotes, P. N., 1993. A G-protein beta-subunit is essential for Dictyostelium development. Genes Dev. 7**,** 986-95.

Liu, Q. R., Lopez-Corcuera, B., Mandiyan, S., Nelson, H., Nelson, N., 1993. Molecular characterization of four pharmacologically distinct gamma-aminobutyric acid transporters in mouse brain [corrected]. J Biol Chem. 268**,** 2106-12.

Liu, Q. R., Lopez-Corcuera, B., Nelson, H., Mandiyan, S., Nelson, N., 1992. Cloning and expression of a cDNA encoding the transporter of taurine and beta-alanine in mouse brain. Proc Natl Acad Sci U S A. 89**,** 12145-9.

Lopez-Corcuera, B., Liu, Q. R., Mandiyan, S., Nelson, H., Nelson, N., 1992. Expression of a mouse brain cDNA encoding novel gamma-aminobutyric acid transporter. J Biol Chem. 267**,** 17491-3.

Maeda, Y., 2011. Cell-cycle checkpoint for transition from cell division to differentiation. Dev Growth Differ. 53**,** 463-81.

Mahadeo, D. C., Parent, C. A., 2006. Signal relay during the life cycle of Dictyostelium. Curr Top Dev Biol. 73**,** 115-40.

Manahan, C. L., Iglesias, P. A., Long, Y., Devreotes, P. N., 2004. Chemoattractant signaling in dictyostelium discoideum. Annu Rev Cell Dev Biol. 20**,** 223-53.

Maruo, T., Sakamoto, H., Iranfar, N., Fuller, D., Morio, T., Urushihara, H., Tanaka, Y., Maeda, M., Loomis, W. F., 2004. Control of cell type proportioning in Dictyostelium discoideum by differentiation-inducing factor as determined by in situ hybridization. Eukaryot Cell. 3**,** 1241-8.

McGeer, P. L., McGeer, E. G., 1976. Enzymes associated with the metabolism of catecholamines, acetylcholine and gaba in human controls and patients with Parkinson's disease and Huntington's chorea. J Neurochem. 26**,** 65-76.

McIntire, S. L., Reimer, R. J., Schuske, K., Edwards, R. H., Jorgensen, E. M., 1997. Identification and characterization of the vesicular GABA transporter. Nature. 389**,** 870-6.

Meldrum, B. S., 1989. GABAergic mechanisms in the pathogenesis and treatment of epilepsy. Br J Clin Pharmacol. 27 Suppl 1**,** 3S-11S.

Myre, M. A., 2012. Clues to gamma-secretase, huntingtin and Hirano body normal function using the model organism Dictyostelium discoideum. J Biomed Sci. 19**,** 41.

Myre, M. A., Lumsden, A. L., Thompson, M. N., Wasco, W., MacDonald, M. E., Gusella, J. F., 2011. Deficiency of huntingtin has pleiotropic effects in the social amoeba Dictyostelium discoideum. PLoS Genet. 7**,** e1002052.

Nagasaki, A., Itoh, G., Yumura, S., Uyeda, T. Q., 2002. Novel myosin heavy chain kinase involved in disassembly of myosin II filaments and efficient cleavage in mitotic dictyostelium cells. Mol Biol Cell. 13**,** 4333-42.

Owens, D. F., Kriegstein, A. R., 2002. Is there more to GABA than synaptic inhibition? Nat Rev Neurosci. 3**,** 715-27.

Palanivelu, R., Brass, L., Edlund, A. F., Preuss, D., 2003. Pollen tube growth and guidance is regulated by POP2, an Arabidopsis gene that controls GABA levels. Cell. 114**,** 47-59.

Perry, T. L., Hansen, S., Kloster, M., 1973. Huntington's chorea. Deficiency of gamma-aminobutyric acid in brain. N Engl J Med. 288**,** 337-42.

Phillips, J. E., Gomer, R. H., 2012. A secreted protein is an endogenous chemorepellant in Dictyostelium discoideum. Proc Natl Acad Sci U S A. 109**,** 10990-5.

Pitt, G. S., Milona, N., Borleis, J., Lin, K. C., Reed, R. R., Devreotes, P. N., 1992. Structurally distinct and stage-specific adenylyl cyclase genes play different roles in Dictyostelium development. Cell. 69**,** 305-15.

Prabhu, Y., Eichinger, L., 2006. The Dictyostelium repertoire of seven transmembrane domain receptors. Eur J Cell Biol. 85**,** 937-46.

Prabhu, Y., Mondal, S., Eichinger, L., Noegel, A. A., 2007a. A GPCR involved in post aggregation events in Dictyostelium discoideum. Dev Biol. 312**,** 29-43.

Prabhu, Y., Muller, R., Anjard, C., Noegel, A. A., 2007b. GrlJ, a Dictyostelium GABAB-like receptor with roles in post-aggregation development. BMC Dev Biol. 7**,** 44.

Raisley, B., Zhang, M., Hereld, D., Hadwiger, J. A., 2004. A cAMP receptor-like G protein-coupled receptor with roles in growth regulation and development. Dev Biol. 265**,** 433-45.

Raper, K. B., 1935. Dictyostelium discoideum, a new species of slime mold from decaying forest leaves. J Agr Res. 50**,** 135-147.

Reddy, P. H., Williams, M., Tagle, D. A., 1999. Recent advances in understanding the pathogenesis of Huntington's disease. Trends Neurosci. 22**,** 248-55.

Rekik, L., Daguin-Nerriere, V., Petit, J. Y., Brachet, P., 2011. gamma-Aminobutyric acid type B receptor changes in the rat striatum and substantia nigra following intrastriatal quinolinic acid lesions. J Neurosci Res. 89**,** 524-35.

Roberts, E., Ayengar, P., Posner, I., 1953. Transamination of gamma-aminobutyric acid and beta-alanine in microorganisms. J Biol Chem. 203**,** 195-204.

Roberts, E., Frankel, S., 1950. gamma-Aminobutyric acid in brain: its formation from glutamic acid. J Biol Chem. 187**,** 55-63.

Saxe, C. L., 3rd, Johnson, R. L., Devreotes, P. N., Kimmel, A. R., 1991. Expression of a cAMP receptor gene of Dictyostelium and evidence for a multigene family. Genes Dev. 5**,** 1-8.

Schaap, P., 2011. Evolution of developmental cyclic adenosine monophosphate signaling in the Dictyostelia from an amoebozoan stress response. Dev Growth Differ. 53**,** 452-62.

Segall, J. E., Bominaar, A. A., Wallraff, E., De Wit, R. J., 1988. Analysis of a Dictyostelium chemotaxis mutant with altered chemoattractant binding. J Cell Sci. 91 (Pt 4)**,** 479-89.

Segall, J. E., Fisher, P. R., Gerisch, G., 1987. Selection of chemotaxis mutants of Dictyostelium discoideum. J Cell Biol. 104**,** 151-61.

Shelp, B. J., Bown, A. W., McLean, M. D., 1999. Metabolism and functions of gamma-aminobutyric acid. Trends Plant Sci. 4**,** 446-452.

Shelp, B. J., Mullen, R. T., Waller, J. C., 2012. Compartmentation of GABA metabolism raises intriguing questions. Trends Plant Sci. 17**,** 57-9.

Sillo, A., Bloomfield, G., Balest, A., Balbo, A., Pergolizzi, B., Peracino, B., Skelton, J., Ivens, A., Bozzaro, S., 2008. Genome-wide transcriptional changes induced by phagocytosis or growth on bacteria in Dictyostelium. BMC Genomics. 9**,** 291.

Siu, C. H., Sriskanthadevan, S., Wang, J., Hou, L., Chen, G., Xu, X., Thomson, A., Yang, C., 2011. Regulation of spatiotemporal expression of cell-cell adhesion molecules during development of Dictyostelium discoideum. Dev Growth Differ. 53**,** 518-27.

Snaar-Jagalska, B. E., Van Es, S., Kesbeke, F., Van Haastert, P. J., 1991. Activation of a pertussis-toxin-sensitive guanine-nucleotide-binding regulatory protein during desensitization of Dictyostelium discoideum cells to chemotactic signals. Eur J Biochem. 195**,** 715-21.

Soghomonian, J. J., Martin, D. L., 1998. Two isoforms of glutamate decarboxylase: why? Trends Pharmacol Sci. 19**,** 500-5.

Spiegel, A. M., Weinstein, L. S., 2004. Inherited diseases involving g proteins and g protein-coupled receptors. Annu Rev Med. 55**,** 27-39.

Srinivasan, K., Wright, G. A., Hames, N., Housman, M., Roberts, A., Aufderheide, K. J., Janetopoulos, C., 2012. Delineating the core regulatory elements critical for directed cell migration by examining folic acid-mediated responses. J Cell Sci.

Steward, F. C., Thompson, J. F., Dent, C. E., 1949. γ-Aminobutyric Acid: A Constituent of the Potato Tuber? Science. 110**,** 439-440.

Sucgang, R., Weijer, C. J., Siegert, F., Franke, J., Kessin, R. H., 1997. Null mutations of the Dictyostelium cyclic nucleotide phosphodiesterase gene block chemotactic cell movement in developing aggregates. Dev Biol. 192**,** 181-92.

Sussman, R., Sussman, M., 1967. Cultivation of Dictyostelium discoideum in axenic medium. Biochem Biophys Res Commun. 29**,** 53-5.

Taniura, H., Sanada, N., Kuramoto, N., Yoneda, Y., 2006. A metabotropic glutamate receptor family gene in Dictyostelium discoideum. J Biol Chem. 281**,** 12336-43.

Tillinghast, H. S., Newell, P. C., 1987. Chemotaxis towards pteridines during development of Dictyostelium. J Cell Sci. 87 (Pt 1)**,** 45-53.

Van Driessche, N., Shaw, C., Katoh, M., Morio, T., Sucgang, R., Ibarra, M., Kuwayama, H., Saito, T., Urushihara, H., Maeda, M., Takeuchi, I., Ochiai, H., Eaton, W., Tollett, J., Halter, J., Kuspa, A., Tanaka, Y., Shaulsky, G., 2002. A transcriptional profile of multicellular development in Dictyostelium discoideum. Development. 129**,** 1543-52.

van Es, S., Weening, K. E., Devreotes, P. N., 2001. The protein kinase YakA regulates g-protein-linked signaling responses during growth and development of Dictyostelium. J Biol Chem. 276**,** 30761-5.

Walker, F. O., Young, A. B., Penney, J. B., Dovorini-Zis, K., Shoulson, I., 1984. Benzodiazepine and GABA receptors in early Huntington's disease. Neurology. 34**,** 1237-40.

Wang, Y., Steimle, P. A., Ren, Y., Ross, C. A., Robinson, D. N., Egelhoff, T. T., Sesaki, H., Iijima, M., 2011. Dictyostelium huntingtin controls chemotaxis and cytokinesis through the regulation of myosin II phosphorylation. Mol Biol Cell. 22**,** 2270-81.

Wise, A., Gearing, K., Rees, S., 2002. Target validation of G-protein coupled receptors. Drug Discov Today. 7**,** 235-46.

Wu, L., Gaskins, C., Zhou, K., Firtel, R. A., Devreotes, P. N., 1994. Cloning and targeted mutations of G alpha 7 and G alpha 8, two developmentally regulated G protein alpha-subunit genes in Dictyostelium. Mol Biol Cell. 5**,** 691-702.

Wu, L., Valkema, R., Van Haastert, P. J., Devreotes, P. N., 1995. The G protein beta subunit is essential for multiple responses to chemoattractants in Dictyostelium. J Cell Biol. 129**,** 1667-75.

Wu, Y., Janetopoulos, C., 2013a. The G alpha subunit Galpha8 inhibits proliferation, promotes adhesion and regulates cell differentiation. Dev Biol.

Wu, Y., Janetopoulos, C., 2013b. Systematic Analysis of gamma-Aminobutyric Acid (GABA) Metabolism and Function in the Social Amoeba Dictyostelium discoideum. J Biol Chem. 288**,** 15280-90.

Wurster, B., Schubiger, K., 1977. Oscillations and cell development in Dictyostelium discoideum stimulated by folic acid pulses. J Cell Sci. 27**,** 105-14.

Zhang, N., Long, Y., Devreotes, P. N., 2001. Ggamma in dictyostelium: its role in localization of gbetagamma to the membrane is required for chemotaxis in shallow gradients. Mol Biol Cell. 12**,** 3204-13.